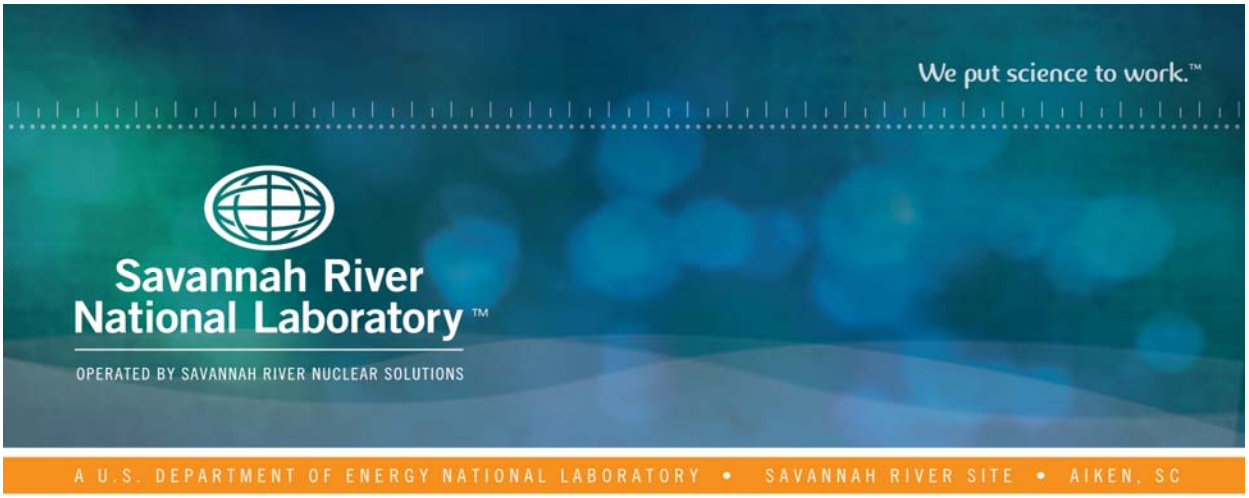

Nitric-Glycolic Flowsheet Evaluation with the Slurry-Fed Melt Rate Furnace

M. S. Williams
D. H. Miller
M. D. Fowley
J. R. Zamecnik

March 2017
SRNL-STI-2017-00072, Revision 0

DISCLAIMER

Printed in the United States of America

Prepared for
U.S. Department of Energy

SRNL-STI-2017-00072
Revision 0

Keywords: *alternate reductant, glycolic, DWPF, melter, offgas, REDOX, hydrogen, glass, cold cap*

Retention: *Permanent*

Nitric-Glycolic Flowsheet Evaluation with the Slurry-Fed Melt Rate Furnace

M. S. Williams
D. H. Miller
M. D. Fowley
J. R. Zamecnik

March 2017

Prepared for the U.S. Department of Energy under contract number DE-AC09-08SR22470.

Savannah River National Laboratory™
OPERATED BY SAVANNAH RIVER NUCLEAR SOLUTIONS

REVIEWS AND APPROVALS

AUTHORS:

M. S. Williams, Process Technology Programs Date

D. H. Miller, Engineering Process Development Date

M. D. Fowley, Immobilization Technology Date

J. R. Zamecnik, Process Technology Programs Date

TECHNICAL REVIEW:

F. C. Johnson, Immobilization Technology Date

W. H. Woodham, Process Technology Programs Date

APPROVAL:

F. N. Pennebaker, Manager Date
Chemical Processing Technologies

D. E. Dooley, Director, Date
Chemical Processing Technologies

E. J. Freed, Manager Date
SRR DWPF & Saltstone Facility Engineering

ACKNOWLEDGEMENTS

The operation of the melter required several start-ups and shutdowns, resulting in multiple schedule adjustments over a period of nearly three months. The authors would like to thank all those involved for their flexibility in working around unanticipated events (including a hurricane) yet remaining vigilant in performing the testing to the highest standards of scientific rigor and safety.

Thanks to the technicians involved in the testing: Jon Duvall, Phyllis Workman, Kim Wyszynski, and Minnie Hightower. The technicians worked twelve-hour day or night shifts for five separate weeks over the three month testing period, including some weekends. Their willingness to be flexible in their time while maintaining the utmost attitude of safety and commitment is greatly appreciated.

Thanks to the scientists and engineers involved in the testing: Charles Crawford, Jake Amoroso, Fabienne Johnson, Frances Williams, Devon McClane, and Wes Woodham. The investigators worked eight-hour shifts around the clock during the testing and many more hours before testing began to ensure that the melter operated optimally under conditions that it had never been operated under before. Their ability to handle the unexpected and troubleshoot unforeseen issues while operating in the unknown is applauded.

Thanks to Jeff Coughlin for designing and drafting the modifications to the melter lid, allowing for previously unavailable additions. Thanks to Andy Foreman for constructing a majority of the offgas and condensate recirculation system as well as many other mechanical modifications. Thanks to Joel Jones for developing the LabVIEW automation and control software. Thanks to Dale Marzolf and Vernon Bush for modifications and troubleshooting of the electrical systems. All of their high quality contributions to the construction of the system are echoed in the robust operation of each individual component as part of the whole system.

Thanks to Whitney Riley, Beverly Wall, Courtney Burckhalter, Kim Wyszynski, and Mark Reboul for analyzing the numerous samples, often with short turnaround time demands and including numerous different types of preparations for a variety of analytical methods. Thanks to Jack Zamecnik and John Pareizs for analyzing the days' and days' worth of offgas data from the instrumentation, ensuring correct baseline corrections and calibrations were accounted for. Their accurate analyses are the keys to understanding and verifying the observations of the experimentation.

Thanks to Holly Hall for coordinating all of the personnel and equipment efforts and ensuring that we were operating according to lab standards. Her ability to organize and direct individuals and efforts was paramount to smooth operations.

EXECUTIVE SUMMARY

The Savannah River National Laboratory (SRNL) was tasked to support validation of the Defense Waste Processing Facility (DWPF) melter offgas flammability model for the nitric-glycolic (NG) flowsheet. The work supports Deliverable 4 of the DWPF & Saltstone Facility Engineering Technical Task Request (TTR)[1] and is supplemental to the Cold Cap Evaluation Furnace (CEF) testing conducted in 2014.[2] The Slurry-fed Melt Rate Furnace (SMRF) was selected for the supplemental testing as it requires significantly less resources than the CEF and could provide a tool for more rapid analysis of melter feeds in the future. The SMRF platform has been used previously to evaluate melt rate behavior of DWPF glasses, but was modified to accommodate analysis of the offgas stream. Additionally, the Melt Rate Furnace (MRF) and Quartz Melt Rate Furnace (QMRF) were utilized for evaluations. MRF data was used exclusively for melt behavior observations and REDuction/OXidation (REDOX) prediction comparisons and will be briefly discussed in conjunction with its support of the SMRF testing. The QMRF was operated similarly to the SMRF for the same TTR task, but will be discussed in a separate future report. The overall objectives of the SMRF testing were to:

1) Evaluate the efficacy of the SMRF as a platform for steady state melter testing with continuous feeding and offgas analysis

2) Generate supplemental melter offgas flammability data to support the melter offgas flammability modelling effort for DWPF implementation of the NG flowsheet.

This report will address the first objective, while the second objective will be addressed in a separate future melter offgas flammability report.

During the first startup in August of 2016, the SMRF was charged with cullet from the 2014 CEF Phase 2 campaign. The melter feed was based on the CEF SB6I Sludge Receipt and Adjustment Tank (SRAT) product developed in 2014, which was diluted to 42 wt.% total solids to facilitate feeding. Additional nitric acid was used to remediate the first feed in order to lower the predicted REDOX ratio value (ratio of Fe^{2+} to total Fe in the glass) to target ~0.00 – 0.10. For successive startups in September and October the melter was charged with SMRF glass produced during the proceeding runs. The second feed was unremediated, predicted to produce a glass with an intermediate REDOX value (target ~0.15 – 0.20). The third feed was remediated with additional glycolic acid to raise the predicted REDOX value to near the upper limit of the acceptable range (target ~0.25 – 0.35). The third feed was also subjected to argon bubbling to assess if bubbled operations were feasible in the SMRF.

Testing consisted of operating at steady state conditions through a variety of melter vapor space (VS) temperatures (~250 – 750°C) with corresponding slurry feed rates (~5 – 30 grams/min). Vapor space temperature targets were achieved through optimization of melter feed rate, melter VS heater power output, and purge air flow rates. Steady state conditions were considered to be achieved when minimal fluctuations were observed in the operational variables with no outside influence and relatively stable offgas compositions.

Notable results from testing with the SMRF platform are as follows:

- Hydrogen concentrations in the offgas typically peaked between 0.015 and 0.06 vol% with one peak up to 0.265 vol%; all significantly below 25% of the lower flammability limit (LFL) established as the operating threshold (1.0 vol%).

- Measured REDOX ($Fe^{2+}/\Sigma Fe$) values of the poured glass from both the Nitric-remediated and unremediated feeds were fully oxidized.

- Over time, the measured REDOX ($Fe^{2+}/\Sigma Fe$) values of the poured glass for the Glycolic-remediated feed were shown to drop from the maximum ~0.12 soon after melt pool turnover to zero by the end of steady state testing.

- Over time, the measured REDOX ($Fe^{2+}/\Sigma Fe$) values of the poured glass for the Bubbled Glycolic-remediated feed were shown to remain stable around ~0.05 for the entirety of testing (~24 hours) after bubbler initiation.

- Steady state conditions were achievable in the range of predicted, scaled operational targets for the SMRF platform.

Observations from testing with the MRF and SMRF platforms follow:

- Cold cap expansion and separation from the melt pool was drastically decreased in both platforms as the targeted REDOX value of the glass was raised.

- The air/water mister modification of the SMRF lid was sufficient to supply all necessary melter air and removed more than sufficient amounts of thermal energy to reach very low VS temperatures (<400°C).

- Measured REDOX ($Fe^{2+}/\Sigma Fe$) values from Nitric-remediated and unremediated glass produced in the MRF followed more closely to predicted values than those from the pour tube of the SMRF.

- Bridging between the melter sides and the chimney, bubblers, and thermocouples in the melter vapor space was significant at lower predicted REDOX feeds and affected transitions between steady state conditions and melt rates of the elevated cold cap.

Based on the SMRF testing observations and results, recommended items for future support of the offgas flammability modelling of the NG flowsheet are as follows:

- Testing and implementation of an *in situ* melt pool and/or pour stream REDOX probe(s) to track the progression of REDOX in the melt as a function of VS temperature, melt pool location, and residence time.

- Modification of the SMRF vessel construction to allow for a deeper melt pool for additional bubbling evaluations and reduced impact of cold cap expansion on the glass overflow chimney.

- Operation of the SMRF at DWPF nominal conditions for an extended period of time (up to 5 consecutive days) to achieve a singular steady state. Extended single steady state testing would deconvolute any effects that may have been due to varying the operating conditions as well as provide true melt rate analyses for the NG flowsheet feed.

TABLE OF CONTENTS

LIST OF TABLES

LIST OF FIGURES

LIST OF ABBREVIATIONS

AD	Analytical Development
CC_{Hot}	Closed Crucible - Hot insertion
CEF	Cold cap Evaluation Furnace
DAS	Data Acquisition System
DWPF	Defense Waste Processing Facility
ELN	Electronic Laboratory Notebook
fs	Full Scale
FTIR	Fourier-Transform Infrared Spectrometer
GC	Gas Chromatograph
gpm	Gallons per Minute
ICP-AES	Inductively Coupled Plasma – Atomic Emission Spectroscopy
in H_2O	Inches of Water
inwc	Inches of Water Column
kg	Kilogram
LFL	Lower Flammability Limit
lpm	Liters per Minute
mlpm	Milliliters per Minute
MRF	Melt Rate Furnace
MS	Mass Spectrometer
NG	Nitric-Glycolic
P&ID	Piping and Instrumentation Diagram
PPE	Personal Protective Equipment
psig	Pounds per Square Inch Gage
QMRF	Quartz Melt Rate Furnace
rdg	Reading
REDOX	Reduction/Oxidation; specifically the $Fe^{2+}/\Sigma Fe$ ratio
sccm	Standard Cubic Centimeters per Minute
scfm	Standard Cubic Feet per Minute
set pt	Set Point
slm	Standard Liters per Minute
SME	Slurry Mix Evaporator
SMRF	Slurry-fed Melt Rate Furnace
SRAT	Slurry Receipt and Adjustment Tank
SRNL	Savannah River National Laboratory
TOC	Total Organic Carbon
TTQAP	Task Technical and Quality Assurance Plan
TTR	Technical Task Request
W	Watts (power)

1.0 Introduction

The Savannah River National Laboratory (SRNL) was tasked to support validation of the Defense Waste Processing Facility (DWPF) melter offgas flammability model for the nitric-glycolic (NG) flowsheet. The work supports Deliverable 4 of the DWPF & Saltstone Facility Engineering Technical Task Request (TTR)[1] and is supplemental to the Cold Cap Evaluation Furnace (CEF) testing conducted in 2014.[2] The Slurry-fed Melt Rate Furnace (SMRF) was selected for the supplemental testing as it requires significantly less resources than the CEF and could provide a tool for more rapid analysis of melter feeds in the future. The SMRF platform has been used previously to evaluate melt rate behavior of DWPF glasses, but was modified to accommodate analysis of the offgas stream. Additionally, the Melt Rate Furnace (MRF) and Quartz Melt Rate Furnace (QMRF) were utilized for additional evaluations. MRF data was used exclusively for melt behavior observations and Reduction/Oxidation (REDOX) prediction comparisons and will be briefly discussed in conjunction with its support of the SMRF testing. The QMRF was operated similarly to the SMRF, but will be discussed in a separate future report. As discussed in the Task Technical and Quality Assurance Plan (TTQAP)[3], the overall objectives of the SMRF testing were to:

1) Evaluate the efficacy of the SMRF as a platform for steady state melter testing with continuous feeding and offgas analysis

2) Generate supplemental melter offgas flammability data to support the melter offgas flammability modelling effort for DWPF implementation of the NG flowsheet.

Due to the novel parameters under which the SMRF was going to be operated, a run plan and detailed R&D directions were written to describe the specific goals and tasks during testing.[4, 5] This report is intended to describe the operating conditions under which the SMRF was tested to support the first objective above. Selected analytical data will be presented as it is relevant to the scope of the discussion. In-depth discussion of offgas chemistry and melter flammability model applicability of the data produced from the SMRF as is applicable to the second objective will be detailed in a separate future melter offgas flammability report.

1.1 Quality Assurance

Requirements for performing reviews of technical reports and the extent of review are established in Manual E7 Procedure 2.60. SRNL documents the extent and type of review using the SRNL Technical Report Design Checklist contained in WSRC-IM-2002-00011, Rev. 2.

Details of various portions of the experiments are contained in the following Electronic Laboratory Notebooks (ELN):

- D. H. Miller, “Alt Reductant Melter Offgas Flammability”, ELN experiment T8786-00095-11.
- M. S. Williams, “Alt Reductant Melter Offgas Flammability – Volume 2”, ELN experiment I7770-00157-17.

2.0 System Description

Figure 2-1. Slurry-Fed Melt Rate Furnace Testing Equipment setup in and around walk-in hood located in 999-1W high bay.

2.1 Slurry-Fed Melt Rate Furnace

Figure 2-1 shows the complete setup in and around the walk-in hood of the 999-1W high bay.

2.1.1 Melter

The SMRF is designed to mimic the heat transfer characteristics of a large-scale joule-heated melter, which is accomplished by providing heat in one dimension through the bottom of an 8" diameter Inconel® 690 crucible using radiant heaters below the crucible. The sides of the crucible are insulated in the melt pool area to minimize radial heat transfer to or from the melt pool and heat exchange with the plenum. This directional heating melter configuration relies on convective and conductive heat transfer between the glass pool and cold cap. The heaters below the crucible were controlled by a thermocouple mounted on the bottom of the crucible and maintained a glass temperature of 1125°C throughout testing. Additional heating (separate from that supplied to the melt pool) is applied to the plenum above the melt pool through radiant heaters that surround the upper part of the crucible. The plenum heaters were controlled by a thermocouple inserted into the vapor space (VS) of the crucible. The melter has an overflow pour tube and a bottom drain tube, both inductively heated where they exit the insulated cabinet. The pour tube is an over flow design similar to the CEF that maintains a glass pool approximately 3.5" deep. A sketch of the SMRF is shown in Figure 2-2 with more in-depth diagrams of the entire system in Appendix A; detailed information pertaining to melter components is listed in Table A-1.

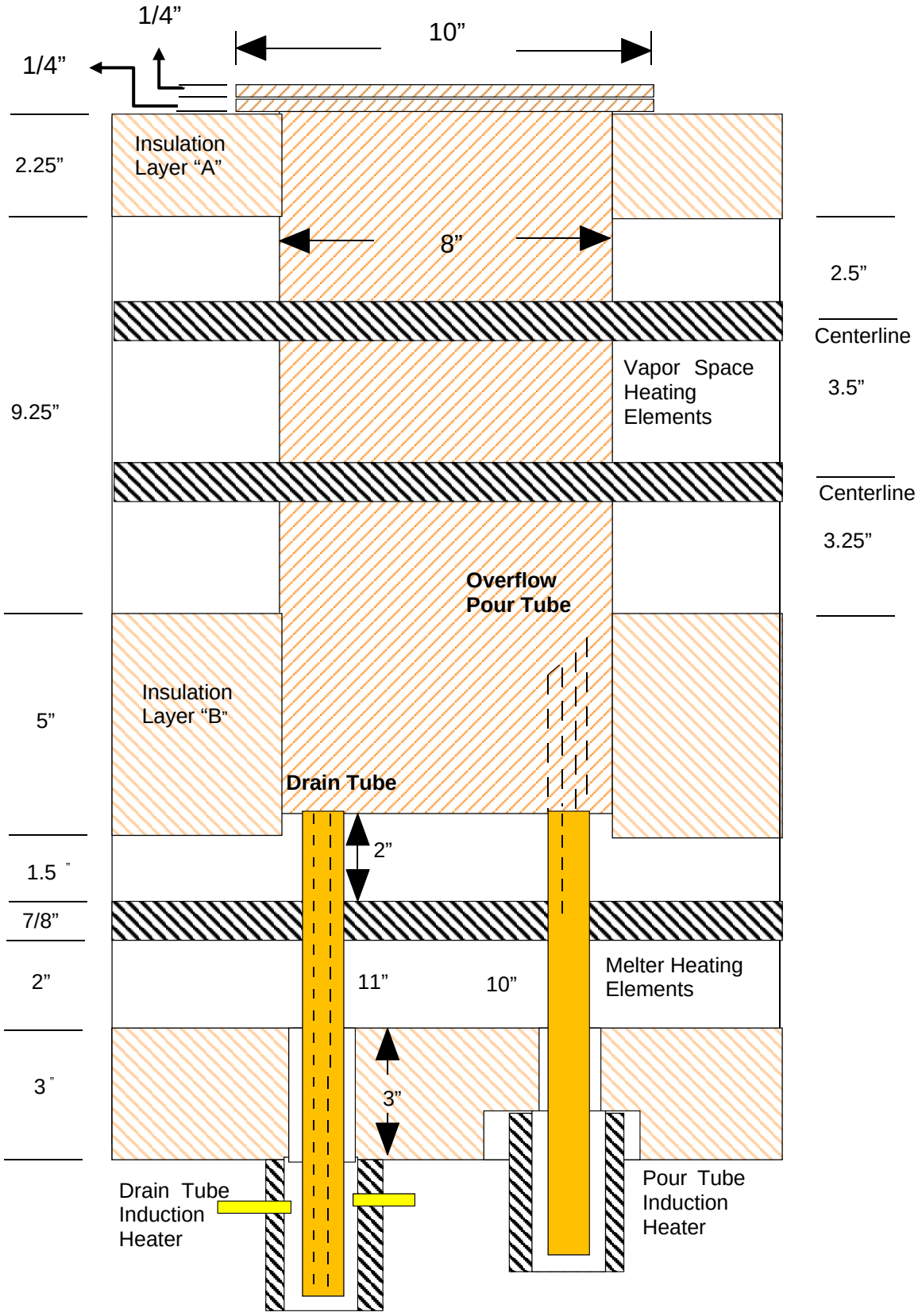

Figure 2-2. Slurry-Fed Melt Rate Furnace Section View

2.1.1.1 Melter Lid

Figure 2-3. Image of melter lid assembled inside walk-in hood.

A new Inconel® top (Figure 2-3) was fabricated for the SMRF to provide the option of operating at a slightly negative pressure and to allow an estimate of air inleakage. The top components are labelled in Figure 2-4 and a brief description is given below.

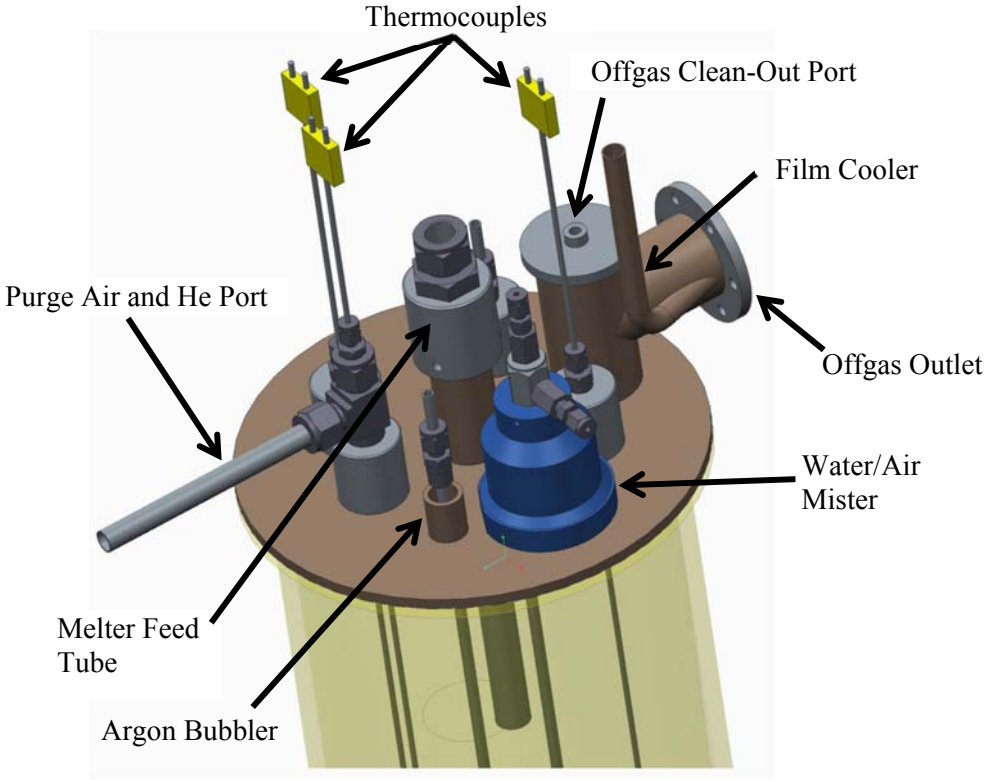

Figure 2-4. SMRF Lid Ports Diagram

In order to minimize the new load being carried by the melter flange, the top and offgas line components were counter balanced with a series of pulleys and weights.

2.1.1.2 Melter Lid Sealing

The new top sat on a ribbon of high temperature gasket material in an attempt to reduce air inleakage. The gasket was fabricated from a ¼" thick rope made of Thermicullite®, which is a high temperature woven fabric reinforced with Inconel® fibers. A thinner version of the rope material was wrapped around the melter top ports prior to sliding the top head components in place.

2.1.1.3 Argon Bubblers

The bubblers are 3/8" outer diameter Inconel® 600 tubing with a 0.049" wall. The closed end had a 1/8" hole drilled in one sidewall approximately ¼" from the end. The bubblers are located ¼" off the bottom of the melter with the hole pointing toward the center. As seen in Figure 2-5, the bubblers are 180˚ apart and approximately 1" from the crucible sidewall.

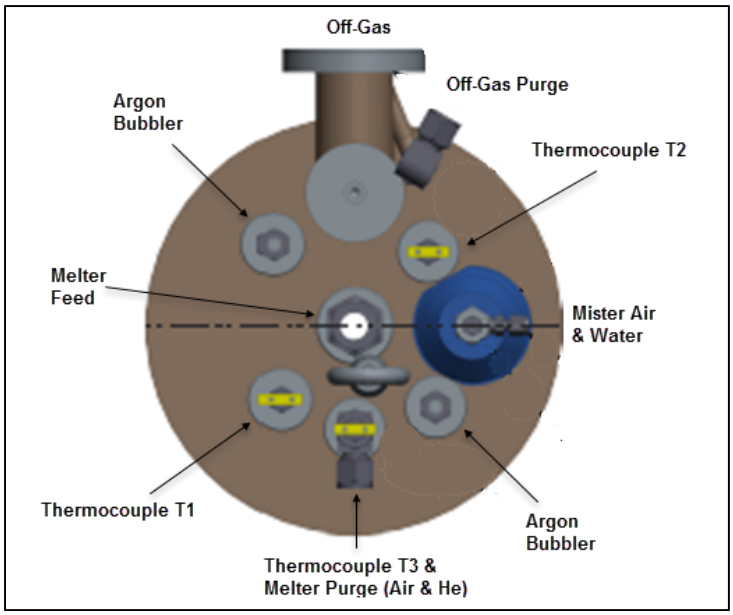

Figure 2-5. SMRF Lid Component Orientation Diagram

Two argon gas flow rates were used during testing. A minimum argon flow of 5 sccm (standard cubic centimeters per minute) per tube was maintained throughout the run for non-bubbled operations to ensure the tubes remained free of glass. A flow of 2356 sccm was used for bubbled operations.

2.1.1.4 Purge Air

The melter purge served as dilution air and also as a possible cooling source for low temperature testing. The purge was introduced into the vapor space through a top port located 180° from the offgas port. The same line was utilized for the addition of the He tracer gas employed in the inleakage calculations.

2.1.1.5 Offgas Port

The offgas port connects the melter to the offgas sampling and ventilation system. The 1-1/2" diameter pipe had a flanged end that connected to the jumper which tied the melter to the quencher/condensate tank assembly. A vertical clean out port, as part of the offgas port, covered with a quartz glass disk also served as a limited cold cap viewing port. A digital video camera was hung above the glass disk and used to record images and video of cold cap and feed dispersion behavior.

2.1.1.6 Film cooler

The offgas cooling air was introduced into the offgas line at the exit of the offgas port. The air inlet was not configured like a traditional slotted film cooler, but consisted of air being injected almost parallel to the vapor flow. This air source served to quickly reduce the exiting gas temperature without contributing to the reactions inside the melter.

2.1.1.7 Mister nozzle

The mister nozzle, utilizing an air/water mixture, produced a fine spray of water that served to cool the offgas without significantly increasing the required amount of air being sent through the system. The droplet size was dependent on water and air flows as well as pressure and was characterized outside the melter prior to operation. The water spray was designed to allow lower VS temperatures to be achieved and still operate within the capacity of the quencher/scrubber. A minimum air flow was maintained at all times to cool the nozzle tip, while water was only added to achieve the lowest temperature test conditions.

2.1.1.8 Helium tracer gas

Helium (He) was introduced into the melter through the air purge line. The helium served as a tracer gas to allow estimates of air inleakage. The helium flow was kept off during the majority of the testing to ensure accurate H_2 readings with the gas chromatograph (GC). Immediately before and after each steady state test condition, the helium flow was turned on to 600 sccm for approximately 5-10 minutes to provide inputs for inleakage calculations. The helium readings were allowed to stabilize on the mass spectrometer (MS) and the GC when starting and finishing a steady state condition.

2.1.1.9 Glass pool thermocouple

An Inconel® sheathed thermocouple, was inserted through the melter lid until the junction was ~1" off the floor of the melter. This measurement was used to give an indication of the glass pool temperature since the melter temperature was controlled by external thermocouples touching the outside wall of the vessel. This thermocouple also indicated movement of hot spots within the glass pool. The thermocouple was raised ~2" later in the run to better represent the lowest molten temperature zone, which would affect pour rates partially due to the intimate contact of the melt pool with the overflow pour tube chimney.

2.1.2 Melter Feed System

Figure 2-6. Image of melter feed system assembled outside of walk-in hood.

The SMRF feed system (Figure 2-6) consisted of an agitated feed tank sitting on a platform scale, a peristaltic feed pump, the melter feed tube assembly and a chiller to provide cooling water to the feed tube assembly; component configuration is diagramed in Figure 2-7.

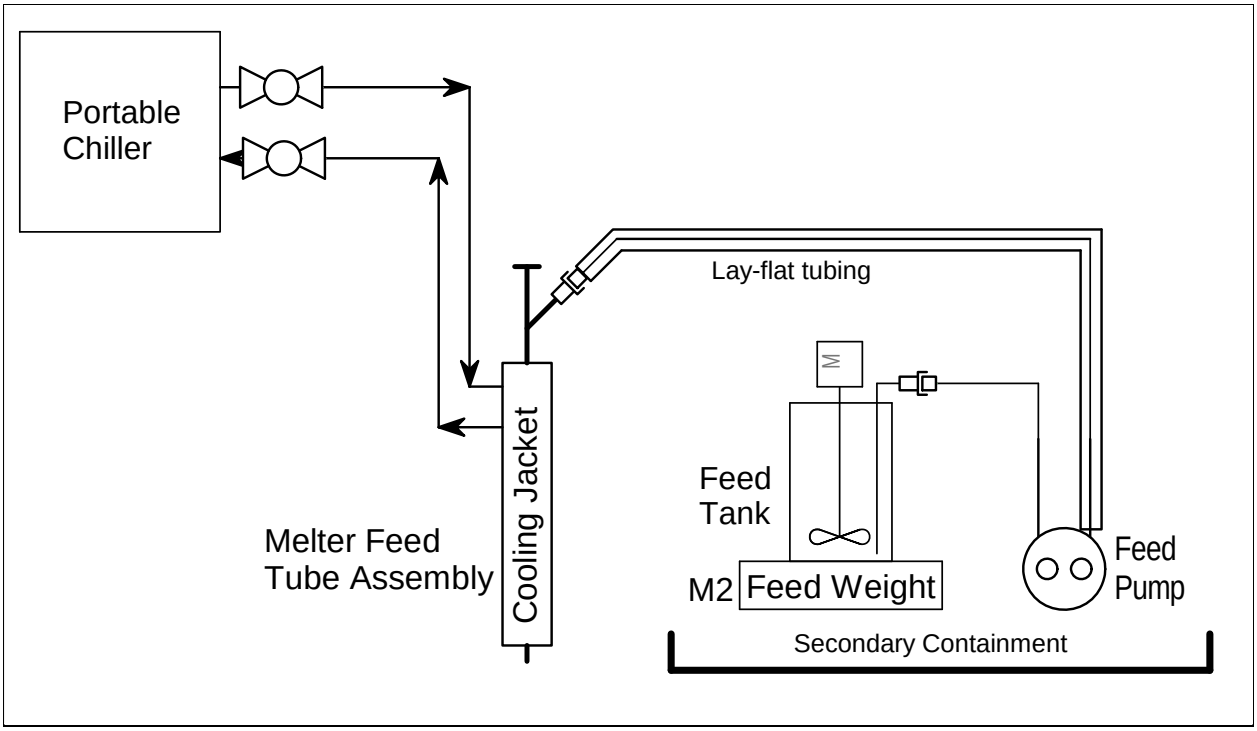

Figure 2-7. SMRF Feed System Diagram

The ~5 gallon stainless steel feed tank was agitated by a ¼ horsepower laboratory mixer using a 3" flat blade impeller. There were no baffles on the container. The agitator speed was controlled by the Data Acquisition System (DAS) and mixing speed was set visually. The speed of the mixer was such that there was minimal air entrainment in the slurry and when probed, minimal solids were felt settling out on the bottom of the pot. The melter feed tube assembly located in the center of the melter lid was constructed from a 3/8" Inconel® tube within a ¾" Inconel® tube chilled water jacket. Feed entered the assembly through a 45° angled branch near the top of the assembly. A removable cap at the top allowed for *in situ* cleaning of the feed tube. A 4.5 KW Neslab HX-150 chiller provided chilled water flow to the water jacket to cool the feed as it entered the melter.

The Master-Flex adjustable-speed peristaltic feed pump was controlled by the DAS. Master-Flex tygon tubing, size L-15, was used for the pump tubing. The tygon tubing ran from the feed inlet wand to the melter feed tube and was wrapped with plastic, "lay-flat" tubing for secondary containment in case of a leak or rupture. A modified fitting was used at the melter feed tube assembly to minimize the stretch of the tygon tubing and create a smooth flow path transition from the tygon to the fitting. The feed inlet wand was made from ¼" stainless steel tubing with the end crimped shut and multiple slots machined into the side above the crimp. The slots allowed feed into the wand and were positioned away from the direction of rotation (downstream side) of feed in the container. The tygon tubing was periodically repositioned in the pump head (moved towards the low pressure side) to relocate the wear spot created by the pump rollers and, on occasion, the entire length of tygon tubing was replaced.

2.1.3 Offgas Quencher & Condensate Circulation System

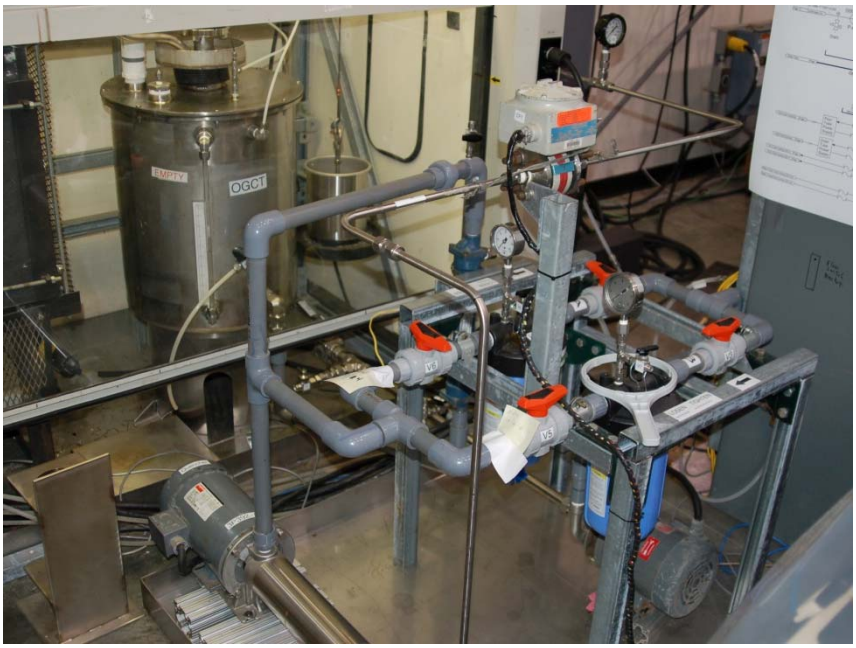

Figure 2-8. Image of Offgas Condensate circulation and filtration system assembled outside of walk-in hood.

The offgas quencher and condensate circulation system are pictured in Figure 2-8 and diagramed in Figure 2-9; the Piping and Instrumentation Diagram (P&ID) component labels are listed in Table A-1. Vapors from the melter were withdrawn using a 1-1/2" Shutte & Koerting gas quencher. The quencher was located at the end of the 2" offgas pipe on top of the condensate tank. The quencher sprayed water into the offgas stream to cool the vapors and remove particulates. The condensate tank was filled with ~10 gallons of water. The tank level was maintained by an overflow line on the side of the tank. Over-flowing condensate collected in a carboy sitting on a platform scale. Condensate samples were taken from this overflow line. The tank vented into the back of a laboratory hood through an in-tank demister (made of coarse stainless steel wool) and 90° nozzle on the lid.

Condensate tank fluid was circulated through a dual filter system using a centrifugal pump to remove particulates. The dual filter configuration provided a means of replacing a filter without stopping the circulation system. A secondary branch after the filters contained a multi-stage centrifugal pump to provide high pressure water flow to the quencher. Both pumps were Variable Frequency Drive (VFD) controlled to optimize pressure and flow in the circulation system and quencher. A heat exchanger in the circulation loop cooled the circulated fluid before it re-entered the condensate tank. The offgas quencher and condensate circulation system were equipped with temperature, pressure and flow instrumentation to monitor the performance of the system. The output of the instruments were recorded and displayed by the DAS.

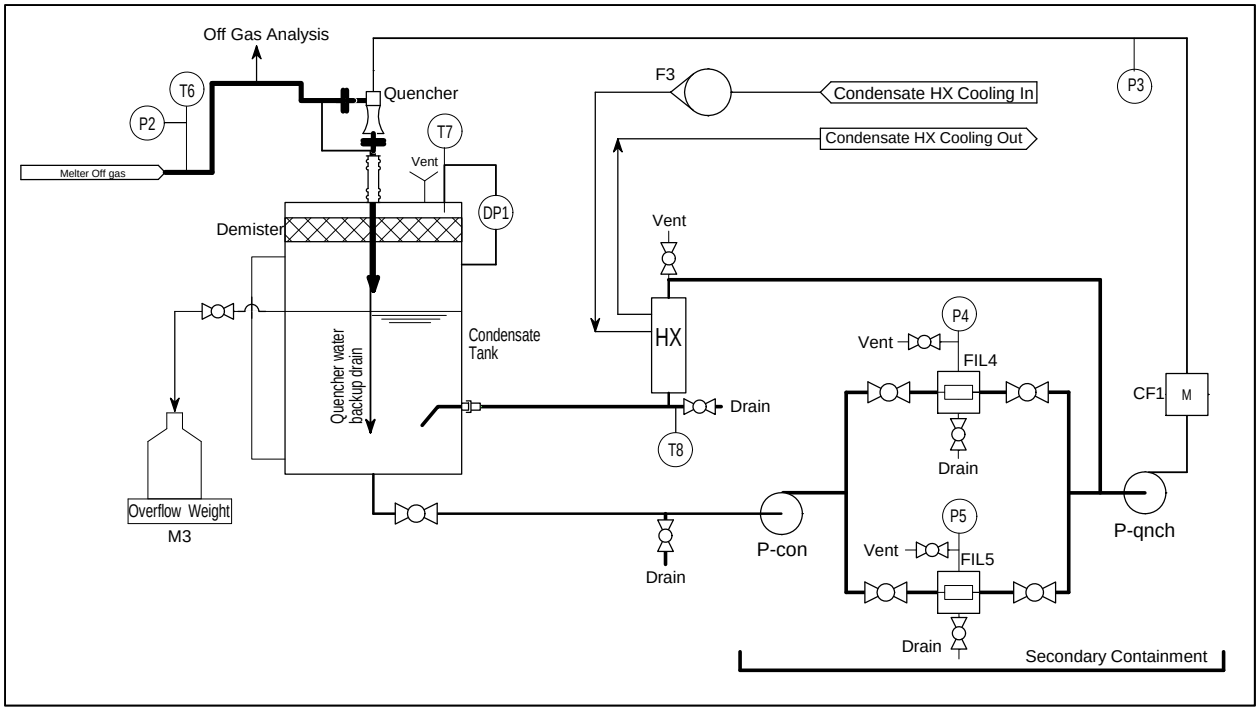

Figure 2-9. SMRF Offgas/Condensate Circulation System Diagram

Offgas analysis was performed by gas sampling from a line located in the offgas pipe between the melter offgas port and the offgas quencher. Vapors from the offgas pipe were drawn into the offgas sampling line, preconditioned, and analyzed by a GC, MS, and Fourier-transform infrared (FTIR) spectrometer.

2.1.4 Data Acquisition System

The DAS consisted of a PC using LabVIEW software provided by R&D Engineering in SRNL. The DAS recorded the output of SMRF instrumentation as well as operational data from the heater controls of the melter heaters. A list of SMRF instrumentation is shown in Table A-1. The DAS screen displayed data from the instrumentation and heaters (Figure A-4). The DAS provided on-screen control of the feed tank agitator speed, feed pump, and system gas flows. Visible and audible alarms on the DAS were associated with critical temperature and pressure readings in the melter and condensate tank as well as with the feed container scale.

2.2 System Checkout

Prior to the start of testing at temperature, each subsystem was checked to verify that it functioned properly. All instruments were successfully operated from the control computer. Alarms and interlocks were verified using simulated signals. Water runs were completed to verify the accuracy of the feed delivery system and weight scales. The data collection, graphing and storage systems were verified during the initial shakedown testing. The mister settings were determined by visually observing the mist produced over a range of air/water flow combinations. Operation of the DAS, computer-instrumentation interface, interlocks, and alarms were also verified.[6]

A performance curve was generated for the air inleakage by measuring the melter pressure over a range of melter air flows and quencher power outputs. The inleakage was measured using a helium tracer to compare the measured air flow to the known inputs. The inleakage was also estimated from the performance curve for the 1-1/2" scrubber using the known water pressures and flows.

The air inleakage into the melter was measured at room temperature before (●) and after (□) the entire testing operation. It was also measured at 400°C before (◇) operation during shakedown testing. The air inleakage in scfm (standard cubic feet per minute, with mass flow controller standard conditions of 70°F and 1 atm (atmospheres)) is plotted versus the melter pressure in Figure 2-10. Negative melter pressures were achieved by pulling a vacuum employing the offgas quencher. Positive melter pressures were achieved by having the purge air exceed the quencher vacuum capacity. These checks were performed to ensure that there would be no excessive, unaccountable offgas loss or dilution due to an overly leaky melter.

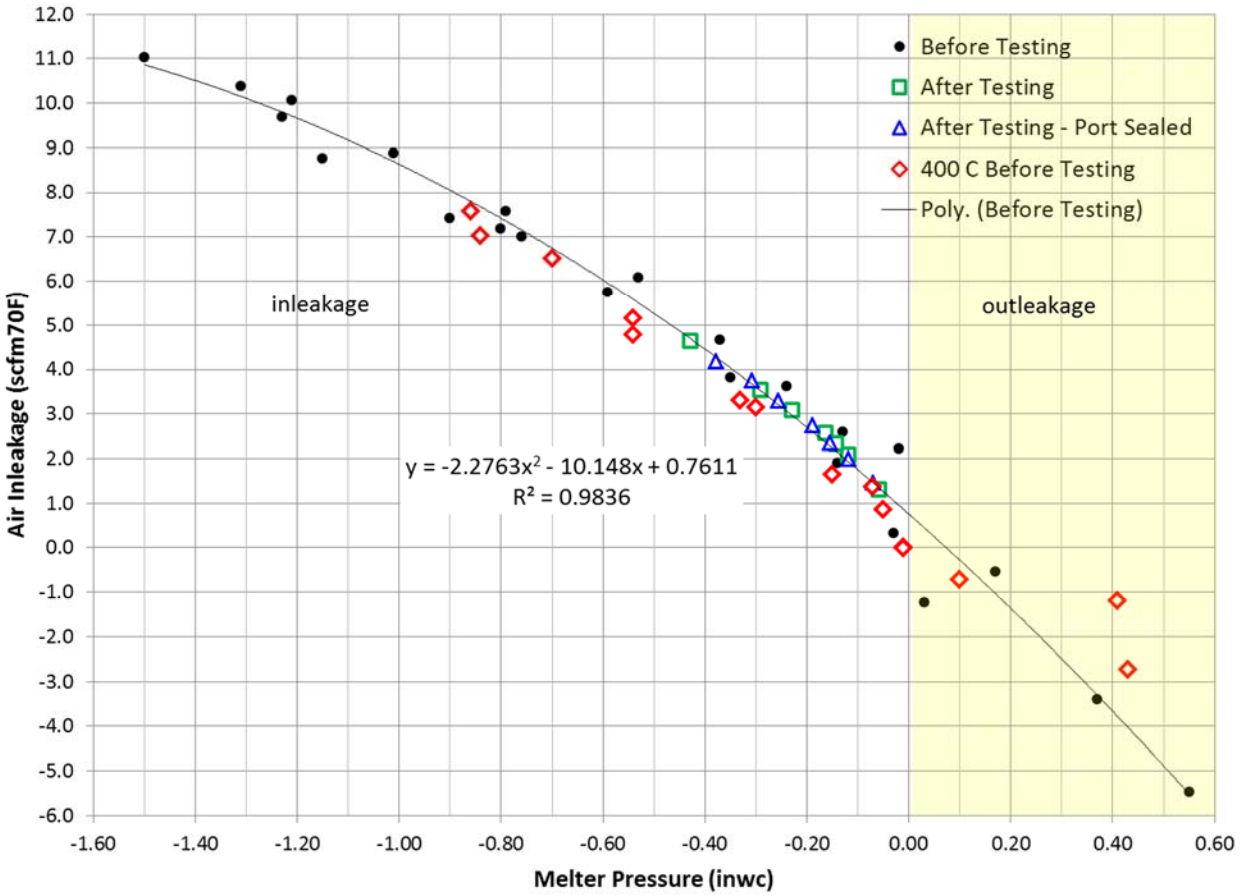

*inwc – inches of water column
*Poly. (Before Testing) – polynomial fit trend line to assist in visualizing trend

Figure 2-10. Melter Air In/Outleakage versus Melter Pressure Testing

In the negative pressure region of Figure 2-10, the air inleakage at 400°C (◇) appears to have been slightly less than at room temperature (● and □), as visualized by all the red diamonds being below the trend line. After melter testing was completed, it was suspected that air inleakage could be occurring at the cap on the offgas line after the film cooler air was added based on energy balance calculations. This port was sealed securely with high vacuum grease and the air inleakage versus vacuum was again measured (Δ). The results showed that there was most likely no significant air inleakage at this location. As compared to the CEF, the overall inleakage was slightly higher, but accountable due to the use of the He tracer gas measurements before and after steady state conditions.

2.3 Modifications

Modifications were made to the melter feed system, the melter feed, and the induction heating power supplies based on initial complications encountered.

2.3.1 Feed System

After experiencing multiple feed stoppages due to plugs in the system, the entire feed system was reviewed and several enhancements were made. The overall weight percent (wt.%) total solids was reduced from ~49% to ~42% by the addition of water to each carboy. Also, all carboys were poured through a mesh screen to remove any large particles.

The type of tubing used in the peristaltic pumps was also changed; a stiffer material was chosen for both its rupture resistance and pumping efficiency. Testing with the addition of a screening basket to the suction tube was performed and later deemed excessive to the standard slotted suction tube due to the prescreening of each carboy. A larger diameter agitator was added to the feed tank to improve the mixing and suspension of solids in the tank. The 9" diameter pitched blade agitator, pictured in Figure 2-11, replaced the ~3" diameter flat blade impeller to cover more of the interior surface of the feed tank bottom and alter the shape of the mixing vortex.

Figure 2-11. Image of large, pitched blade agitator and slotted feed suction tube modifications assembled outside walk-in hood

Additionally, the outer diameter of the stainless steel suction tube where connected to the flexible rubber tubing was mechanically reduced by thinning the tube wall thickness. This size reduction was performed to attempt to decrease stress on the rubber due to stretching over a similarly sized rigid tube. Special crimps were used rather than hose clamps to secure the connection without deforming or scoring the rubber tubing. A Swagelok connector welded to stainless steel tubing with a reduced wall thickness was used to attach the discharge end of the flexible tubing to the melter feed tube. Crimp connectors were also used at this junction.

The feed line was positioned to provide a gradual elevation increase from the pump discharge to the melter feed tube. This configuration was done to minimize low spots that might promote settling of melter feed components. The discharge tubing was longer than needed to allow periodic repositioning of the section under the pump rotor. The excess was coiled around a large cylinder to maintain the gradual

elevation increase. Clear, lay flat tubing covered the entire length of the flexible tubing with the exception of the portion inside the pump guard. The ends of the lay flat tubing were secured with tape to provide secondary containment in the event of a rupture

2.3.2 Camera

A small digital color camera along with a recording device were added to the system to allow both still images and video to be taken of the melter plenum at various stages during the testing. Direct observations of the cold cap, feed, and melter components were permitted through the offgas clean out port and water/air mister port. A mount was added directly over the offgas clean out port so the camera could be held in place directly over a quartz disc that covered the opening. The clock on the recording device was synchronized to the control computer to provide real time information when reviewing the images.

Occasionally the camera was held over the mister port which provided a clearer image of the cold cap under the feed tube discharge. This could only be accomplished during non-steady state conditions to prevent changing the vapor space conditions. Typical images (externally illuminated) of the melter interior from these two locations are shown in Figure 2-12.

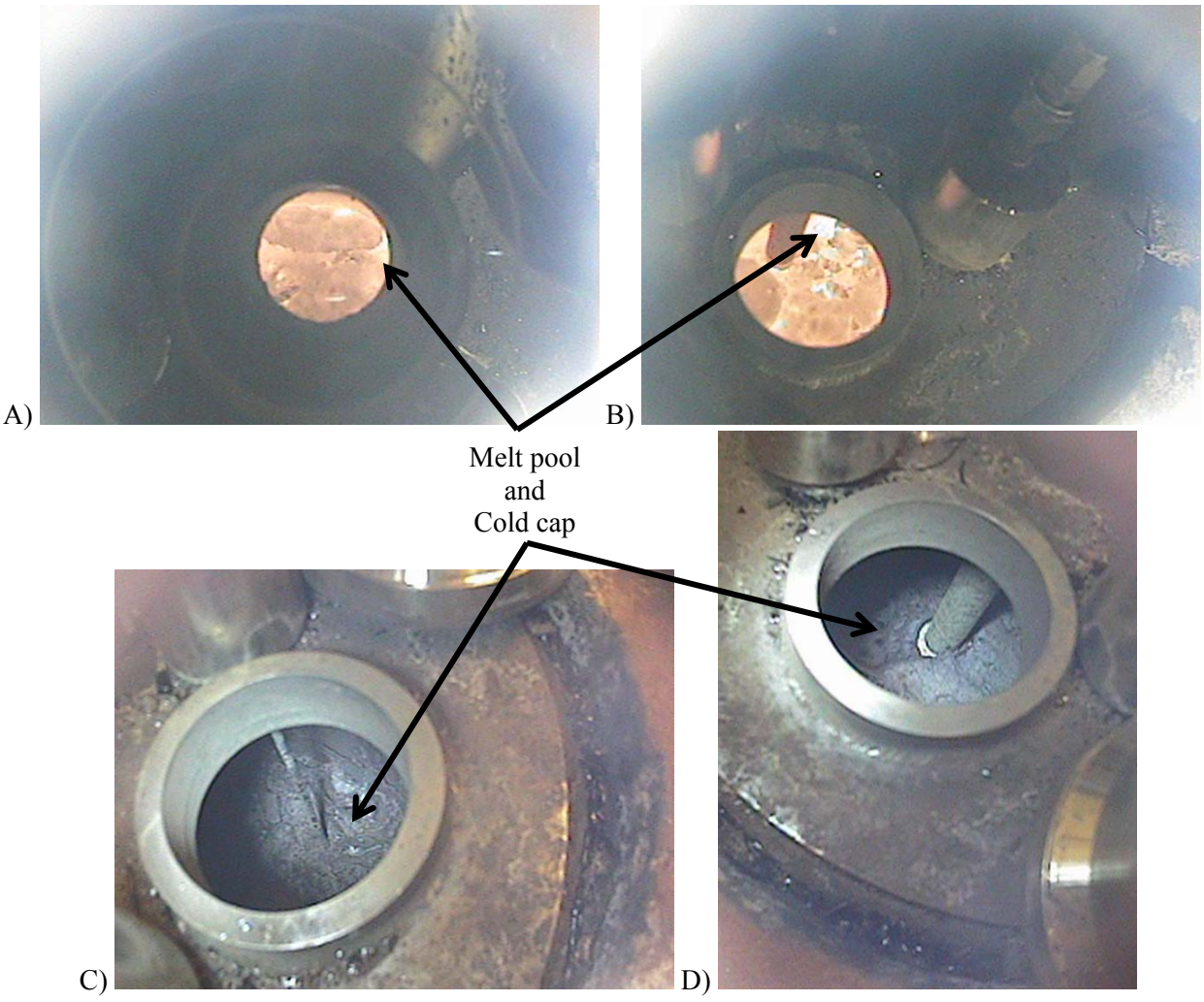

Figure 2-12. Typical images (externally illuminated) from the offgas port (A) and mister port (B, C, and D).

The offgas port was appropriate for viewing the cold cap in relation to the edge of the melter to help in determining cold cap coverage. Viewing through the mister port was utilized to observe the cold cap in relation to the feed tube and pour tube chimney. Both ports provided views of the bubblers to examine cold cap effects as a function of bubbler activity.

2.3.3 Induction power supply

During the initial SMRF testing, the 3kW induction heater on the drain tube heater failed to tune properly prior to shutdown of the melter. The induction heater on the pour tube heater was transferred to the drain tube heater to allow for shutdown and draining of the melter and a replacement for the pour tube heater was put in place. A spare 5kW power supply was identified as a suitable replacement and subsequent testing demonstrated successful tuning to the pour tube. Though both power supplies were not used at the same time, having two separate, functional power supplies aided in smooth operation of the induction heaters of the melter. The original (left) and replacement (right) controllers are shown in Figure 2-13.

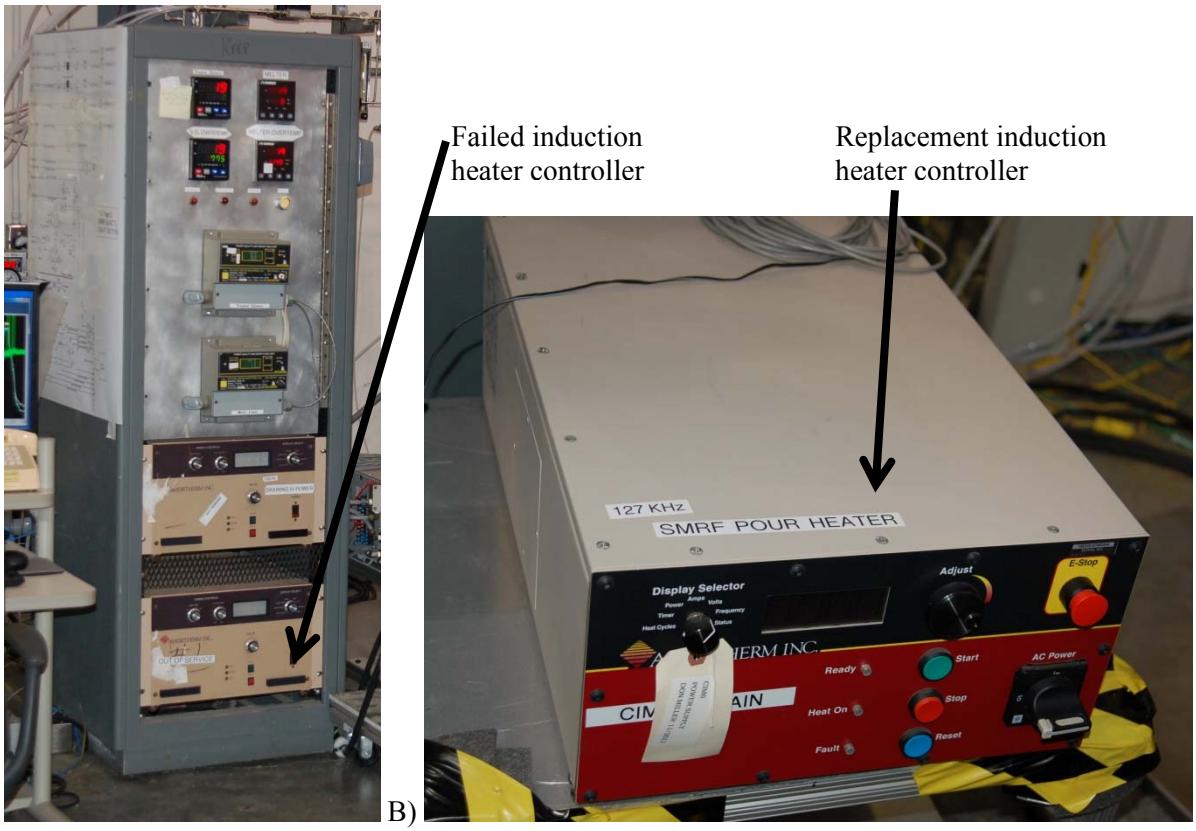

Figure 2-13. A) SMRF Heaters Control Cabinet and B) Replacement Pour Tube Induction Heater Controller

3.0 Experimental Procedure

3.1 Feed Preparation

The melter feed utilized in this testing was based on 100% acid stoichiometry Sludge Batch 6 (SB6I) Sludge Receipt and Adjustment Tank (SRAT) product and was initially developed for CEF Phase 2 testing in 2014.[2] The frit added to the sludge was composition Frit 418[7] and was loaded at a 36% waste

loading.[a][8] Carboys were individually loaded with sludge and frit and remediated with water and/or acid. Remediations consisted of adding water to all carboys to decrease the weight percent total solids and acids to some to produce two additional melter feeds. The total solids were reduced from ~49 wt.% to ~42 wt.% for each prepared carboy based on analysis of each as they were prepared. Nitric acid (designated Nitric-remediated) or glycolic acid (designated Glycolic-remediated) were added to adjust the predicted REDOX ratio targets of the final glass products. REDOX values were predicted using the Interim REDOX model incorporating the glycolate and antifoam terms.[9] The remediations were performed to produce feeds that would expand the range of testing above and below the typical operating range of feed REDOX values. Glasses were prepared to verify the REDOX values for each remediation utilizing the Closed Crucible Hot Insertion (CC_{Hot}) and MRF methods. The CC_{Hot} method for glass production followed that detailed in the REDOX procedure[10] while glasses prepared via the MRF were vitrified according to ITS-WI-0067[11] utilizing 4" diameter stainless steel beakers. The predicted and measured REDOX values for the feed verification are listed in Table 3-1.

Table 3-1. SMRF Feed REDOX Analyses.

Melter Feed Remediation	Predicted $Fe^{2+}/\Sigma Fe$	CC_{Hot} Measured $Fe^{2+}/\Sigma Fe$	MRF Measured $Fe^{2+}/\Sigma Fe$
Nitric-remediated	0.03	0.04	0.07
Unremediated	0.16	0.14	0.20
Glycolic-remediated	0.27	0.47	0.59

Each carboy was mixed for ~30 minutes prior to transfer into the feed tank. Details of the compositions of each batch of melter feed are listed in Appendix B.

3.2 Initial Startup

For initial startup of the SMRF, the vessel was charged with ~7kg of cullet from the 2014 CEF Phase 2 experiment. This cullet represented glass made from the Nitric-remediated NG flowsheet feed that was utilized during the 2014 CEF Phase 2 testing and the first feed to be employed in this testing. Once loaded, the melter was ramped to 1125°C and the VS heaters were set to 750°C in automatic mode. After arriving at operational temperature, the melter was allowed to soak and stabilize for ~2 hours. Once stable, feeding was initiated at a high rate (~40 grams/min) to fill the feed line and build the initial cold cap. After the cold cap was established by observing the drop in VS temperature and visually noting the melt pool surface coverage through the viewing ports, the feed rate and VS heater (in manual mode) were reduced to the target conditions. The first 24 hours of the initial operation were utilized to turn over the melt pool contents from the loaded cullet to the added feed and establish operational guides for actual performance of the melter under the modified running conditions (i.e. continuous feeding and offgas sampling). Subsequent melter startups followed the same process, but used SMRF glass produced during the previous run as the starting cullet.

3.3 Testing Conditions

Table 3-2 summarizes the target testing conditions for each of the feeds employed. The testing conditions progressed through the target VS temperatures from highest to lowest after each feed turnover period. The VS heater power outputs and feed rate targets were based on conditions observed in the CEF-2 2014 testing; the actual power outputs and feed rates observed resulted from evaluations of the cold cap through the various view ports and the stability of the achieved VS temperatures. The various VS temperatures were evaluated in order to support melter offgas flammability modeling validation.

[a] Viscosity of the target melter feed composition at 1150°C was predicted using the THERMO® calculation. The predicted viscosity was within 40-60 poise; therefore, no viscosity remediation (i.e. addition of $LiBO_2$) was necessary.

Table 3-2. Summary of Target Steady State Testing Conditions

Feed Remediation	Target VS Temperatures (°C)	Target VS Heater Power Outputs (W, %)	Target Feed Rates (grams/min)	Target Mister Water Flow (rotameter units)
Nitric-remediated	650, 550, 450, 350, <300	3000 (75%), 2000 (50%), 1000 (25%), 600 (15%), 0 (0%)	17, 14, 11, 8, 5	0, 0, 0, 0, 10
Unremediated (as-received)				
Glycolic-remediated				

The three feed remediations were utilized to correlate with the CEF-2 2014 testing (nitric remediation) and to provide a wide range of feeds with respect to predicted glass REDOX values (Table 3-1). The only feed that was operated under bubbling conditions[b] was the Glycolic-remediated feed.

3.3.1 Steady State Test Conditions

During testing, the desired steady state condition for the melter was controlled by the following parameters:

- Vapor space temperature (±25°C)
- Feed rate (±1 gram/min)
- Offgas readings (±15%)
- Cold cap coverage
- Melter vessel air purge (±15%)

The variables were adjusted to approach a steady state condition aimed at each of the target VS temperatures. Once an optimized combination of each variable for each steady state was determined, an attempt was made to maintain the steady state for a time period between one and two hours. Plots in Appendix E display the periods denoted as steady states, in terms of VS temperatures and heater power outputs, in the larger context of each feed run.

3.3.2 Sampling and Analyses

Samples were pulled during the course of testing on regular intervals for the analysis of glass composition, glass REDOX, melter feed composition, and condensate composition along with the constant analysis of the offgas composition. Analyses of each sample type pulled are detailed in the associated appendices.

Melter feed slurry samples were pulled directly from the stirred melter feed tank approximately 10 minutes after each feed addition to the pot. This sampling method ensured that the sample was well mixed and represented what was actually being fed to the melter at that time. A condensate sample was taken at the offgas condensate tank overflow line every four hours or as condensate was available.[c] Melter feed samples and condensate samples were analyzed for cations, anions, weight percent solids, pH, and density.[12-20] Samples of melter feed were also submitted to the Analytical Development (AD) laboratory and the DWPF laboratory for comparative total organic carbon (TOC) measurements.[20] Melter feed compositional analyses are detailed in Appendix B and details of the condensate analyses are listed in Appendix C.

[b] "Bubbling conditions" refers to the bubblers operating at scaled flows typical of DWPF; a minimum flow of argon was run through the bubblers at all other times during testing to keep the bubblers clear of glass.

[c] Condensate production was slow during some portions of testing making sampling frequencies greater than four hours in some situations while waiting for sufficient condensate to accumulate.

Condensate recirculation filters were collected and dried to be analyzed for entrained solids. Due to the lack of significant solids present in the filters, these were not analyzed beyond acquiring dried weights.

Glass samples were taken directly from the pour tube or the drain pans under the SMRF every two hours. Often the glass would form a droplet and come off the end of the pour tube intermittently. In those cases, the droplet was collected as the sample as opposed to waiting for a constant stream to fill the collection cup. Compositions of select glass samples were determined by Inductively Coupled Plasma – Atomic Emission Spectroscopy (ICP-AES) and the $Fe^{2+}/\Sigma Fe$ ratio was determined utilizing UV/Vis spectroscopy.[21,12] Detailed glass analyses are shown in Appendix D

The offgas composition was constantly analyzed via GC, MS, and FTIR. The time frames for each analysis were ~4 minutes for the GC, ~16 seconds for FTIR, and ~7 seconds for MS. Various species are analyzed with each instrument with some redundancies to ensure accurate measurements (Table 3-3). Detailed offgas analyses for each species monitored are listed in Appendix F.

Table 3-3. Offgas Speciation by Instrumentation

Offgas Species	GC	MS	FTIR
H_2	X	X	
He	X	X	
CO			X
CO_2	X	X	X
O_2	X	X	
N_2	X	X	
N_2O	X		X
NO		X	X
NO_2		X	X
Ar		X	

The GC was calibrated using a standard calibration gas containing He, H_2, O_2, N_2, CO_2 and N_2O. The calibration was verified prior to the initiation of each melter startup and checked with room air. Concentrations of N_2 and O_2 measured in air before and after testing were used to perform linear interpolation corrections of the data. The introduction of tracer He gas before and after steady states allowed for continual in/out leakage calculations while not masking the H_2 reading during the steady state as the He and H_2 elution times in the GC are very close.

The MS was calibrated using a series of cylinders of standard calibration gas mixtures. Each gas mixture was National Institute of Standards and Technology (NIST) traceable and the certificates of analysis are reported in the associated electronic laboratory notebook (ELN).[d]

The FTIR uses internal calibration spectra to generate concentration data; the uncertainty of each analysis is based on the accuracy of the calibration setup and the interferences of overlapping analytes.

4.0 Results and Discussion

4.1 Melter Operations and Steady State Conditions

Melter operations were performed according to the target conditions (Table 3-2) with minor alterations required while running. The feed rates estimated from the 2014 CEF testing gave good starting points to approach steady state conditions.

[d] Documentation for MS calibration gases is in the electronic laboratory notebook T7909-00035-02.

During the first wave of testing with the Nitric-remediated feed the targets were more drastically missed based on incorrect observations of the cold cap behavior. Only minor deviations were required to produce stable cold caps and VS temperatures for most other tests. Overfeeding occurred, as can be observed by comparing the actual feed rates (Table 4-1) to the predicted feed rates (Table 3-2) for the first two steady states. This resulted in the third steady state being in a state of underfeeding as the cold cap was still oversized from the first two overfed data points. Similar observations can be made concerning the VS heater power as additional power had to be supplied to the melter to overcome the excess cooling produced from the overfeeding. Lessons learned from this testing resulted in more linear extrapolations of feeding and heating data for the next three series.

Down to ~450°C, the VS temperature was controlled by adjusting the power output to the VS heaters. In the CEF testing, lower temperatures were achieved by adding additional purge air. However, the addition of the air/water mister to the SMRF allowed for the lowest VS temperatures to be achieved without the addition of excess purge air diluting low concentration analytes (i.e. hydrogen). As the VS heater power was reduced to zero watts, a minimum VS temperature was maintained due to heating from the melt pool. The addition of the water mist was sufficient to reduce the temperature of the vapor space gases to the lowest target points. Additionally, the thermodynamics of this process made the VS temperature control very stable. The mister needed to be used only at the very lowest temperatures where the carry-over heat from the melter had to be overcome, or when the bubblers were at scaled bubbling rates and the bubbles carried hot gas from the melt pool into the vapor.

Table 4-1 through Table 4-4 details the steady state conditions for each feed/test; graphical figures are in Appendix E.

Table 4-1. Nitric-Remediated Steady State Conditions.

Average Actual Steady State Temp. (°C)	Average Vapor Space Heater Power Output (W)	Average Steady State Feed rate (g/min)	Average Water Mister Flow (rotameter units)
628	3200	38	0
496	2400	30	0
381	710	12	0
238	0	11	10

Table 4-2. Unremediated Steady State Conditions.

Average Actual Steady State Temp. (°C)	Average Vapor Space Heater Power Output (W)	Average Steady State Feed rate (g/min)	Average Water Mister Flow (rotameter units)
606	2850	24	0
501	1990	22	0
432	950	13	0
321	450	10	0
222	0	7	16

Table 4-3. Glycolic-Remediated Steady State Conditions.

Average Actual Steady State Temp. (°C)	Average Vapor Space Heater Power Output (W)	Average Steady State Feed rate (g/min)	Average Water Mister Flow (rotameter units)
616	2650	22	0
529	1800	18	0
421	1000	11	0
324	330	10	0
208	0	6.5	23

Table 4-4. Bubbled Glycolic-Remediated Steady State Conditions.

Average Actual Steady State Temp. (°C)	Average Vapor Space Heater Power Output (W)	Average Steady State Feed rate (g/min)	Average Water Mister Flow (rotameter units)
641	1620	25	0
499	720	21	0
364	0	13	18
239	0	7	36

Along with observations of temperature and power stability, steady states were verified based on cold cap observations. Figure 4-1 A) thru D) show the various stages of cold cap coverage from initial building through complete coverage.

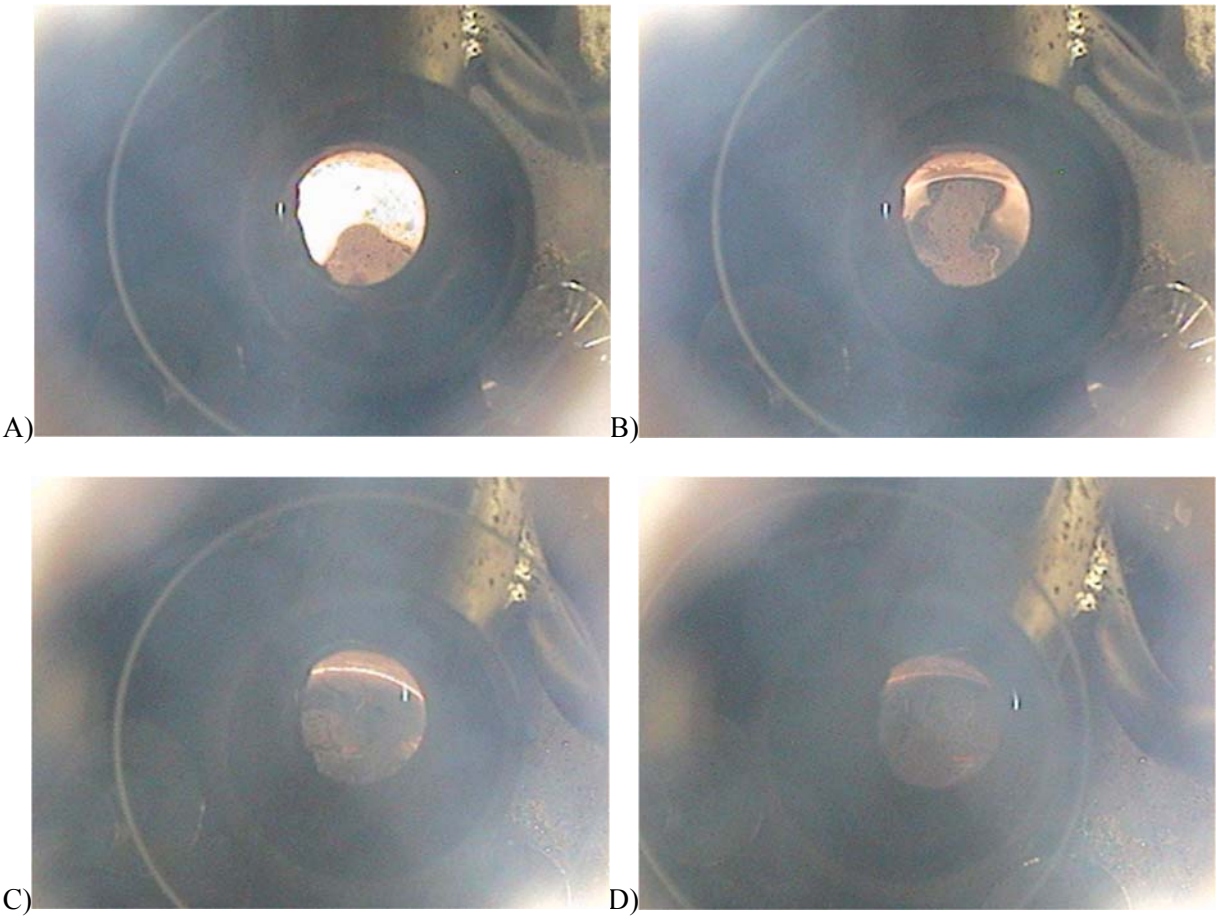

Figure 4-1. Views from the offgas port of A) initial cold cap formation, B) continued cold cap building, C) near complete cold cap coverage, and D) a steady state cold cap.

The cold cap was observed to excessively build during times of feeding material at low VS temperatures and low feed rates. Without sufficient energy from the VS heaters to assist melting the feed, the only source of energy was the melt pool. To compound the situation, offgas-related expansion and bridging of the cold cap was observed when feeding material with a low predicted REDOX value (<0.15 predicted $Fe^{2+}/\Sigma Fe$ ratio). Significant offgasing in the cold cap and at the cold cap-melt pool interface caused separation of the cold cap from the main heat source during low VS temperature conditions. Offgas within the cold cap produced a foamy cold cap that expanded up to and some times over the top of the pour tube chimney. The crust periodically bridged the gap between the vessel walls and the chimney, bubblers, or thermocouples extending through the vapor space. Bridging suspended the cold cap as the melt pool dropped away due to pouring. This caused separation between the cold cap and the melt pool slowing the conversion of feed to glass.

To eliminate the bridged or excess cold cap that would build during these periods of testing, between some steady states the melter vapor space was reheated to ~750°C. This reheating of the melter vapor space would soften the dried cold cap, allowing it to rejoin the melt pool. However, this also exposed the top of the melt pool to the purge air. This exposure of the melt pool to the purge air without the buffering factor of the cold cap is a possible contributor to the overly oxidizing environment within the melter. As the feed REDOX increased, the cold cap behavior became much more stable and responsive to adjustments.

The addition of bubbling to the melt pool did not add any significant complications to operations. The bubbles were observed through the cold cap even as the VS temperature was reduced and the cold cap became more viscous. The bubbling did not result in foaming of the cold cap or separation of the cold cap from the melt pool. Instead, the bubbles helped move hot glass from the bottom of the melt pool to the cold cap, improving connection with and melting of the feed material. This effect can be easily seen when visually comparing the glass pour rates of the unbubbled and bubbled feeds during their respective steady state regions.

As seen in Figure 4-2, as the melter vapor space approached lower and lower temperatures, the unbubbled glass ceased to pour whereas the bubbled glass maintained positive pour rates. The graph plots the glass pan weight of the SMRF as a function of time through the various steady state conditions. The left portion of the graph is the unbubbled Glycolic-remediated testing; the right portion is the bubbled testing. Within each section, the glass pan weights of each steady state vapor space are highlighted and fit with a linear trend line. The slopes of the trend lines relate to the glass pour rates in approximate grams per hour. Each section's label corresponds to the average VS temperature of that specific steady state region. The slope of each trend line shows that the unbubbled testing resulted in slower and slower pour rates (trend lines closer to slope 0 grams per hour) as the VS temperature decreased. On the other hand, the bubbled testing trend line slopes remained high (significantly positive number of grams per hour) translating to continued high pour rates.

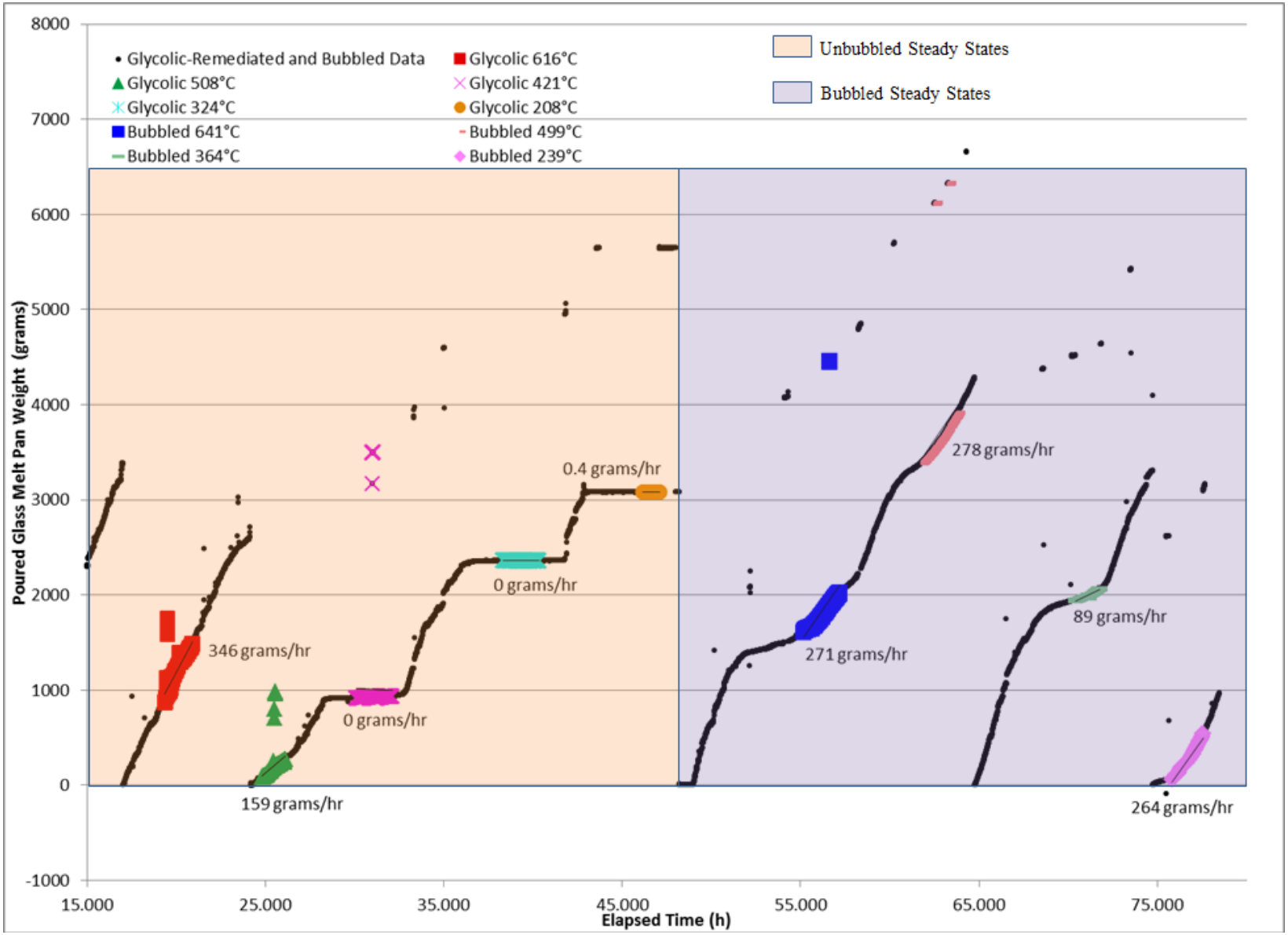

Figure 4-2. Poured Glass Pan Weight for Glycolic-remediated Unbubbled and Bubbled Steady State Tests

4.2 Offgas Compositions

The composition of the offgas was continually recorded by GC, MS, and FTIR. The addition of a trace amount of helium gas before and after each steady state period allowed for the tracking of purge gas and out/inleakage dilution effects. The species of interest and method of analysis are listed in Table 3-3.

A general overview of the offgas analysis for this testing is presented here; a discussion of the relation of the offgas to the melter flammability calculations and modelling will be presented in a separate future melter offgas flammability report. Since flammability is the major concern of this testing, H_2 will be the focus of this discussion; offgas concentration analyses as a function of run time are displayed in Appendix F for each monitored species. The concentration of each species was normalized to the offgas flow as determined by the helium tracer.

The main components of the flammability concern within the melter are hydrogen and carbon monoxide (CO). The goal is to remain below 25% of the lower flammability limit (LFL) for each species. The LFL for hydrogen is 4 vol%; therefore, the objective of this testing was to remain below 1 vol% hydrogen in the melter offgas. For CO, the LFL is 12.5 vol% making the limit for this testing just over 3 vol%. Figure 4-3 thru Figure 4-6 display the observed hydrogen in the offgas for each of the three feeds and bubbled testing along with helium readings to aid in delineating the accepted steady state regions; CO concentration together with hydrogen concentration observed during steady states of each feed and bubbling are presented in Figure F-3, Figure F-4, Figure F-17, Figure F-18, Figure F-30, and Figure F-37. The accepted steady state regions are highlighted.

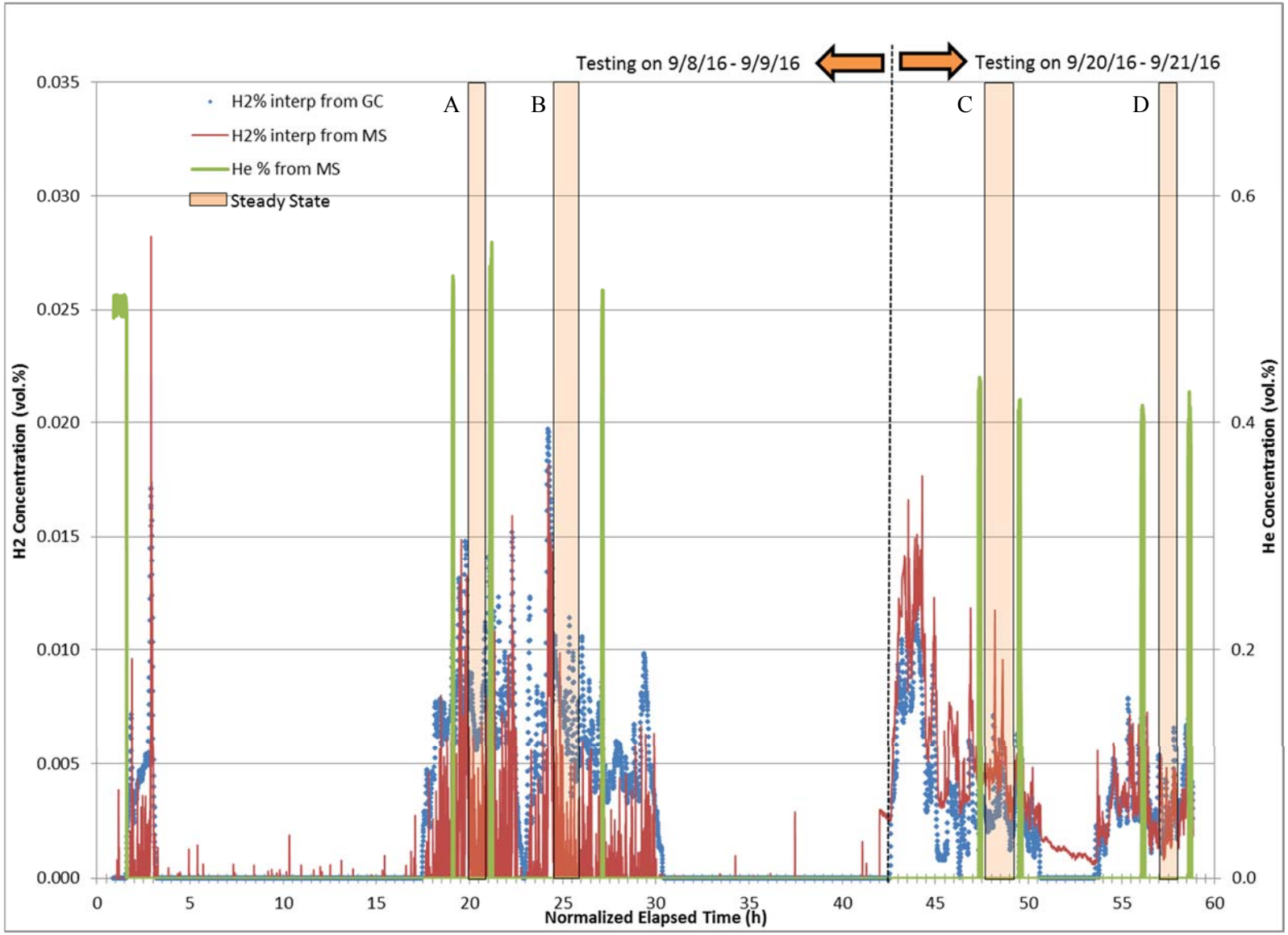

Figure 4-3. Nitric-Remediated Feed – H_2% and He%. Steady State Temperatures (°C): A) 628, B) 496, C) 381, and D) 238.

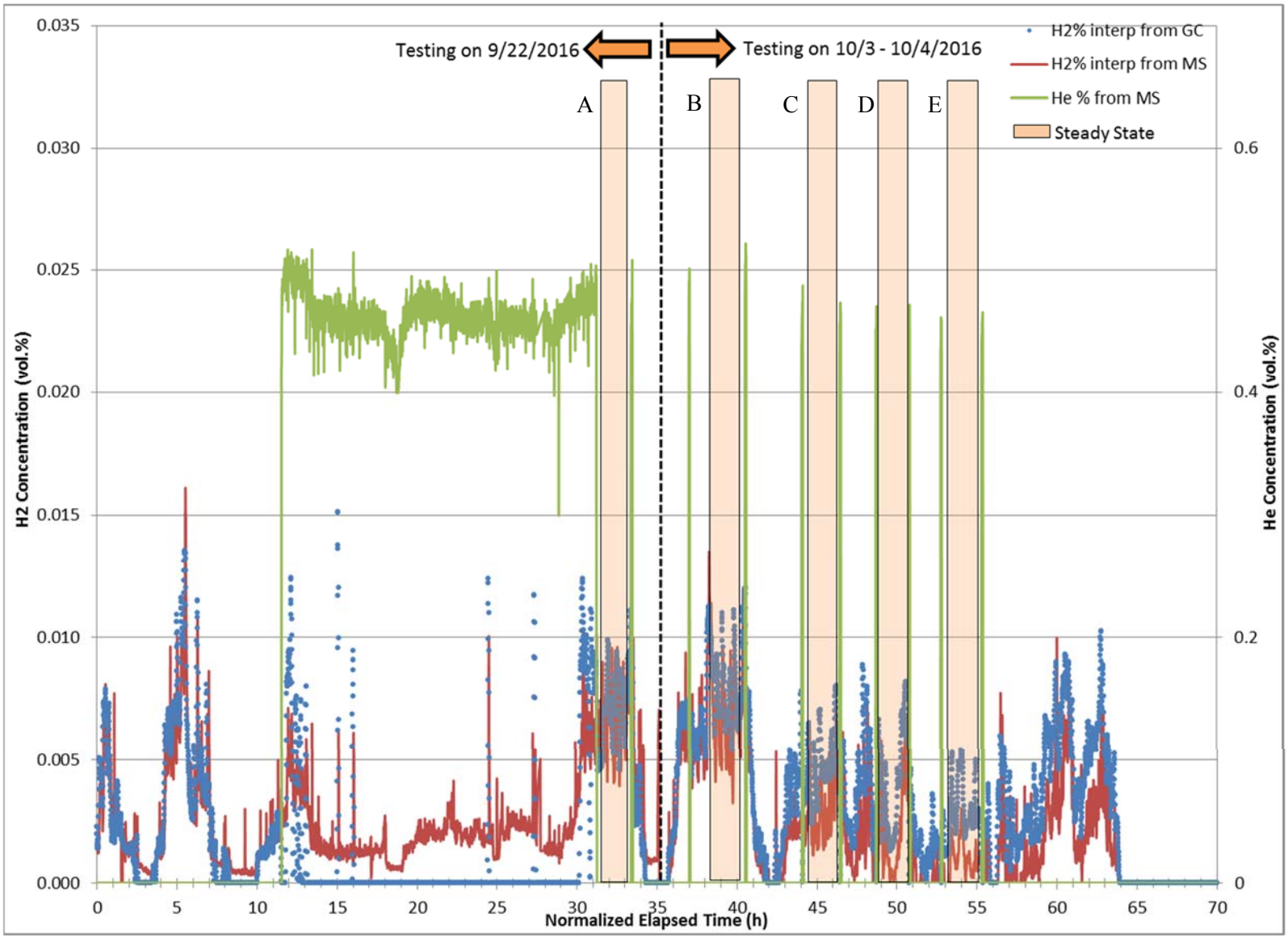

Figure 4-4. Unremediated Feed - H_2% and He%. Steady State Temperatures (°C): A) 606, B) 501, C) 432, D) 321, and E) 222.

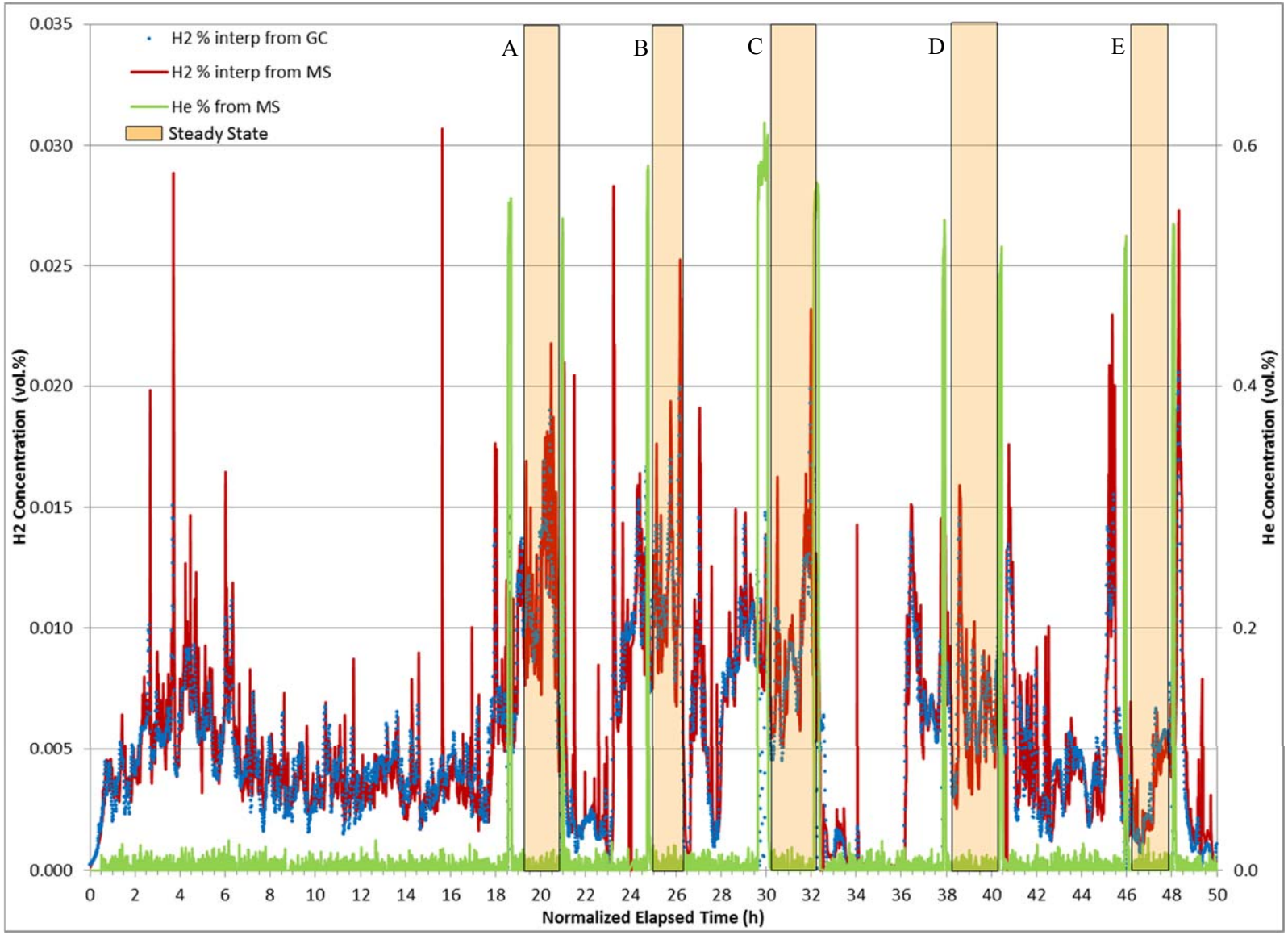

Figure 4-5. Glycolic-Remediated Feed - H_2% and He%. Steady State Temperatures (°C): A) 616, B) 508, C) 421, D) 324, and E) 208.

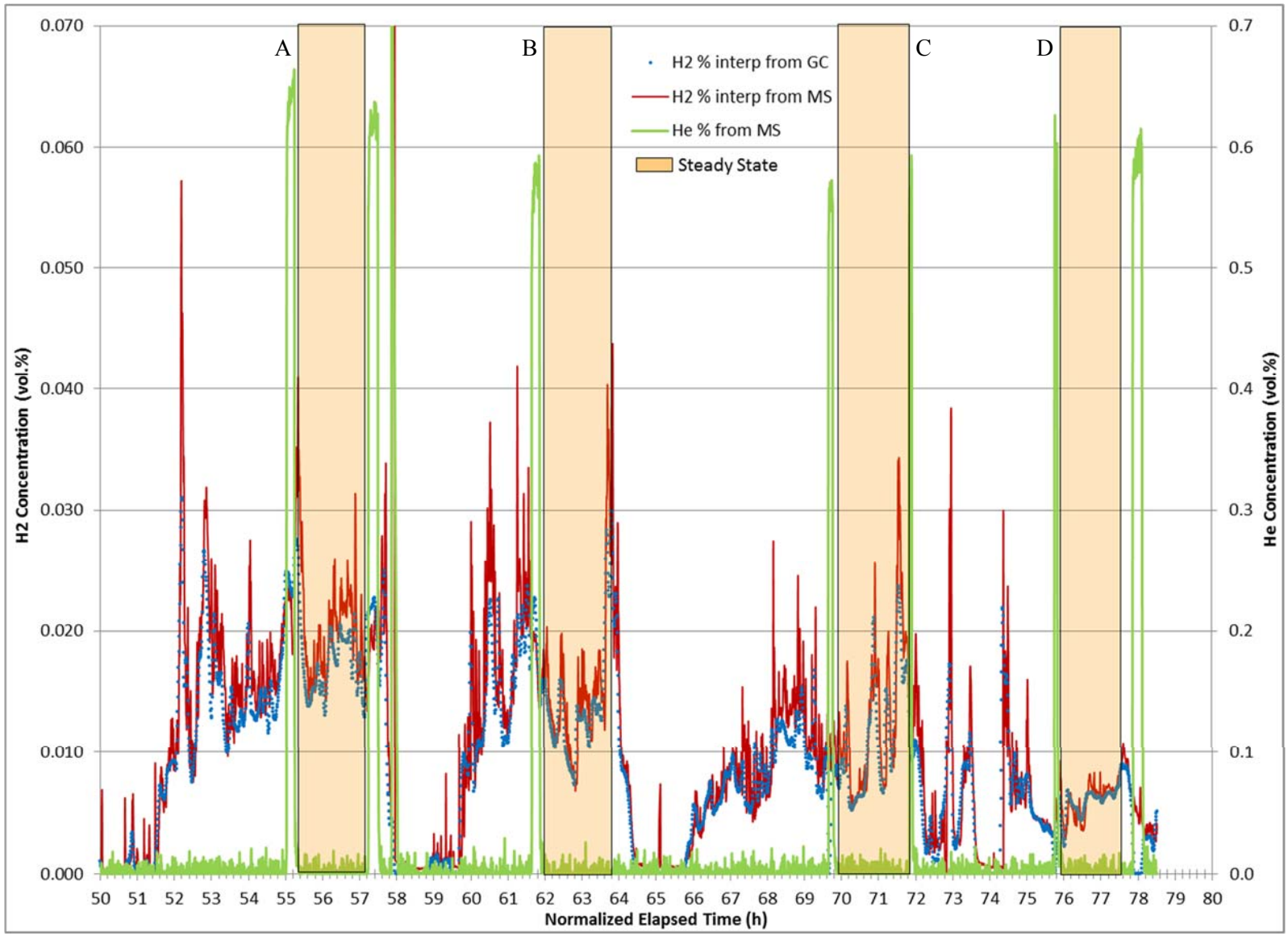

Figure 4-6. Bubbled Glycolic-Remediated Feed - H_2% and He%. Steady State Temperatures (°C): A) 641, B) 499, C) 364, and D) 239.

The offgas results show that as more glycolic acid is added to the feed and it becomes more reducing (i.e. higher REDOX $Fe^{2+}/\Sigma Fe$ ratio) the percentage of evolved hydrogen increases. This release increases again with the introduction of scaled DWPF flow of argon to the bubblers. Overall, the H_2 generation in the NG flowsheet feed is well below 25% of the LFL (1 vol%).

4.3 Glass REDOX measurements

While one of the goals of this testing was to feed the SMRF with feeds of varying targeted REDOX values as measured by CC_{Hot}, interpreting REDOX results of the poured glass was not the primary testing objective. Further testing primarily targeting optimal operating conditions for controlled REDOX of the poured glass at nominal DWPF conditions would be required to provide more interpretation of the REDOX behavior for the NG flowsheet.

Not all glass samples collected from the SMRF testing were analyzed. It is possible that another specimen may have exhibited a higher REDOX value than what is documented in this report and that the trend over time may have been different with further analyses.

Table 4-5 lists the measured REDOX values of select glasses collected from the SMRF over time; the REDOX values from CC_{Hot} and MRF testing were reported earlier (Table 3-1). CC_{Hot} and MRF measurements for the Nitric-remediated and unremediated feeds tended to average closer to the predicted REDOX values than the SMRF, but the values for the Glycolic-remediated feed were divergent for all testing methods. All SMRF REDOX values measured from testing during Nitric-remediated feeding and unremediated feeding were <0.03 $Fe^{2+}/\Sigma Fe$. The highest SMRF REDOX value in the analyzed sample set was measured just after completion of turnover to the Glycolic-remediated feed, 0.12 $Fe^{2+}/\Sigma Fe$. From this high value, the measured REDOX values of glasses collected throughout the Glycolic-remediated feeding to the SMRF appears to steadily drop, eventually reaching <0.03 before beginning bubbled operations. Once bubbled SMRF operations began, REDOX values of the glass appear to increase to ~0.05 and hold relatively steady throughout bubbled operations.

Table 4-5. Poured Glass REDOX measurements

Sample ID	Fe^{2+}	Fe^{3+}	ΣFe	Fe^{2+}/ Fe^{3+}	$Fe^{2+}/ \Sigma Fe$	Experimental Phase
SMRF-G-44	<0.01	0.353	0.353	All Fe^{3+}	<0.03 (All Fe^{3+})	End of Nitric-to-Unremediated Turnover
SMRF-G-59	<0.01	0.525	0.525	All Fe^{3+}	<0.03 (All Fe^{3+})	Unremediated steady state testing – 250°C
SMRF-G-63	<0.01	0.535	0.535	All Fe^{3+}	<0.03 (All Fe^{3+})	Middle of Unremediated –to-Glycolic Turnover
SMRF-G-74	0.060	0.451	0.511	0.132	0.117	Glycolic-remediated steady state testing - 650°C
SMRF-G-80	0.048	0.474	0.522	0.101	0.092	Glycolic-remediated steady state testing – 550°C
SMRF-G-82	0.016	0.400	0.416	0.040	0.038	Glycolic-remediated steady state testing – 250°C
SMRF-G-86	<0.01	0.604	0.604	All Fe^{3+}	<0.03 (All Fe^{3+})	Start of Bubbled steady state testing - 650°C
SMRF-G-90	0.034	0.599	0.633	0.057	0.054	Bubbled steady state testing - 550°C
SMRF-G-95	0.026	0.480	0.506	0.054	0.051	Bubbled steady state testing - 400°C
SMRF-G-98	0.028	0.380	0.407	0.073	0.068	Bubbled steady state testing - 300°C
SMRF-G-100	0.018	0.495	0.513	0.036	0.035	Final Drain
SMRF-G-101	0.053	0.455	0.507	0.116	0.104	Final Drain

A) 

B) 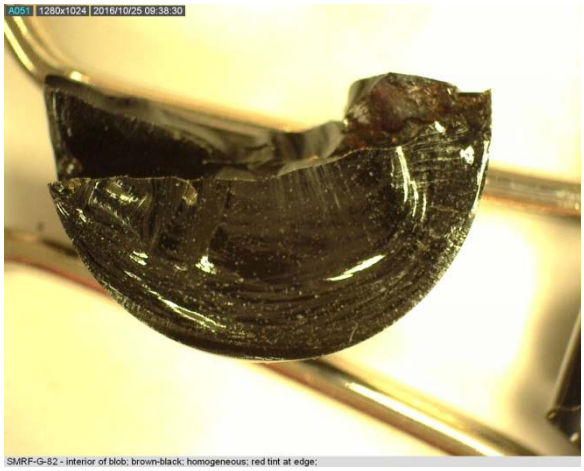

Figure 4-7. Glass sampled from the A) melter pour tube (SMRF-G-74) and B) drain pan (SMRF-G-82).

Visual examination of the glasses provided support for the observation of oxidized REDOX values (Figure 4-7). The oxidized SMRF glasses have a tell-tale reddish hue whereas more reduced glasses would have had a yellowish or greenish hue.

4.4 Compositional Analyses

Along with the glass samples, samples were pulled from the melter feed tank and the offgas condensate tank and analyzed for chemical composition. Detailed composition results are reported in the appendices; results relevant to the melter offgas flammability calculations will be discussed in a separate future report.

The composition analyses of the melter feed slurries are averaged in Table 4-6; individual samples are detailed in Appendix B. Comparison between the averaged melter feed composition and the predicted[e] melter feed composition demonstrates that melter feeds were batched accurately.

[e] Based on the analyzed composition of the SRAT product and the nominal composition of Frit 418.

Table 4-6. Predicted versus Average Melter Feed Tank Cation Composition

Element	Predicted Composition		Averaged Measured Composition
	Elemental Wt.%		Elemental Wt.%
Al	5.04		4.78
B	1.59		1.63
Ba	0.05		<0.101
Ca	0.45		0.38
Cr	0.06		0.07
Cu	0.04		<0.101
Fe	8.04		7.43
K	0.15		0.13
Li	2.19		2.34
Mg	0.38		0.32
Mn	2.44		2.34
Na	8.65		8.30
Ni	1.08		0.88
S	0.11		0.11
Si	23.30		24.25
Ti	<0.100		<0.100
Zn	0.04		<0.100
Zr	0.08		0.10

Comparison of the individual supernate analyses revealed predictable trends in the feeds with acid additions: higher metal concentrations in the supernate, lower supernate pH values, and increased supernate concentrations of conjugate base anions (nitrate in the case of Nitric-remediated, glycolate in the case of Glycolic-remediated). TOC measurements, performed by DWPF and AD, confirmed the correct acid additions as they showed higher organic carbon concentrations for the Glycolic-remediated feed than was seen in the Nitric-remediated or unremediated feeds. Analyses are reported in Appendix B, Table B-4 through Table B-9.

Select condensate samples were analyzed for cations, anions, total solids, pH and density. The corresponding condensate filters were weighted to examine for solids entrainment. The analyses of the condensate showed increasing sulfur, sodium, lithium, nitrite, and nitrate concentrations in the condensate as time progressed through testing, which is consistent with scrubbing NOx/SOx gases. For the condensate filters, the delta weight change for each only ranged from 1.0 to 8.4 grams, rendering analysis impractical.[f]

The predicted glass composition, based on the melter feed as well as the average measured glass composition, is listed in Table 4-7.

[f] The fraction of mass lost due to filtration from the overall removed condensate is predicted to be negligible.

Table 4-7. Predicted and Average Measured Glass Compositions Based on SB6I SRAT Composition

Elemental Oxide	Predicted Wt.%		Average Measured Wt.%
Al_2O_3	9.53		10.93
B_2O_3	5.12		4.83
BaO	0.06		<0.11
CaO	0.64		0.55
Cr_2O_3	0.10		0.18
CuO	0.05		<0.13
Fe_2O_3	11.49		12.77
K_2O	0.18		0.19
Li_2O	5.12		4.67
MgO	0.63		0.52
MnO	3.15		3.19
Na_2O	11.67		12.62
NiO	1.37		1.39
SO_4	0.32		0.42
SiO_2	49.85		46.16
ZnO	0.05		<0.12
ZrO_2	0.10		0.14
Total	99.42		98.92

When compared to the measured glass compositions of two glass samples pulled during the run (Table D-2), the oxide values are all ±10-15%, demonstrating that the glass produced was consistent with the melter feed analyses.

5.0 Conclusions

The SMRF was operated continuously for 3 to 5 days at a time, five separate times over a period of nearly three months to support Deliverable 4 of the TTR.[1] The separate future report discussing the melter offgas flammability calculations will complete this deliverable.

Operations were targeted at establishing steady state conditions at a variety of melter VS temperatures and feed rates with feeds of varying targeted REDOX values. The primary objective of this testing was to provide supplemental data to the melter offgas flammability modelling calculations for DWPF implementation of the NG flowsheet. In addition to the melter offgas, the REDOX values of the poured glass were examined to compare to the predictive REDOX model and the 2014 CEF Phase 2 testing.

The results of this testing demonstrated that the modified SMRF is operable in a continuously-fed mode for the purpose of producing melter offgas data. The feed rates scaled well to those calculated based on the CEF. The melter and VS temperatures were well-controlled and stable. The addition of the air/water mister provided VS temperature control at the low temperature range with the added benefit of not excessively diluting the offgas stream, which would complicate analysis of the low concentration analytes. This additional functionality is of significant benefit to future work requiring evaluations of melter operations where it is impractical to operate a larger scale melter (i.e. the CEF).

SMRF testing provided sufficient data to supplement the previous melter offgas flammability modelling effort. Additional details concerning the implications of the data to the modelling will be detailed in a separate future melter offgas flammability report. Preliminary observations of the offgas data support the

trend that reduced volumes of flammable gases (i.e. hydrogen, CO) are produced from the NG flowsheet feed. The specific impact of flammable antifoam degradation products on the melter offgas flammability was not evaluated as monitoring during the 2014 CEF study showed complete combustion of organics in the offgas.

Information relating cold cap behavior to the predicted REDOX of the feed was gleaned from the visual observations of the MRF and SMRF feeds during vitrification. Oxidized feeds were observed to foam in both the MRF and SMRF, impacting total glass produced in the MRF beakers and melt pouring behavior in the SMRF; reduced feeds demonstrated better melt properties in both platforms.

As in the 2014 CEF Phase 2 testing, the measured REDOX of the glass poured from the melter was significantly lower than the predicted values; however, non-zero values were observed. The $Fe^{2+}/\Sigma Fe$ ratio measurements briefly peaked at ~0.12 near the beginning of steady state testing for the Glycolic-remediated feed. During bubbling operations, the analyzed REDOX values plateaued near 0.05.

6.0 Recommendations, Path Forward or Future Work

For additional or future testing, the following recommendations are suggested to improve the operation of the SMRF and our understanding of the Nitric-Glycolic flowsheet:

- Testing and implementation of an *in situ* melt pool or pour stream REDOX probe(s) to track the progression of REDOX in the melt as a function of vapor space temperature, melt pool location, and residence time.

- Modification of the SMRF vessel construction to allow for a deeper melt pool and reduced impact of cold cap expansion on the glass overflow chimney.

- Operation of the SMRF at DWPF nominal conditions for an extended period of time (up to 5 consecutive days) to achieve a singular steady state. Extended single steady state testing would deconvolute any effects that may have been due to varying the operating conditions as well as provide true melt rate analyses for the NG flowsheet feed.

7.0 References

1. E. W. Holtzscheiter, "**Nitric-Glycolic Acid Flowsheet Melter Flammability Testing**", Savannah River Remediation, Aiken, SC, HLW-DWPF-TTR-2013-0002, rev. 1, (2016).

2. F. C. Johnson, M. E. Stone and D. H. Miller, "**Alternate Reductant Cold Cap Evaluation Furnace Phase II Testing**", U.S. Dept. of Energy, Savannah River National Laboratory, Aiken, SC, SRNL-STI-2014-00157, rev. 0, (2014).

3. D. H. Miller, "**Task Technical and Quality Assurance Plan for Alternative Reductant Melter Offgas Flammability Evaluation**", U.S. Dept. of Energy, Savannah River National Laboratory, Aiken, SC, SRNL-RP-2016-00018, rev. 1, (2016).

4. M. S. Williams, D. H. Miller and J. R. Zamecnik, "**Planned Experimentation for the Alternate Reductant Melter Offgas Flammability Evaluation**", U.S. Dept. of Energy, Savannah River National Laboratory, Aiken, SC, SRNL-L3100-2016-00074, rev. 0, (2016).

5. D. H. Miller, "**R&D Directions for SMRF Testing with 2014 CEF Feed**", U.S. Dept. of Energy, Savannah River National Laboratory, Aiken, SC, SRNL-L3100-2016-00107, rev. 1, (2016).

6. J. D. Jones, "**SMRF DAC Application Software**", U.S. Dept. of Energy, Savannah River National Laboratory, Aiken, SC, B-SWCD-A-00725, rev. 0, (2016).

7. P. L. Bovan, "**Specification for Procurement of DWPF Glass Frit**", Savannah River Remediation, X-SPP-S-00018, rev. 10, (2012).

8. C. M. Jantzen and T. B. Edwards, "**Defense Waste Processing Facility (DWPF) Viscosity Model: Revisions for Processing High TiO2 Glasses**", U.S. Dept. of Energy, Savannah River National Laboratory, Aiken, SC, SRNL-STI-2016-00115, rev. 0, (August 2016).

9. C. M. Jantzen, M. S. Williams, J. R. Zamecnik and D. M. Missimer, "**Interim Glycol Flowsheet REDuction/OXidation (REDOX) Model for the Defense Waste Processing Facility (DWPF)**", U.S. Dept. of Energy, Savannah River National Laboratory, Aiken, SC, SRNL-STI-2015-00702, rev. 0, (2016).

10. C. M. Jantzen, "**Heat Treatment of Waste Slurries for REDOX and Corrosion Analyses**", U.S. Dept. of Energy, Savannah River National Laboratory, Aiken, SC, Manual L29, ITS-0052, rev. 5, (2016).

11. D. H. Miller, "**Preparing Batches and Melting in the Dry Fed Melt Rate Furnace (MRF)**", U.S. Dept. of Energy, Savannah River National Laboratory, Aiken, SC, ITS-WI-0067, current rev., (2015).

12. D. R. Best, "**Dissolution of Glass, Sludge, and Slurry Samples Using Na2O2/NaOH/HCl**", U.S. Dept. of Energy, Savannah River National Laboratory, Aiken, SC, Manual L29, ITS-0040, current rev., (2013).

13. D. R. Best, "**Lithium Metaborate Fusion Preparation**", U.S. Dept. of Energy, Savannah River National Laboratory, Aiken, SC, Manual L29, ITS-0071, current rev., (2015).

14. D. R. Best, "**Lithium Tetraborate Fusion Preparation**", U.S. Dept. of Energy, Savannah River National Laboratory, Aiken, SC, Manual L29, ITS-0070, current rev., (2015).

15. D. R. Best, "**Aqua Regia Dissolutions of Passivated Hydride Materials**", U.S. Dept. of Energy, Savannah River National Laboratory, Aiken, SC, ECPT-ITS-WI-0036, current rev., (2014).

16. W. T. Riley, "**Sample Dissolution Using Potassium Hydroxide Fusion**", U.S. Dept. of Energy, Savannah River National Laboratory, Aiken, SC, Manual L29, ITS-0035, rev. 3, (2015).

17. W. T. Riley, "**Calibration, Verification, and Operation of the Agilent 730 ES Inductively Coupled Plasma-Atomic Emission Spectrometer**", U.S. Dept. of Energy, Savannah River National Laboratory, Aiken, SC, Manual L29, ITS-0079, rev. 6, (2016).

18. D. R. Best, "**Anion Analysis Using the Dionex DX-500 and ICS-5000 Ion Chromatograph**", U.S. Dept. of Energy, Savannah River National Laboratory, Aiken, SC, Manual L29, ITS-0027, current rev., (2011).

19. J. M. Pareizs, "**Weight Percent Solids Determination Using a Furnace or Oven**", U.S. Dept. of Energy, Savannah River National Laboratory, Aiken, SC, Manual L29, ITS-0078, rev. 1, (2012).

20. F. C. Johnson, "**Standardization Instructions for Fisher Scientific Accumet Basic Benchtop Meters (AB150, AB200, and AB250)**", U.S. Dept. of Energy, Savannah River National Laboratory, Manual L29, ITS-0212, rev. 1, (2016).

21. D. R. Best, "**Determining Fe2+/Fe3+ and Fe2+/Fe(Total) Using UV VIS Spectrometer**", U.S. Dept. of Energy, Savannah River National Laboratory, Aiken, SC, Manual L29, ITS-0042, current rev., (2014).

8.0 Appendices

Appendix A. Supplemental Equipment Diagrams

Appendix B. Supplemental Melter Feed Analytical Data

Appendix C. Supplemental Condensate Analytical Data

Appendix D. Supplemental Glass Analytical Data

Appendix E. Supplemental Melter Operations Data

Appendix F. Supplemental Offgas Analysis Data

Appendix A. Supplemental Equipment Diagrams

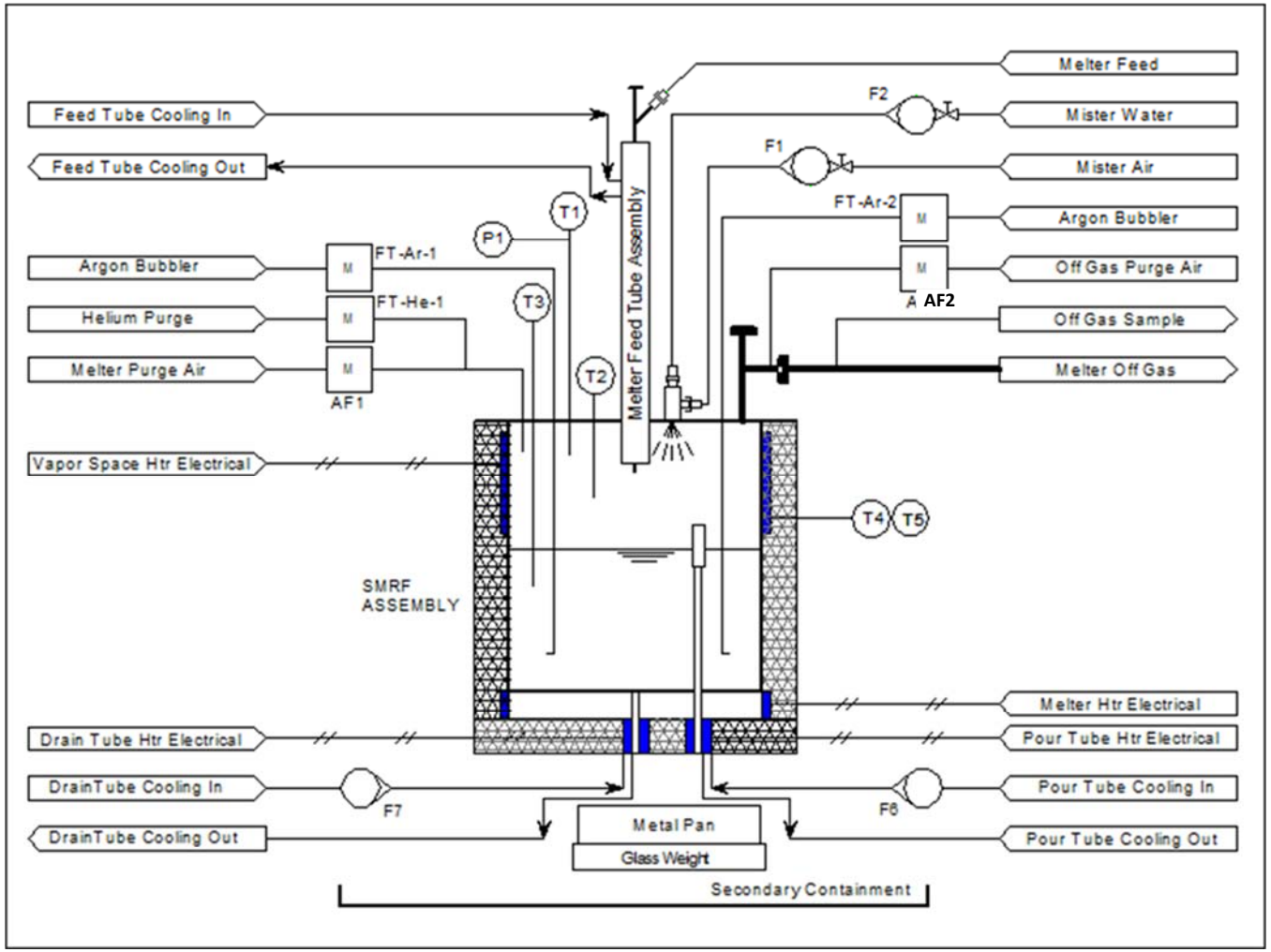

Figure A-1. Detailed SMRF Diagram

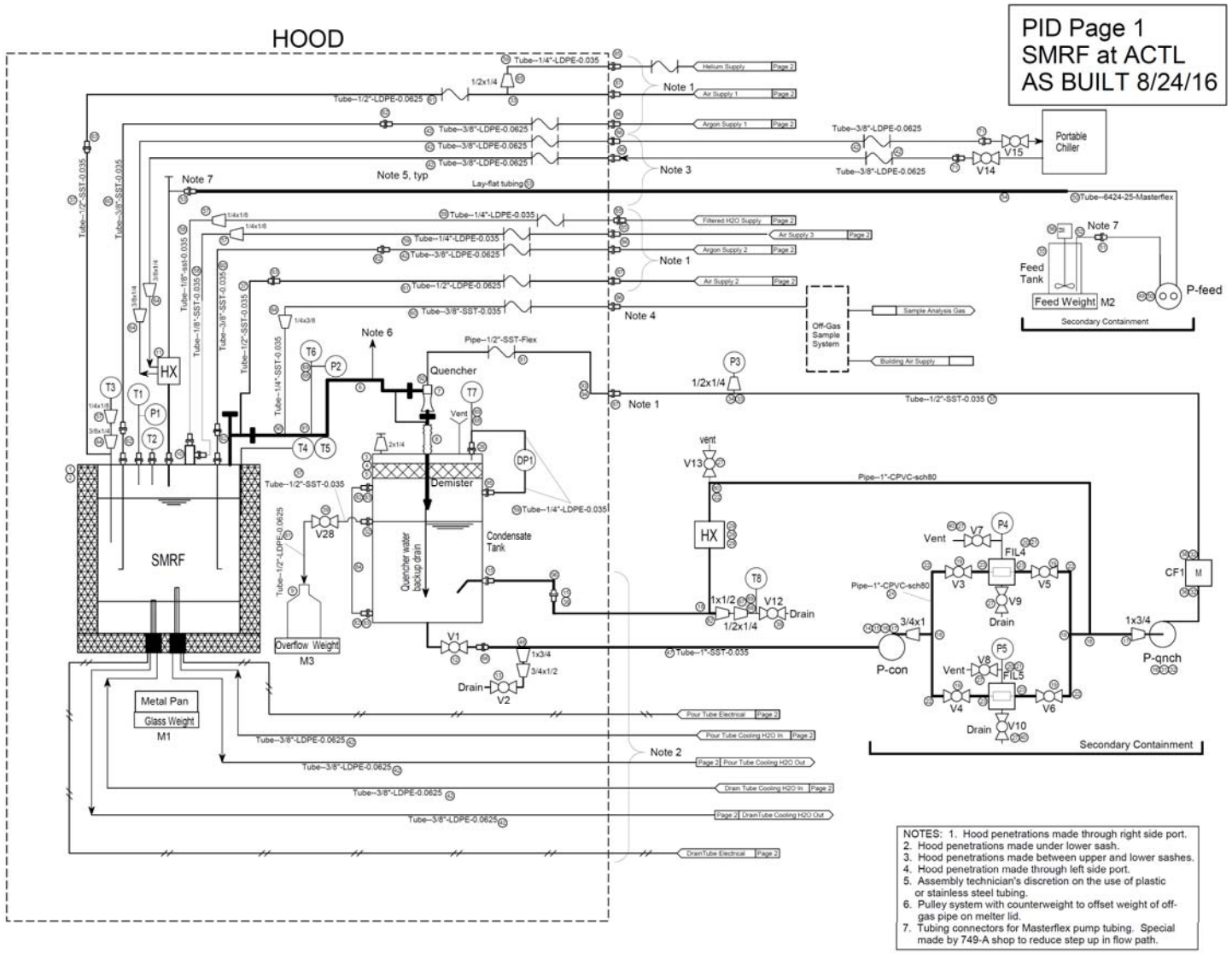

Figure A-2. Complete SMRF P&ID

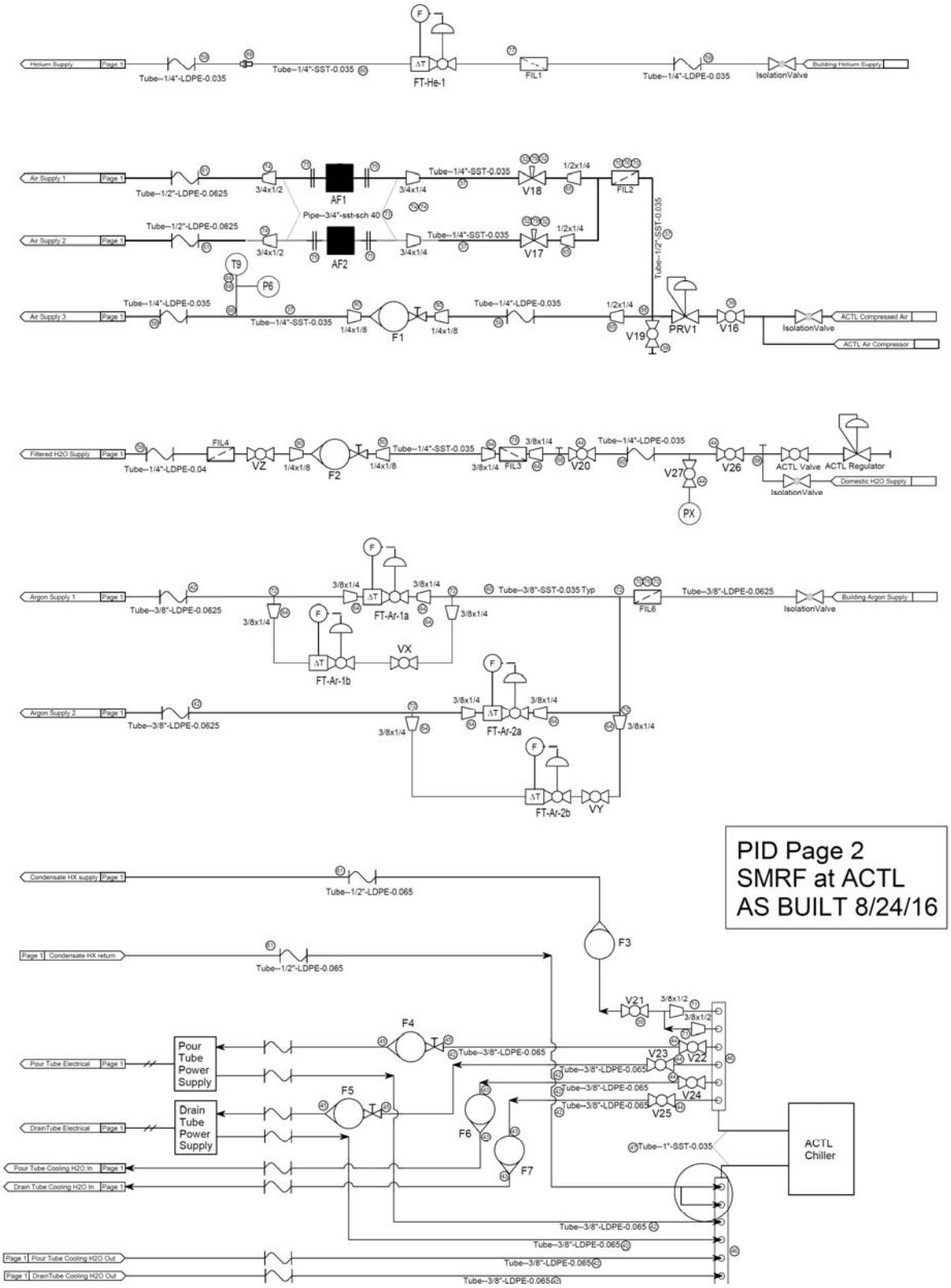

Figure A-3. SMRF Support Systems P&ID

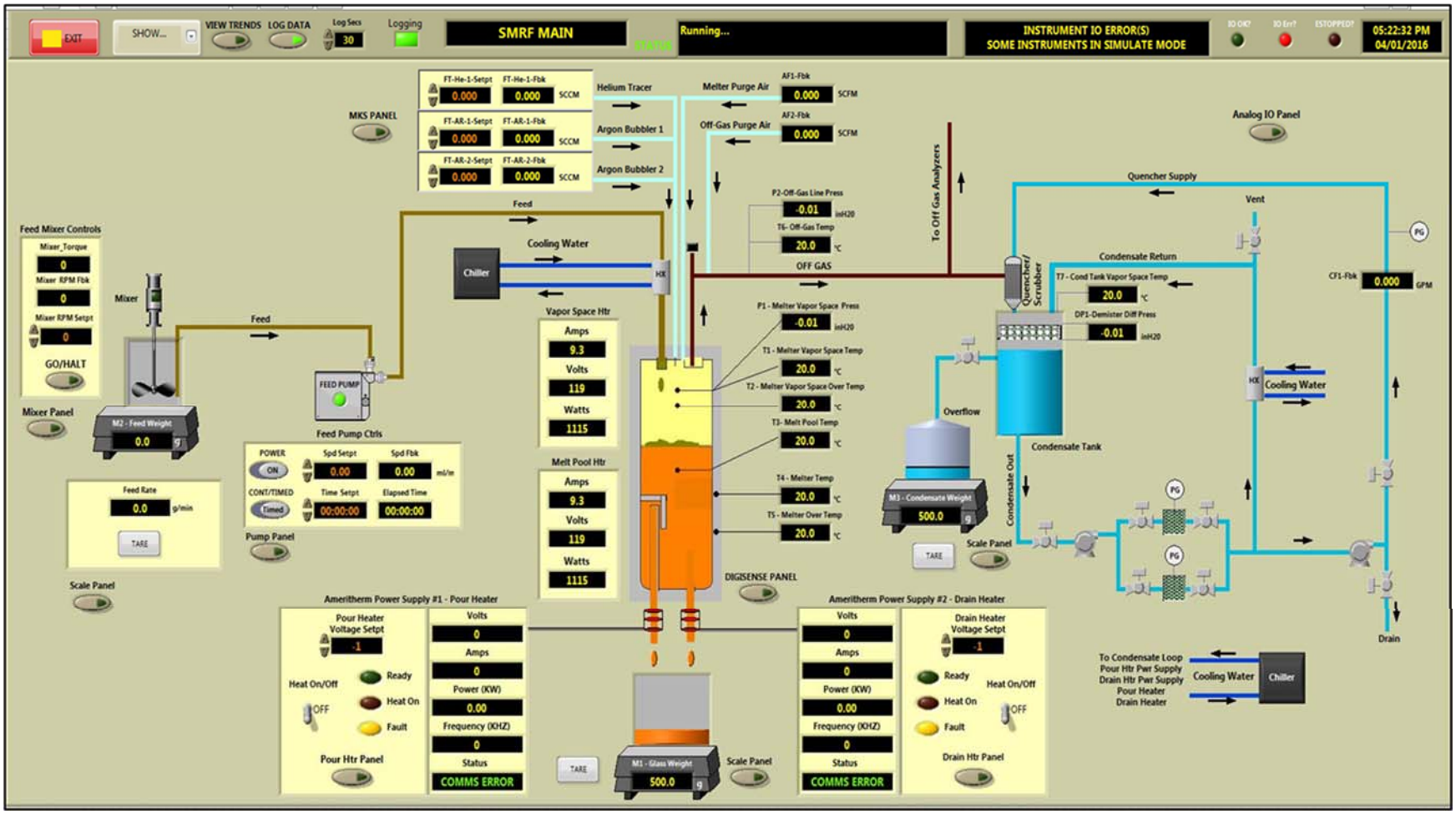

Figure A-4. SMRF Data Acquisition Display

Table A-1. SMRF Instrumentation.

P&ID Desig.	Description	Manufacturer, Part Number	Measuring & Test Equipment (M&TE) Number	Calibrated Range	Tolerance
P1	Melter vapor space pressure	Rosemont 1151DP3E22	TR-03104	-15 to +15 in H2O	0.5 % fs
P2	Off-Gas line pressure	Rosemont 1151DP3E22	TR-03106	-15 to +15 in H2O	0.5 % fs
P3	Quencher supply line pressure	Span 02-0012-T	TR-40282	0 - 160 psig	1 % fs
P4	Filter (FIL4) inlet pressure	Ashcroft Duralife	N/A	0 - 30 psig	3-2-3 % span
P5	Filter (FIL5) inlet pressure	Ashcroft 1008	N/A	0 - 30 psig	3-2-3 % span
P6	Rotameter F1 outlet pressure	USG, 100 psig	N/A	0 - 100 psig	3-2-3 % span
DP1	Condensate demister differential pressure	Rosemont 1151DP3E	TR-03103	0 - 30 in H2O	0.5 % fs
T1	Melter vapor space temperature	Omega HKIN-18U-18	ITS-TC0053	100 - 1100°C	2.2°C or 0.75 % rdg (greater value)
T2	Melter vapor space over-temperature	Omega HKIN-18U-18	ITS-TC0054	100 - 1100°C	2.2°C or 0.75 % rdg (greater value)
T3	Melt pool temperature	Omega CAIN-18U-24-NHX	ITS-TC0070	100 - 1100°C	2.2°C or 0.75 % rdg (greater value)
T4	Melter temperature	Omega HKIN-18U-18	ITS-TC0055	100 - 1100°C	2.2°C or 0.75 % rdg (greater value)
T5	Melter over-temperature	Omega HKIN-18U-18	ITS-TC0056	100 - 1100°C	2.2°C or 0.75 % rdg (greater value)
T6	Off-gas line gas temperature	Omega HKIN-18U-6	ITS-TC0051	100 - 1100°C	2.2°C or 0.75 % rdg (greater value)
T7	Condensate tank vapor space temperature	Omega HKIN-18U-18	ITS-TC0064	100 - 1100°C	2.2°C or 0.75 % rdg (greater value)
T8	Rotameter F1 outlet temperature, with display	Omega GEQSS-116G-12	TR-40030	0 - 100°C	1.7°C or 0.5 % rdg (greater value)
T9	Condensate temperature	Omega HKIN-18U-18	ITS-TC0065	100 - 1100°C	2.2°C or 0.75 % rdg (greater value)
M1	Glass pour weight	Hardy Instrm. HI-1212SBU	ITS-BL011	0 - 20 Kg	0.75 % rdg
M2	Feed pot weight	Hardy Instrm. HI-1212SBU	ITS-BL005	0 - 20 Kg	0.75 % rdg
M3	Condensate overflow weight	Hardy Instrm. HI-1212SBU	ITS-BL007	0 - 20 Kg	0.75 % rdg
CF1	Quencher supply flow rate	Fischer-Porter 10D1475DM07	TR-40067	0 - 12 gpm	(0.5 %rdg + 1 %fs)

Table A-1. SMRF Instrumentation (continued)

P&ID Desig.	Description	Manufacturer, Part Number	Measuring & Test Equipment (M&TE) Number	Calibrated Range	Tolerance
AF1	Melter purge air flow rate	KURZ 504FTB-12	TR-40153	0 - 12 scfm	(1 %rdg + 0.5 %fs)
AF2	Off-gas purge air flow rate	KURZ 504FTB-12	TR-40154	0 - 12 scfm	(1 %rdg + 0.75 %fs)
FT-AR-1a	Argon bubbler 1 flow rate, low flow	MKS 1179A12CS1BV	FC100-10	0 - 100 sccm	2 % rdg
FT-AR-1b	Argon bubbler 1 flow rate, high flow	MKS GE50A013104SBV020	FC10K-13	0 - 10000 sccm	2 % set pt
FT-AR-2a	Argon bubbler 2 flow rate, low flow	MKS 1179A51CS1BV	FC50-03	0 - 50 sccm	2 % rdg
FT-AR-2b	Argon bubbler 2 flow rate, high flow	MKS GE50A013104SBV020	FC10K-12	0 - 10000 sccm	1 % set pt
FT-He-1	Helium tracer gas flow rate	MKS GE50A013503SBV020	FC5K-21	0 - 5000 sccm	1 % set pt
F1	Melter spray nozzle, air flow rate	Brooks 1355 w/ R-6-15-B, Sapphire	TR-03786	0 - 30 lpm air	4 lpm
F2	Melter spray nozzle, water flow rate	Brooks 1355 w/ R-2-15-C, Glass	N/A	0 - 85 mlpm H2O	7.5 %fs
F3	Condensate heat exchanger coolant flow rate	Omega FL 75A	N/A	0 - 5 gpm	3 %fs
F4	Pour tube power supply coolant flow rate	Omega FL5003A-V	N/A	0 - 2 gpm	5 %fs
F5	Drain tube power supply coolant flow rate	Omega FL5003A-V	N/A	0 - 2 gpm	5 %fs
F6	Pour tube coolant flow rate	Omega FL 75A	N/A	0 - 5 gpm	3 %fs

in H_2O – inches of water; fs or span – full scale; psig – pounds per square inch, gage; rdg – reading; kg – kilogram; gpm – gallons per minute; scfm – standard cubic feet per minute; sccm – standard cubic centimeters per minute; set pt – setpoint; lpm – liters per minute; mlpm H_2O – milliliters per minute of H_2O

Appendix B. Supplemental Melter Feed Analytical Data

Table B-1. Source Sludge Composition (Sludge Batch 6I SRAT Product Drum 35)

Element	Elemental Wt.%		Ni	2.99
Al	14.01		P	<0.100
Ba	0.14		Pd	<0.100
Ca	1.26		Rh	<0.100
Cr	0.18		Ru	<0.100
Cu	0.12		S	0.30
Fe	22.32		Si	1.57
K	0.42		Sn	<0.100
Mg	1.05		Ti	<0.100
Mn	6.79		Zn	0.11
Na	13.49		Zr	0.21
Oxide	**Oxide Wt. %**		NiO	3.80
Al_2O_3	26.47		P_2O_5	<0.23
BaO	0.16		PdO	<0.12
CaO	1.77		RhO_2	<0.13
Cr_2O_3	0.27		RuO_4	<0.16
CuO	0.16		SO_4	0.89
Fe_2O_3	31.92		SiO_2	3.36
K_2O	0.51		SnO	<0.11
MgO	1.75		TiO_2	<0.17
MnO	8.75		ZnO	0.14
Na_2O	18.20		ZrO_2	0.28
Caustic Quenched Anions	**Concentration (mg/kg)**		SO_4	1770
F	<500		C_2O_4	1780
Cl	<500		PO_4	<500
NO_2	<500		HCO_2	3190
NO_3	67650		$C_2H_3O_3$	51050
Total Solids (wt. %)	33.5%		**Calcined Solids (wt. %)**	18.7%
Insoluble Solids (wt. %)	18.7%		**Soluble Solids (wt. %)**	14.7%
pH	5.72			

Table B-2. Undiluted, Remediated Melter Feed Carboys Slurry Anions Analyses (mg/kg)

Carboy	F	$C_2H_3O_3$	HCO_2	Cl	NO_2	NO_3	SO_4	C_2O_4	PO_4
SMRF-FD-1	<500	35400	1250	<500	<500	51400	1275	1070	<500
SMRF-FD-2	<500	35100	1210	<500	<500	50800	1255	1080	<500
SMRF-FD-3	<500	34600	1215	<500	<500	50000	1240	1050	<500
SMRF-FD-4	<500	33950	1270	<500	<500	53500	1300	979	<500
SMRF-FD-5	<500	34600	1265	<500	<500	59500	1225	1195	<500
SMRF-FD-6	<500	34900	1225	<500	<500	59050	1260	1190	<500
SMRF-FD-7	<500	34500	1240	<500	<500	57450	1230	1170	<500
SMRF-FD-8	<500	36750	2005	<500	<500	59150	1370	1515	<500
SMRF-FD-9	<500	41450	1620	<500	<500	49300	1210	1130	<500
SMRF-FD-10	<500	44000	1975	<500	<500	50300	1405	1435	<500
SMRF-FD-11	<500	43600	1950	<500	<500	49600	1385	1470	<500
SRMF-FD-12	<500	43750	1950	<500	<500	49850	1375	1415	<500
SMRF-FD-13	<500	43850	2260	<500	<500	53650	1435	1425	<500
SMRF-FD-14	<500	44100	2085	<500	<500	50500	1400	1510	<500
SMRF-FD-15	<500	43550	2115	<500	<500	50200	1355	1505	<500

Table B-3. Sampling Timeline.

Sample Type	Sample ID	Date Sampled	Time Sampled	Feed Remediation
Melter Feed Tank Slurry	SMRF-MFT-1	9/8/2016	---	Nitric
	SMRF-MFT-2	9/9/2016	1300	
	SMRF-MFT-3	9/20/2016	1450	
	SMRF-MFT-4	9/20/2016	1930	
	SMRF-MFT-5	9/21/2016	0700	Unremediated
	SMRF-MFT-6	9/21/2016	1300	
	SMRF-MFT-7	9/21/2016	1935	
	SMRF-MFT-8	9/22/2016	0215	
	SMRF-MFT-9	9/22/2016	1300	
	SMRF-MFT-10	10/3/2016	1400	
	SMRF-MFT-11	10/3/2016	1918	
	SRMF-MFT-12	10/4/2016	1034	Glycolic
	SMRF-MFT-13	10/4/2016	1341	
	SMRF-MFT-14	10/17/2016	1139	
	SMRF-MFT-15	10/17/2016	1608	
	SMRF-MFT-16	10/17/2016	2200	
	SMRF-MFT-17	10/18/2016	0235	
	SMRF-MFT-18	10/18/2016	0852	
	SMRF-MFT-19	10/18/2016	1206	
	SMRF-MFT-20	10/19/2016	0400	
	SMRF-MFT-21	10/19/2016	0823	
	SMRF-MFT-22	10/19/2016	1850	Bubbled Glycolic
	SMRF-MFT-23	10/20/2016	0400	
	SMRF-MFT-24	10/20/2016	0904	
Glass Samples	SMRF-G-1	8/9/2016	1430	Nitric
	SMRF-G-2	8/9/2016	1630	
	SMRF-G-3	8/9/2016	1650	
	SMRF-G-4	8/9/2016	1830	
	SMRF-G-5	8/10/2016	0036	
	SMRF-G-6	8/10/2016	0237	
	SMRF-G-7	8/10/2016	0439	
	SMRF-G-8	8/10/2016	0642	
	SMRF-G-9	8/10/2016	0845	
	SMRF-G-10	8/10/2016	1045	
	SMRF-G-11	8/10/2016	1255	

Table B-3 (continued). Sampling Timeline.

Sample Type	Sample ID	Date Sampled	Time Sampled	Feed Remediation
Glass Samples	SMRF-G-12	8/10/2016	1909	Nitric
	SMRF-G-13	8/10/2016	2110	
	SMRF-G-14	8/11/2016	0230	
	SMRF-G-15	8/11/2016	0446	
	SMRF-G-16	8/11/2016	0648	
	SMRF-G-17	8/11/2016	2322	
	SMRF-G-18	9/9/2016	1145	
	SMRF-G-19	9/9/2016	1400	
	SMRF-G-20	9/9/2016	1550	
	SMRF-G-21	9/9/2016	1810	
	SMRF-G-22	9/9/2016	2035	
	SMRF-G-23	9/20/2016	1630	
	SMRF-G-24	9/20/2016	1832	
	SMRF-G-25	9/20/2016	2031	
	SMRF-G-26	9/20/2016	2232	
	SMRF-G-27	9/21/2016	0030	
	SMRF-G-28	9/21/2016	0235	
	SMRF-G-29	9/21/2016	0435	
	SMRF-G-30	9/21/2016	0635	
	SMRF-G-31	9/21/2016	0935	Unremediated
	SMRF-G-32	9/21/2016	1200	
	SMRF-G-33	9/21/2016	1400	
	SMRF-G-34	9/21/2016	1615	
	SMRF-G-35	9/21/2016	1818	
	SMRF-G-36	9/21/2016	2020	
	SMRF-G-37	9/21/2016	2220	
	SMRF-G-38	9/22/2016	0025	
	SMRF-G-39	9/22/2016	0230	
	SMRF-G-40	9/22/2016	0432	
	SMRF-G-41	9/22/2016	0630	
	SMRF-G-42	9/22/2016	0830	
	SMRF-G-43	9/22/2016	1030	
	SMRF-G-44	9/22/2016	1140	
	SMRF-G-45	9/22/2016	1340	
	SMRF-G-46	9/22/2016	1540	

Table B-3 (continued). Sampling Timeline.

Sample Type	Sample ID	Date Sampled	Time Sampled	Feed Remediation
Glass Samples	SMRF-G-47	9/22/2016	1725	Unremediated
	SMRF-G-48	9/23/2016	0220	
	SMRF-G-49	9/23/2016	0440	
	SMRF-G-50	10/3/2016	1531	
	SMRF-G-51	10/3/2016	1728	
	SMRF-G-52	10/3/2016	1930	
	SMRF-G-53	10/3/2016	2131	
	SMRF-G-54	10/3/2016	2332	
	SMRF-G-55	10/4/2016	0130	
	SMRF-G-56	10/4/2016	0335	
	SMRF-G-57	10/4/2016	0520	
	SMRF-G-58	10/4/2016	0730	
	SMRF-G-59	10/4/2016	0910	
	SMRF-G-60	10/4/2016	1210	Glycolic
	SMRF-G-61	10/4/2016	1420	
	SMRF-G-62	10/4/2016	1625	
	SMRF-G-63	---	---	
	SMRF-G-64	10/17/2016	1344	
	SMRF-G-65	10/17/2016	1538	
	SMRF-G-66	10/17/2016	1740	
	SMRF-G-67	10/17/2016	1950	
	SMRF-G-68	10/17/2016	2140	
	SMRF-G-69	10/17/2016	2340	
	SMRF-G-70	10/18/2016	0240	
	SMRF-G-71	10/18/2016	0440	
	SMRF-G-72	10/18/2016	0505	
	SMRF-G-73	10/18/2016	0704	
	SMRF-G-74	10/18/2016	0907	
	SMRF-G-75	10/18/2016	1105	
	SMRF-G-76	10/18/2016	1307	
	SMRF-G-77	10/18/2016	1458	
	SMRF-G-78	10/18/2016	1835	
	SMRF-G-79	10/18/2016	2055	
	SMRF-G-80	10/18/2016	2235	
	SMRF-G-81	10/19/2016	0525	

Table B-3 (continued). Sampling Timeline.

Sample Type	Sample ID	Date Sampled	Time Sampled	Feed Remediation
Glass Samples	SMRF-G-82	10/19/2016	0710	Glycolic
	SMRF-G-83	10/19/2016	1130	
	SMRF-G-84	10/19/2016	1343	
	SMRF-G-85	10/19/2016	1546	Bubbled Glycolic
	SMRF-G-86	10/19/2016	1750	
	SMRF-G-87	10/19/2016	2010	
	SMRF-G-88	10/19/2016	2145	
	SMRF-G-89	10/19/2016	2345	
	SMRF-G-90	10/20/2016	0205	
	SMRF-G-91	10/20/2016	0350	
	SMRF-G-92	10/20/2016	0605	
	SMRF-G-93	10/20/2016	0808	
	SMRF-G-94	10/20/2016	0957	
	SMRF-G-95	10/20/2016	1122	
	SMRF-G-96	10/20/2016	1305	
	SMRF-G-97	10/20/2016	1510	
	SMRF-G-98	10/20/2016	1715	
	SMRF-G-99	10/20/2016	---	
	SMRF-G-100	---	---	from Final Drain material
	SMRF-G-101	---	---	
Condensate Solutions	SMRF-C-1	8/10/2016	0425	Nitric
	SMRF-C-2	8/10/2016	0825	
	SMRF-C-3	8/10/2016	1322	
	SMRF-C-4	8/10/2016	1836	
	SMRF-C-5	8/10/2016	2240	
	SMRF-C-6	9/9/2016	1412	
	SMRF-C-7	9/9/2016	1820	
	SMRF-C-8	9/9/2016	2235	
	SMRF-C-9	9/20/2016	1759	
	SMRF-C-10	9/20/2016	2205	
	SMRF-C-11	9/21/2016	0427	
	SMRF-C-12	9/21/2016	0830	Unremediated
	SMRF-C-13	9/21/2016	1230	
	SMRF-C-14	9/21/2016	1630	
	SMRF-C-15	9/21/2016	2245	

Table B-3 (continued). Sampling Timeline.

Sample Type	Sample ID	Date Sampled	Time Sampled	Feed Remediation
Condensate Solutions	SMRF-C-16	9/22/2016	0405	Unremediated
	SMRF-C-17	9/22/2016	0805	
	SMRF-C-18	9/22/2016	1230	
	SMRF-C-19	9/22/2016	1630	
	SMRF-C-20	10/3/2016	1832	
	SMRF-C-21	10/3/2016	2233	
	SMRF-C-22	10/4/2016	0235	
	SMRF-C-23	10/4/2016	0630	
	SMRF-C-24	10/4/2016	1030	Glycolic
	SMRF-C-25	10/4/2016	1415	
	SMRF-C-26	10/17/2016	1547	
	SMRF-C-27	10/17/2016	2050	
	SMRF-C-28	10/17/2016	2240	
	SMRF-C-29	10/18/2016	0440	
	SMRF-C-30	10/18/2016	0846	
	SMRF-C-31	10/18/2016	1245	
	SMRF-C-32	10/18/2016	1645	
	SMRF-C-33	10/18/2016	2040	
	SMRF-C-34	10/18/2016	2350	
	SMRF-C-35	10/19/2016	0440	
	SMRF-C-36	10/19/2016	0840	
	SMRF-C-37	10/19/2016	1245	
	SMRF-C-38	10/19/2016	1639	
	SMRF-C-39	10/19/2016	2040	Bubbled Glycolic
	SMRF-C-40	10/20/2016	0040	
	SMRF-C-41	10/20/2016	0440	
	SMRF-C-42	10/20/2016	0900	
	SMRF-C-43	10/20/2016	1310	
	SMRF-C-44	10/20/2016	1708	

Table B-4. Diluted, Remediated Melter Feed Tank Slurry Cations Analyses (elemental wt. %)

	Element (wt. %)								
Sample	**Al**	**B**	**Ba**	**Ca**	**Cr**	**Cu**	**Fe**	**K**	**Li**
SMRF-MFT-1	4.85	1.55	<0.100	0.39	0.08	<0.100	7.52	0.11	2.34
SMRF-MFT-2	3.87	1.82	<0.100	0.33	0.07	<0.100	5.90	0.10	2.57
SMRF-MFT-3	4.58	1.69	<0.100	0.39	0.08	0.11	7.01	0.13	2.30
SMRF-MFT-4	4.48	1.71	<0.100	0.35	0.07	<0.100	6.81	0.11	2.33
SMRF-MFT-5	5.99	1.46	<0.100	0.43	0.09	<0.100	9.02	0.14	1.94
SMRF-MFT-6	5.02	1.67	<0.100	0.39	0.08	<0.100	7.63	0.12	2.23
SMRF-MFT-7	4.37	1.66	<0.100	0.36	0.07	<0.100	6.60	0.11	2.33
SMRF-MFT-8	4.88	1.60	<0.100	0.38	0.08	<0.100	7.42	0.11	2.25
SMRF-MFT-9	4.81	1.58	<0.100	0.37	0.08	<0.100	7.35	0.11	2.25
SMRF-MFT-10	5.11	1.63	<0.100	0.41	0.08	0.09	7.98	0.16	2.25
SMRF-MFT-11	4.70	1.64	<0.100	0.38	0.07	0.09	7.30	0.14	2.37
SRMF-MFT-12	4.76	1.64	<0.100	0.37	0.07	0.10	7.33	0.15	2.39
SMRF-MFT-13	4.70	1.68	<0.100	0.38	0.07	0.07	7.21	0.15	2.40
SMRF-MFT-14	4.97	1.57	<0.100	0.39	0.07	<0.100	7.85	0.13	2.41
SMRF-MFT-15	4.93	1.63	<0.100	0.39	0.07	<0.100	7.69	0.13	2.40
SMRF-MFT-16	4.72	1.59	<0.100	0.39	0.07	<0.100	7.47	0.13	2.42
SMRF-MFT-17	4.90	1.64	<0.100	0.39	0.07	<0.100	7.76	0.13	2.40
SMRF-MFT-18	4.70	1.68	<0.100	0.38	0.07	<0.100	7.46	0.13	2.45
SMRF-MFT-19	4.77	1.68	<0.100	0.38	0.07	<0.100	7.60	0.13	2.36
SMRF-MFT-20	4.88	1.61	<0.100	0.39	0.07	<0.100	7.84	0.13	2.35
SMRF-MFT-21	4.92	1.60	<0.100	0.40	0.07	<0.100	7.85	0.13	2.31
SMRF-MFT-22	4.84	1.55	<0.100	0.39	0.07	<0.100	7.77	0.14	2.36
SMRF-MFT-23	4.54	1.57	<0.100	0.38	0.07	<0.100	7.03	0.12	2.35
SMRF-MFT-24	4.39	1.68	<0.100	0.36	0.07	<0.100	6.85	0.12	2.45

Table B-4 (continued). Diluted, Remediated Melter Feed Tank Slurry Cations Analyses (elemental wt. %)

	Element (wt. %)								
Sample	**Mg**	**Mn**	**Na**	**Ni**	**S**	**Si**	**Ti**	**Zn**	**Zr**
SMRF-MFT-1	0.32	2.39	8.46	0.92	0.12	24.60	<0.100	<0.100	0.10
SMRF-MFT-2	0.27	1.89	7.81	0.76	0.09	27.12	<0.100	<0.100	0.09
SMRF-MFT-3	0.32	2.31	8.60	0.92	0.12	24.18	<0.100	<0.100	0.10
SMRF-MFT-4	0.28	2.06	8.17	0.83	0.11	24.25	<0.100	<0.100	0.09
SMRF-MFT-5	0.38	2.79	9.19	1.08	0.15	20.54	<0.100	<0.100	0.12
SMRF-MFT-6	0.33	2.39	8.59	0.95	0.12	23.57	<0.100	<0.100	0.11
SMRF-MFT-7	0.29	2.12	8.31	0.82	0.10	24.23	<0.100	<0.100	0.09
SMRF-MFT-8	0.31	2.32	8.67	0.91	0.12	23.37	<0.100	<0.100	0.10
SMRF-MFT-9	0.31	2.33	8.55	0.90	0.11	23.39	<0.100	<0.100	0.10
SMRF-MFT-10	0.34	2.64	8.77	0.94	0.12	23.70	<0.100	<0.100	<0.100
SMRF-MFT-11	0.31	2.35	8.00	0.87	0.10	24.61	<0.100	<0.100	<0.100
SRMF-MFT-12	0.31	2.24	7.95	0.83	0.10	24.70	<0.100	<0.100	<0.100
SMRF-MFT-13	0.31	2.26	7.70	0.84	0.10	24.85	<0.100	<0.100	<0.100
SMRF-MFT-14	0.33	2.44	8.26	0.90	0.11	24.34	<0.100	<0.100	0.10
SMRF-MFT-15	0.32	2.41	8.27	0.87	0.11	24.35	<0.100	<0.100	0.10
SMRF-MFT-16	0.32	2.33	8.28	0.89	0.11	24.48	<0.100	<0.100	0.10
SMRF-MFT-17	0.32	2.46	8.24	0.88	0.11	24.51	<0.100	<0.100	0.10
SMRF-MFT-18	0.31	2.34	8.18	0.85	0.11	25.26	<0.100	<0.100	0.09
SMRF-MFT-19	0.31	2.39	8.31	0.85	0.11	24.71	<0.100	<0.100	0.09
SMRF-MFT-20	0.32	2.45	8.32	0.88	0.12	24.35	<0.100	<0.100	0.10
SMRF-MFT-21	0.33	2.46	8.28	0.92	0.12	23.84	<0.100	<0.100	0.10
SMRF-MFT-22	0.32	2.43	8.27	0.89	0.11	24.12	<0.100	<0.100	0.09
SMRF-MFT-23	0.31	2.21	8.07	0.85	0.12	23.86	<0.100	<0.100	0.09
SMRF-MFT-24	0.29	2.14	7.92	0.81	0.10	25.04	<0.100	<0.100	0.09

Table B-5. Diluted, Remediated Melter Feed Tank Slurry Anions Analyses (mg/kg)

	Anions (mg/kg)								
Sample	**F**	**Cl**	**NO_2**	**NO_3**	**C_2O_4**	**SO_4**	**PO_4**	**HCO_2**	**$C_2H_3O_3$**
SMRF-MFT-1	<500	<500	<500	50450	1145	1450	<500	1060	27650
SMRF-MFT-2	<500	<500	<500	45250	1010	1315	<500	1130	26350
SMRF-MFT-3	<500	<500	<500	51250	1145	1485	<500	1415	27900
SMRF-MFT-4	<500	<500	<500	48650	1160	1510	<500	1395	29900
SMRF-MFT-5	<500	<500	<500	49100	1165	1735	<500	1065	31000
SMRF-MFT-6	<500	<500	<500	45050	1100	1635	<500	921	30000
SMRF-MFT-7	<500	<500	<500	43950	1085	1545	<500	901	31350
SMRF-MFT-8	<500	<500	<500	45200	1105	1635	<500	917	29950
SMRF-MFT-9	<500	<500	<500	45100	1180	1625	<500	972	29750
SMRF-MFT-10	<500	<500	<500	44850	1015	1565	<500	900	29350
SMRF-MFT-11	<500	<500	<500	43000	1065	1545	<500	1035	28350
SRMF-MFT-12	<500	<500	<500	48200	1190	1650	<500	1510	37550
SMRF-MFT-13	<500	<500	<500	45400	1125	1600	<500	1415	38350
SMRF-MFT-14	<500	<500	<500	44750	912	1330	<500	1620	38450
SMRF-MFT-15	<500	<500	<500	43550	878	1320	<500	1445	37700
SMRF-MFT-16	<500	<500	<500	43000	881	1315	<500	1510	37450
SMRF-MFT-17	<500	<500	<500	43000	858	1165	<500	1435	37200
SMRF-MFT-18	<500	<500	<500	42700	840	1175	<500	1485	37050
SMRF-MFT-19	<500	<500	<500	42750	853	1185	<500	1355	37150
SMRF-MFT-20	<500	<500	<500	42100	836	1185	<500	1535	36400
SMRF-MFT-21	<500	<500	<500	42350	824	1195	<500	1535	36450
SMRF-MFT-22	<500	<500	<500	42900	850	1270	<500	1525	36950
SMRF-MFT-23	<500	<500	<500	42500	824	1220	<500	1450	37150
SMRF-MFT-24	<500	<500	<500	42250	806	1180	<500	1470	36600

Table B-6. Diluted, Remediated Melter Feed Tank Slurry Solids Data, pH, and Density

Sample	Total Solids	Insoluble Solids	Calcined Solids	pH	Density (g/cm^3)	Supernate Density (g/cm^3)
SMRF-MFT-1	40.5%	31.1%	31.4%	4.20	1.32	1.09
SMRF-MFT-2	43.4%	34.9%	35.2%	4.11	1.34	1.09
SMRF-MFT-3	40.3%	30.1%	31.1%	3.69	1.32	1.10
SMRF-MFT-4	43.7%	34.0%	34.6%	3.69	1.35	1.10
SMRF-MFT-5	37.9%	27.7%	27.6%	6.09	1.29	1.09
SMRF-MFT-6	41.4%	32.0%	31.7%	6.14	1.31	1.09
SMRF-MFT-7	44.4%	35.3%	34.8%	6.23	1.35	1.09
SMRF-MFT-8	42.4%	33.0%	32.7%	6.21	1.33	1.09
SMRF-MFT-9	42.8%	33.6%	33.0%	6.20	1.34	1.09
SMRF-MFT-10	40.1%	30.2%	30.3%	6.07	1.35	1.09
SMRF-MFT-11	43.6%	34.2%	33.9%	6.06	1.30	1.09
SRMF-MFT-12	46.9%	36.1%	36.0%	5.45	1.35	1.11
SMRF-MFT-13	45.3%	35.3%	35.1%	5.40	1.18	1.11
SMRF-MFT-14	44.1%	33.9%	34.0%	4.95	1.33	1.10
SMRF-MFT-15	43.7%	33.6%	33.6%	4.89	1.34	1.10
SMRF-MFT-16	44.0%	34.1%	34.2%	4.90	1.35	1.10
SMRF-MFT-17	43.3%	33.1%	33.4%	4.92	1.35	1.10
SMRF-MFT-18	44.2%	34.3%	34.3%	4.94	1.35	1.10
SMRF-MFT-19	43.5%	33.6%	33.7%	5.01	1.35	1.09
SMRF-MFT-20	43.0%	32.9%	33.2%	5.06	1.33	1.09
SMRF-MFT-21	42.5%	32.5%	32.6%	5.01	1.34	1.09
SMRF-MFT-22	43.3%	33.2%	33.5%	4.96	1.34	1.10
SMRF-MFT-23	44.8%	34.9%	35.1%	5.00	1.36	1.10
SMRF-MFT-24	45.4%	36.0%	35.7%	5.04	1.37	1.10

Table B-7. Diluted, Remediated Melter Feed Tank Supernate Cations Analyses (wt.%)

	Element (wt. %)								
Sample	**Al**	**B**	**Ba**	**Ca**	**Cr**	**Cu**	**Fe**	**K**	**Li**
SMRF-MFT-1	149	39.8	1.27	1160	1.82	94.2	161	506	125
SMRF-MFT-2	182	38.2	1.23	1105	1.83	94.7	189	464	119
SMRF-MFT-3	286	20.6	1.46	1390	2.32	103	527	476	81.6
SMRF-MFT-4	287	21.4	1.44	1410	2.21	106	512	557	86.9
SMRF-MFT-5	12.8	50.3	0.78	941	0.48	5.81	20.0	558	132
SMRF-MFT-6	12.1	46.6	0.72	932	0.75	5.48	16.8	558	129
SMRF-MFT-7	12.1	51.7	0.78	965	0.58	5.19	18.5	578	135
SMRF-MFT-8	12.4	49.2	0.74	953	0.55	5.20	18.3	528	132
SMRF-MFT-9	12.1	48.4	0.77	954	0.53	5.35	18.5	541	132
SMRF-MFT-10	10.9	58.4	0.75	895	0.59	5.06	19.4	598	136
SMRF-MFT-11	10.5	49.1	0.73	929	0.63	5.27	18.8	618	119
SRMF-MFT-12	64.3	47.7	1.14	1300	1.65	60.0	192	695	149
SMRF-MFT-13	65.1	45.3	1.04	1210	1.48	56.0	181	648	140
SMRF-MFT-14	60.4	43.6	0.93	1120	1.32	50.7	161	596	130
SMRF-MFT-15	67.2	43.3	0.92	1100	1.35	54.3	174	584	127
SMRF-MFT-16	71.1	43.9	0.95	1090	1.38	56.7	182	587	128
SMRF-MFT-17	66.3	42.6	0.90	1075	1.32	52.6	170	561	127
SMRF-MFT-18	64.6	42.5	0.90	1080	1.29	51.8	167	576	127
SMRF-MFT-19	59.8	42.5	0.88	1075	1.22	46.9	151	580	125
SMRF-MFT-20	52.0	41.5	0.88	1130	1.18	43.4	142	570	125
SMRF-MFT-21	53.8	40.9	0.87	1115	1.21	45.8	148	561	123
SMRF-MFT-22	54.7	41.2	0.91	1120	1.22	48.0	156	578	124
SMRF-MFT-23	54.7	42.5	0.90	1120	1.20	46.5	157	590	127
SMRF-MFT-24	54.4	42.8	0.90	1120	1.16	44.9	151	595	126

Table B-7 (continued). Diluted, Remediated Melter Feed Tank Supernate Cations Analyses (mg/L)

Sample	Mg	Mn	Na	Ni	S	Si	Ti	Zn	Zr
SMRF-MFT-1	1195	9415	22700	2805	601	314	0.62	83.8	<0.100
SMRF-MFT-2	1135	9015	21100	2725	570	201	0.65	80.9	<0.100
SMRF-MFT-3	1280	10100	24600	2555	619	724	1.26	73.3	<0.100
SMRF-MFT-4	1300	10300	23850	2605	619	453	1.26	75.2	<0.100
SMRF-MFT-5	1070	8280	25350	1650	659	194	<0.100	16.4	<0.100
SMRF-MFT-6	1040	8105	25050	1620	648	840	<0.100	16.3	<0.100
SMRF-MFT-7	1070	8285	25900	1640	672	414	<0.100	15.8	<0.100
SMRF-MFT-8	1080	8365	24800	1655	664	448	<0.100	15.3	<0.100
SMRF-MFT-9	1060	8275	25750	1635	663	425	<0.100	15.4	<0.100
SMRF-MFT-10	1060	8035	26950	1615	635	346	<1.00	15.0	<0.100
SMRF-MFT-11	1085	8285	27200	1680	635	490	<1.00	15.9	<0.100
SRMF-MFT-12	1420	10800	29500	3120	748	737	1.01	77.1	<0.100
SMRF-MFT-13	1320	10300	28150	2945	695	547	0.94	71.1	<0.100
SMRF-MFT-14	1215	9765	26200	2750	673	449	0.94	67.1	<0.100
SMRF-MFT-15	1195	9550	25700	2750	652	471	0.99	68.3	<0.100
SMRF-MFT-16	1190	9535	26450	2765	649	401	1.03	70.1	<0.100
SMRF-MFT-17	1170	9535	25800	2690	645	439	0.97	66.5	<0.100
SMRF-MFT-18	1180	9655	25700	2695	641	368	0.95	66.5	<0.100
SMRF-MFT-19	1170	9545	25950	2670	632	342	0.87	64.0	<0.100
SMRF-MFT-20	1190	9620	25650	2665	643	379	0.80	61.4	<0.100
SMRF-MFT-21	1180	9480	25250	2635	640	423	0.84	63.0	<0.100
SMRF-MFT-22	1190	9550	25100	2650	643	404	0.87	64.1	<0.100
SMRF-MFT-23	1200	9695	26300	2705	652	238	0.86	64.6	<0.100
SMRF-MFT-24	1200	9750	26200	2725	640	251	0.84	64.2	<0.100

Table B-8. Select Diluted, Remediated Melter Feed Tank Supernate Anions Analyses (mg/L)

	Anions (mg/L)								
Sample	**F**	**Cl**	**NO_2**	**NO_3**	**C_2O_4**	**SO_4**	**PO_4**	**HCO_2**	**$C_2H_3O_3$**
SMRF-MFT-1	<100	442	<100	75250	745	1515	1830	1025	17400
SMRF-MFT-2	<100	389	<100	72100	806	1575	<100	1755	17200
SMRF-MFT-4	<100	437	<100	80850	993	1415	<100	2145	21700
SMRF-MFT-17	<100	466.5	<100	73150	859.5	1620	<100	1115	27550
SMRF-MFT-19	<100	453.5	<100	72300	830	1640	<100	1070	27000
SMRF-MFT-21	<100	451	<100	71600	810	1625	<100	1340	26200
SMRF-MFT-22	<100	460.5	<100	73650	848	1710	<100	1395	27150
SMRF-MFT-24	<100	466.5	<100	74250	849	1710	<100	1150	27800

Table B-9. Melter Feed Tank Total Organic Carbon (TOC) Analyses (ppm)

Sample	Average TOC (DWPF)	Average TOC (SRNL AD)		Sample	Average TOC (DWPF)	Average TOC (SRNL AD)
SMRF-MFT-1	10899	10070		SMRF-MFT-13	13569	17097
SMRF-MFT-2	9488	9901		SMRF-MFT-14	13344	13593
SMRF-MFT-3	11517	11202		SMRF-MFT-15	13901	12791
SMRF-MFT-4	12412	10574		SMRF-MFT-16	12295	13254
SMRF-MFT-5	10546	10812		SMRF-MFT-17	12786	14125
SMRF-MFT-6	10140	10516		SMRF-MFT-18	13528	14146
SMRF-MFT-7	9721	10682		SMRF-MFT-19	13185	13780
SMRF-MFT-8	9805	11368		SMRF-MFT-20	11792	12935
SMRF-MFT-9	9254	10705		SMRF-MFT-21	12824	13296
SMRF-MFT-10	10240	10633		SMRF-MFT-22	12739	12500
SMRF-MFT-11	9837	11531		SMRF-MFT-23	12786	12898
SRMF-MFT-12	14582	14860		SMRF-MFT-24	12556	17285

Appendix C. Supplemental Condensate Analytical Data

Table C-1. Averaged Condensate Cation Compositions

	Cations (mg/L)																		
Sample	Al	Ba	Ca	Cr	Cu	Fe	K	Li	Mg	Mn	Na	Ni	P	S	Si	Sn	Ti	Zn	Zr
SMRF-C-11	3.69	<1.0	5.14	<1.0	1.59	<1.0	2.12	<1.0	<1.0	4.56	50.3	<1.0	<1.0	1.62	7.38	<1.0	<1.0	<1.0	<1.0
SMRF-C-23	<1.0	<1.0	4.79	<1.0	<1.0	<1.0	2.24	<1.0	<1.0	2.97	60.2	<1.0	<1.0	2.24	5.64	<1.0	<1.0	<1.0	<1.0
SMRF-C-37	<1.0	<1.0	5.28	<1.0	<1.0	<1.0	2.28	1.08	<1.0	<1.0	75.4	<1.0	<1.0	2.94	4.27	<1.0	<1.0	<1.0	<1.0
SMRF-C-44	<1.0	<1.0	4.53	<1.0	<1.0	<1.0	2.27	1.24	<1.0	<1.0	76.7	<1.0	<1.0	7.83	2.64	<1.0	<1.0	<1.0	<1.0

Table C-2. Averaged Condensate Anion Compositions

	Anions (mg/L)							
Sample	F	Cl	NO_2	NO_3	SO_4	C_2O_4	$C_2H_3O_3$	HCO_2
SMRF-C-11	<100	<100	<100	599.5	<100	<100	<100	<100
SMRF-C-23	<100	<100	<100	731.5	<100	<100	<100	<100
SMRF-C-37	<100	<100	321	903	<100	<100	<100	<100
SMRF-C-44	<100	<100	416.5	818	<100	<100	<100	<100

Table C-3. Condensate Solids Data, Density and pH

Sample	Total Solids	Density (g/cm^3)	pH
SMRF-C-11	<0.10%	0.99757	3.69
SMRF-C-23	<0.10%	0.99770	7.05
SMRF-C-37	0.10%	0.99796	7.65
SMRF-C-44	0.24%	0.99811	8.32

Appendix D. Supplemental Glass Analytical Data

Table D-1. Averaged MRF REDOX Measurements

Sample	Remediation	Fe^{2+}	ΣFe	Fe^{3+}	Fe^{2+}/Fe^{3+}	$Fe^{2+}/\Sigma Fe$
MRF-16-2	Unremediated	0.075	0.363	0.289	0.258	0.205
MRF-16-3	HNO_3-remediated	0.023	0.298	0.275	0.083	0.076
MRF-16-4	$NaNO_3$-remediated	0.034	0.321	0.287	0.119	0.106
MRF-16-5	Glycolic/NaOH-remediated	0.250	0.423	0.173	1.448	0.591

Table D-2. Poured Glass Elemental Composition

	SMRF-G-17			SMRF-G-22	
Elements (Oxides)	Elemental wt.%	Oxide wt.%		Elemental wt.%	Oxide wt.%
Al (Al_2O_3)	6.01	11.37		5.55	10.48
B (B_2O_3)	1.46	4.70		1.54	4.95
Ba (BaO)	<0.100	<0.11		<0.100	<0.11
Ca (CaO)	0.42	0.58		0.37	0.52
Cr (Cr_2O_3)	0.15	0.22		0.09	0.14
Cu (CuO)	<0.100	<0.13		<0.100	<0.13
Fe (Fe_2O_3)	9.48	13.56		8.37	11.97
K (K_2O)	0.17	0.20		0.15	0.18
Li (Li_2O)	2.12	4.57		2.22	4.76
Mg (MgO)	0.34	0.56		0.29	0.48
Mn (MnO)	2.56	3.31		2.37	3.06
Na (Na_2O)	9.43	12.73		9.30	12.56
Ni (NiO)	1.20	1.52		0.99	1.26
P (P_2O_5)	<0.100	<0.23		<0.100	<0.23
S (SO_4)	0.15	0.45		0.13	0.38
Si (SiO_2)	21.40	45.79		21.74	46.52
Sn (SnO)	<0.100	<0.11		<0.100	<0.11
Ti (TiO_2)	<0.100	<0.17		<0.100	<0.17
Zn (ZnO)	<0.100	<0.12		<0.100	<0.12
Zr (ZrO_2)	0.10	0.14		0.10	0.13

Appendix E. Supplemental Melter Operations Data

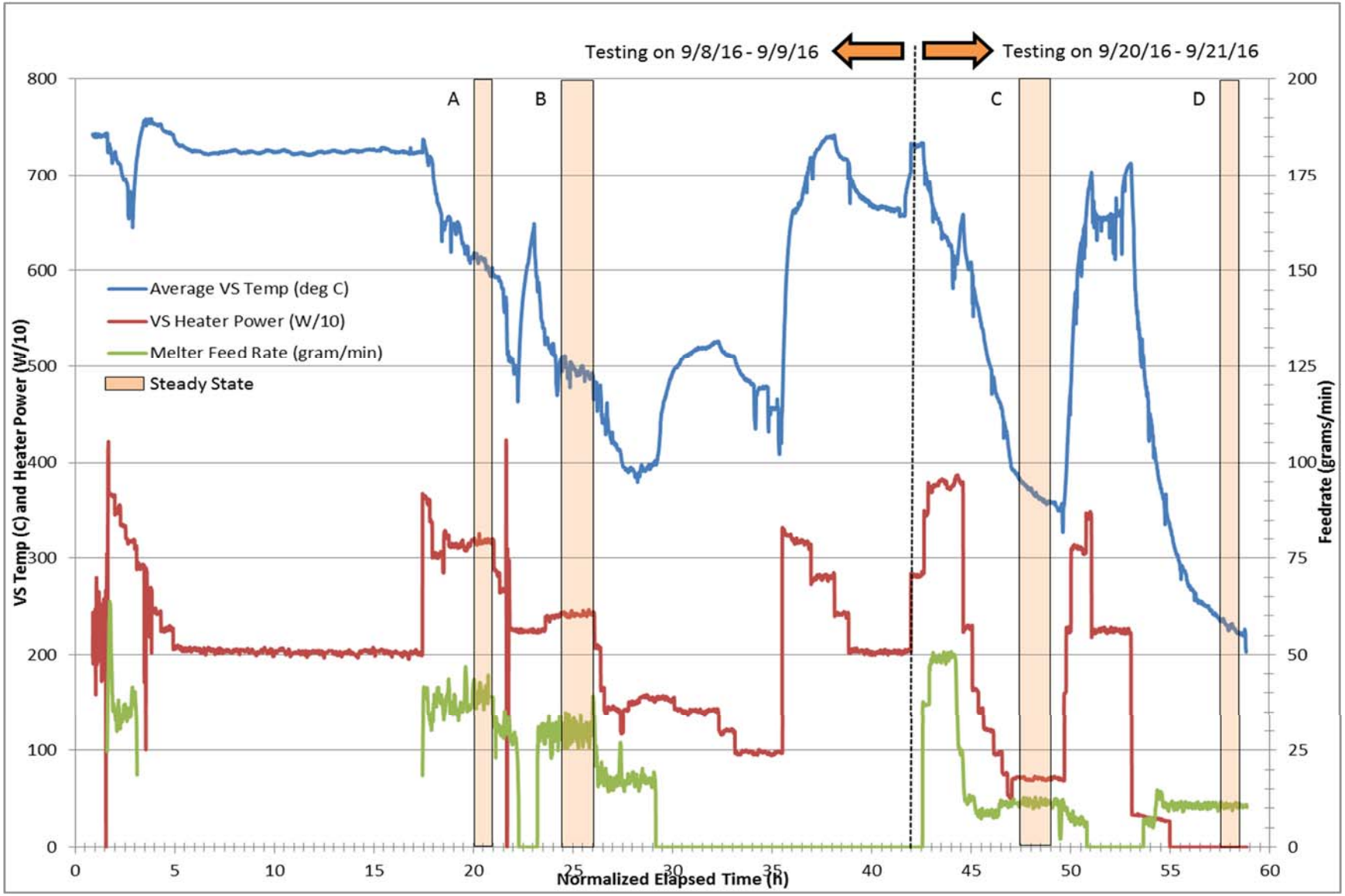

Figure E-1. HNO_3-Remediated Feed Vapor Space Temperature, Vapor Space Heater Power, and Melter Feed Rate as a Function of Normalized Elapsed Time; Steady State Temperatures A) 628, B) 496, C) 381, and D) 238.

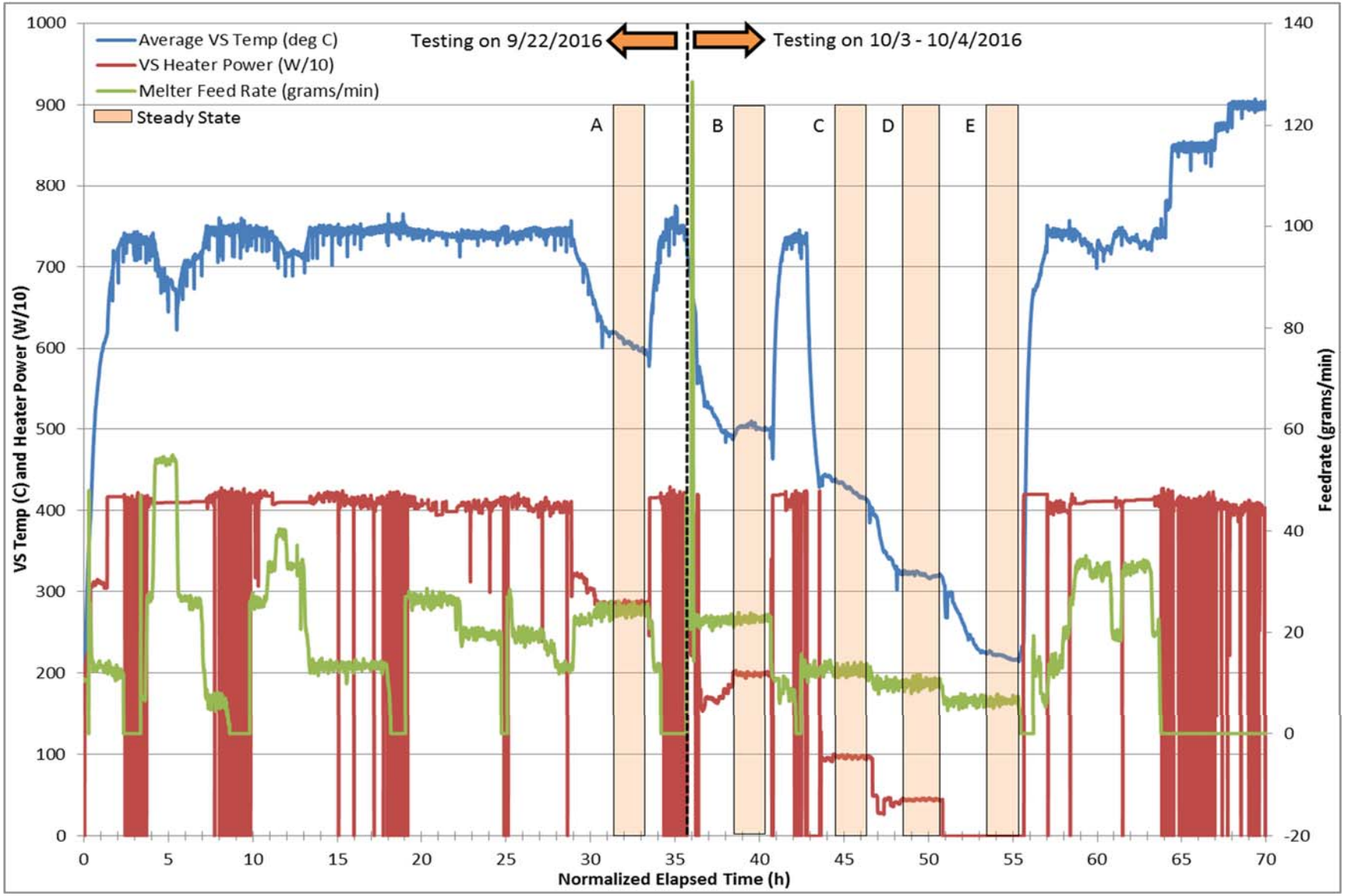

Figure E-2. Unremediated Feed Vapor Space Temperature, Vapor Space Heater Power, and Melter Feed Rate as a Function of Normalized Elapsed Time: Steady State Temperatures: A) 606, B) 501, C) 432, D) 321, and E) 222.

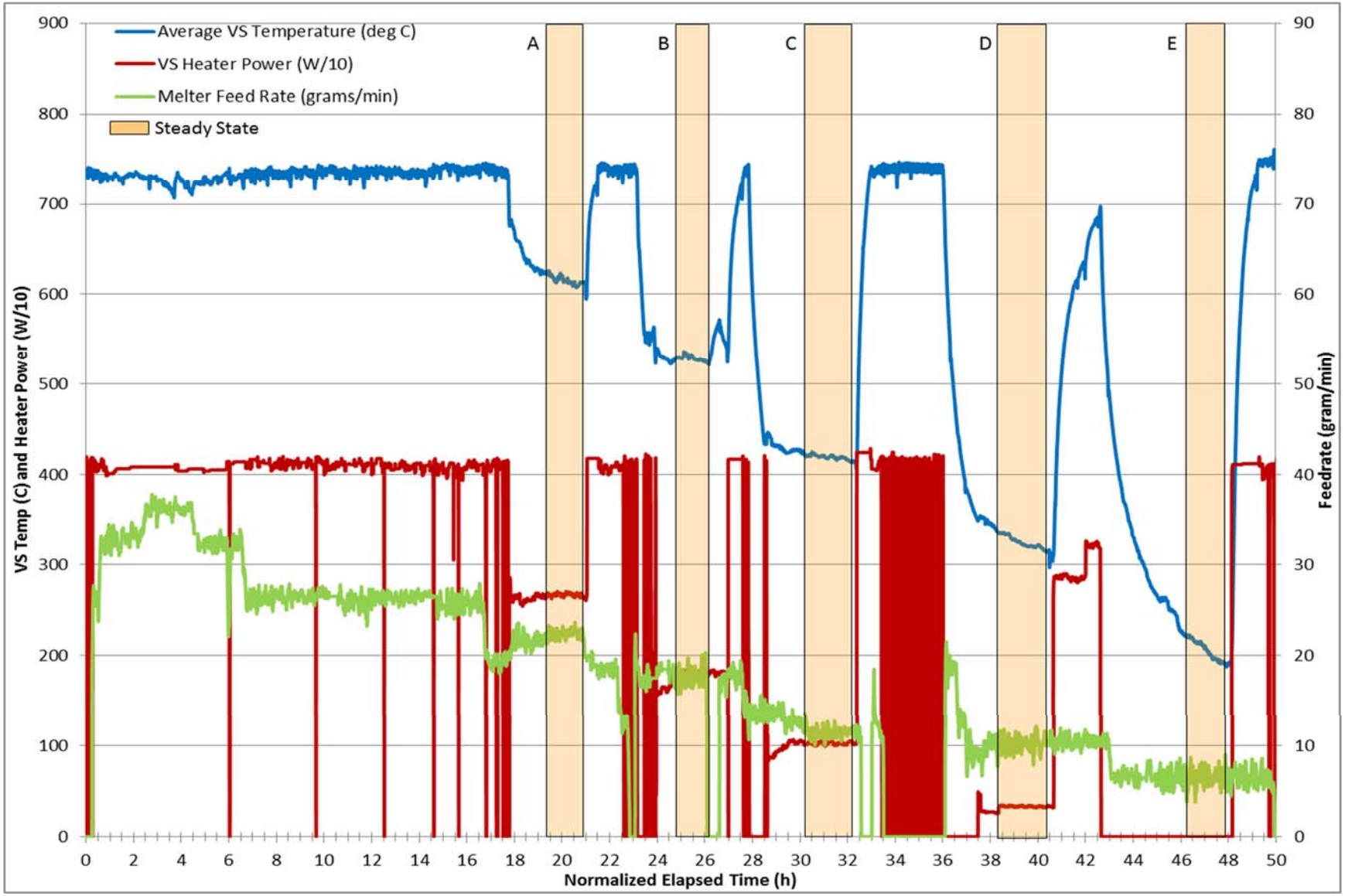

Figure E-3. Glycolic-Remediated Feed Vapor Space Temperature, Vapor Space Heater Power, and Melter Feed Rate as a Function of Normalized Elapsed Time: Steady State Temperatures: A) 616, B) 508, C) 421, D) 324, and E) 208.

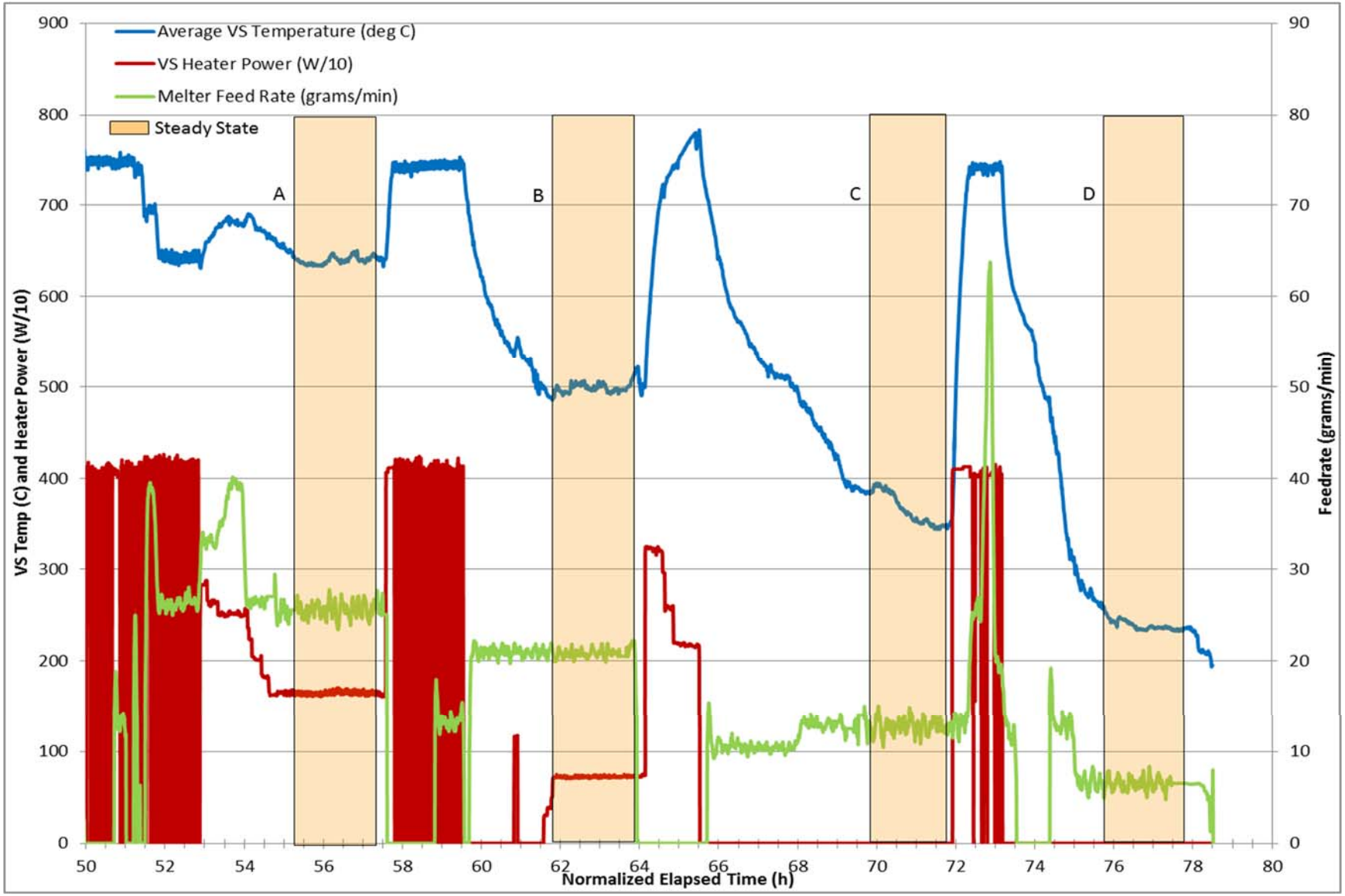

Figure E-4. Bubbled Glycolic-Remediated Feed Vapor Space Temperature, Vapor Space Heater Power, and Melter Feed Rate as a Function of Normalized Elapsed Time: Steady State Temperatures: A) 641, B) 499, C) 364, and D) 239.

Appendix F. Supplemental Offgas Analysis Data

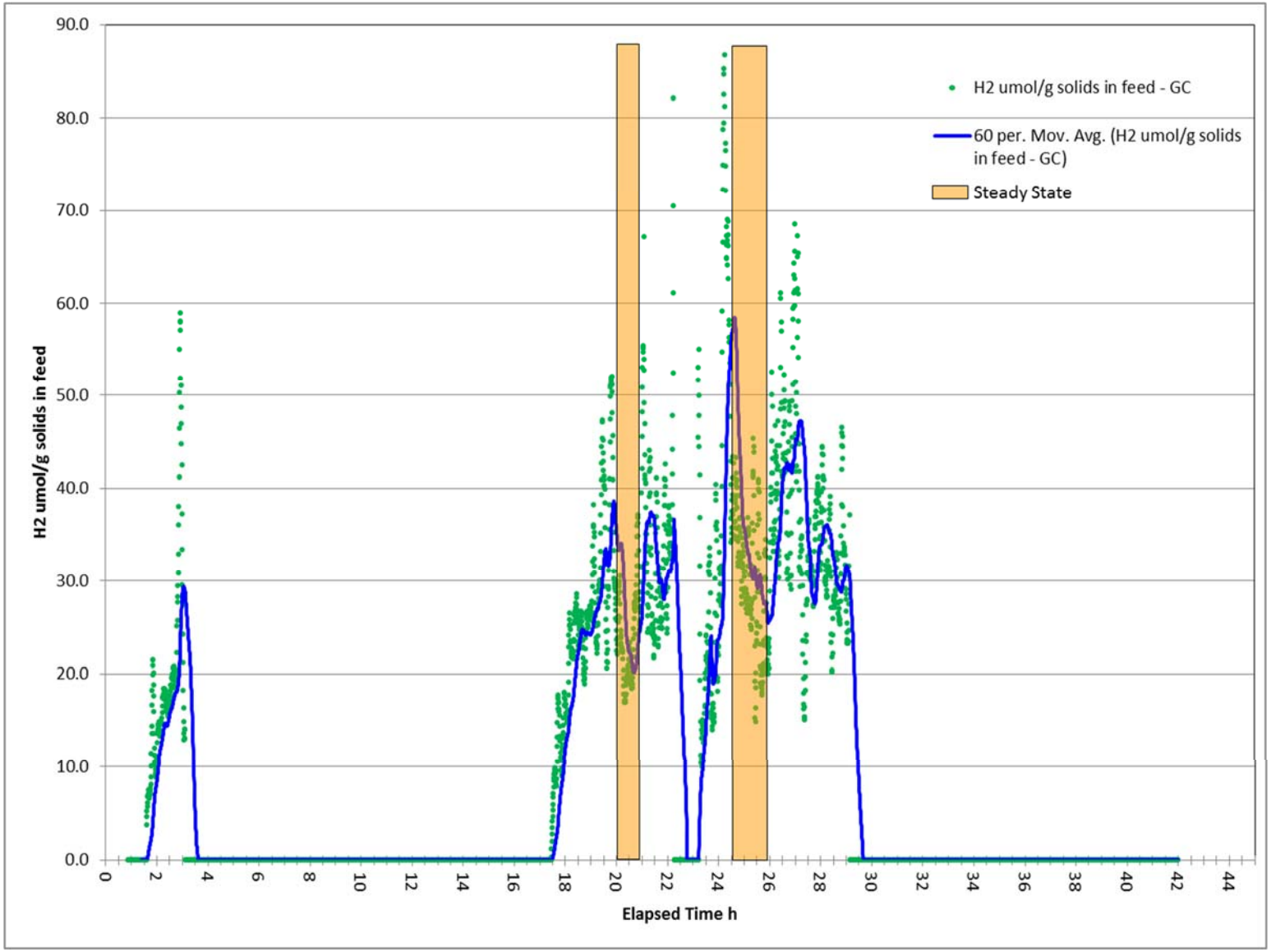

Figure F-1. Nitric-Remediated Feed - H_2 µmol per Gram of Solids in Melter Feed as a Function of Time during High VS Temperature Steady States (628 and 496°C from left to right)

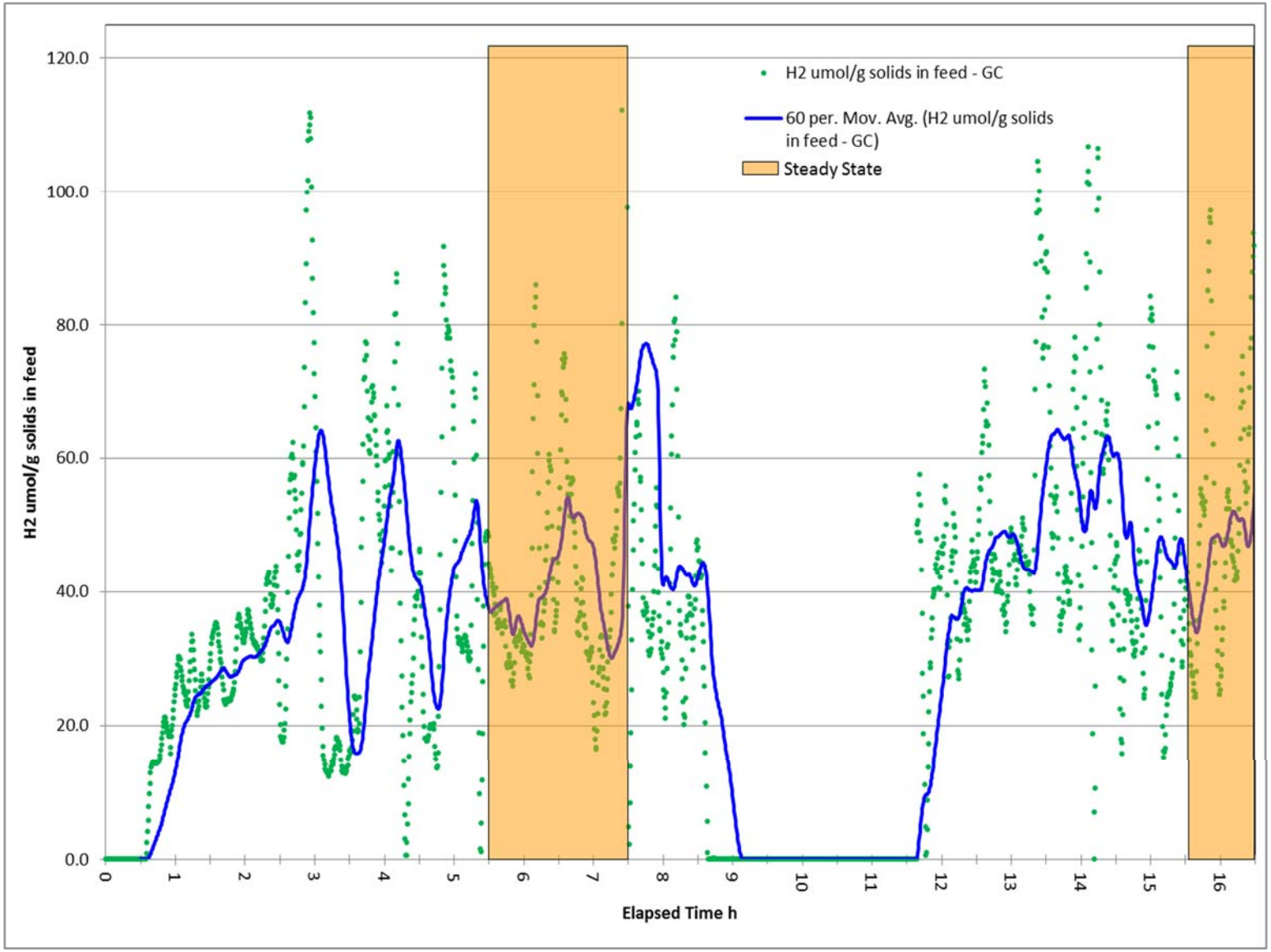

Figure F-2. Nitric-Remediated Feed - H_2 µmol per Gram of Solids in Melter Feed as a Function of Time during Low VS Temperature Steady States (381 and 238°C from left to right)

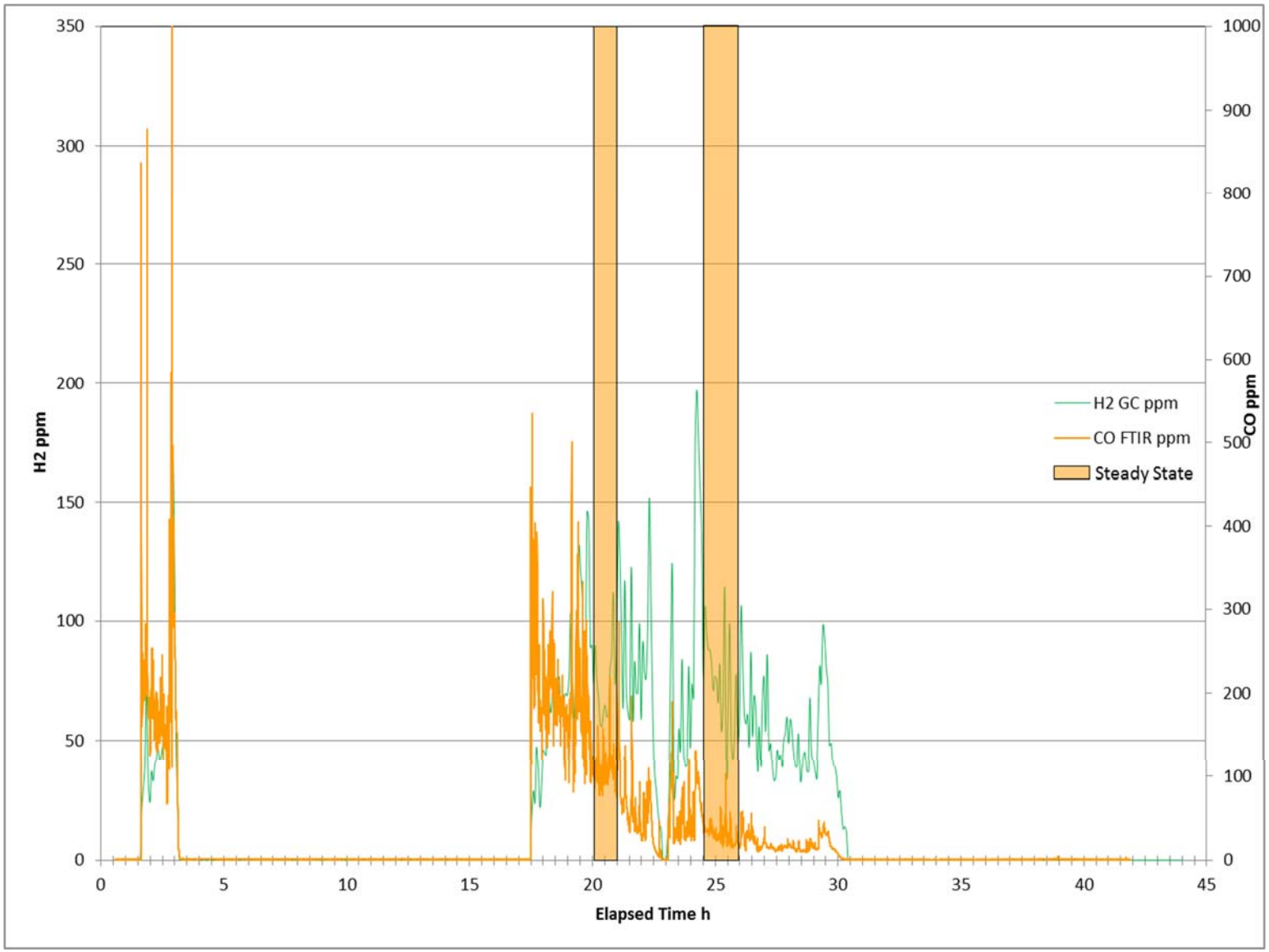

Figure F-3. Nitric-Remediated Feed - H_2 ppm and CO ppm during High VS Temperature Steady States (628 and 496°C from left to right)

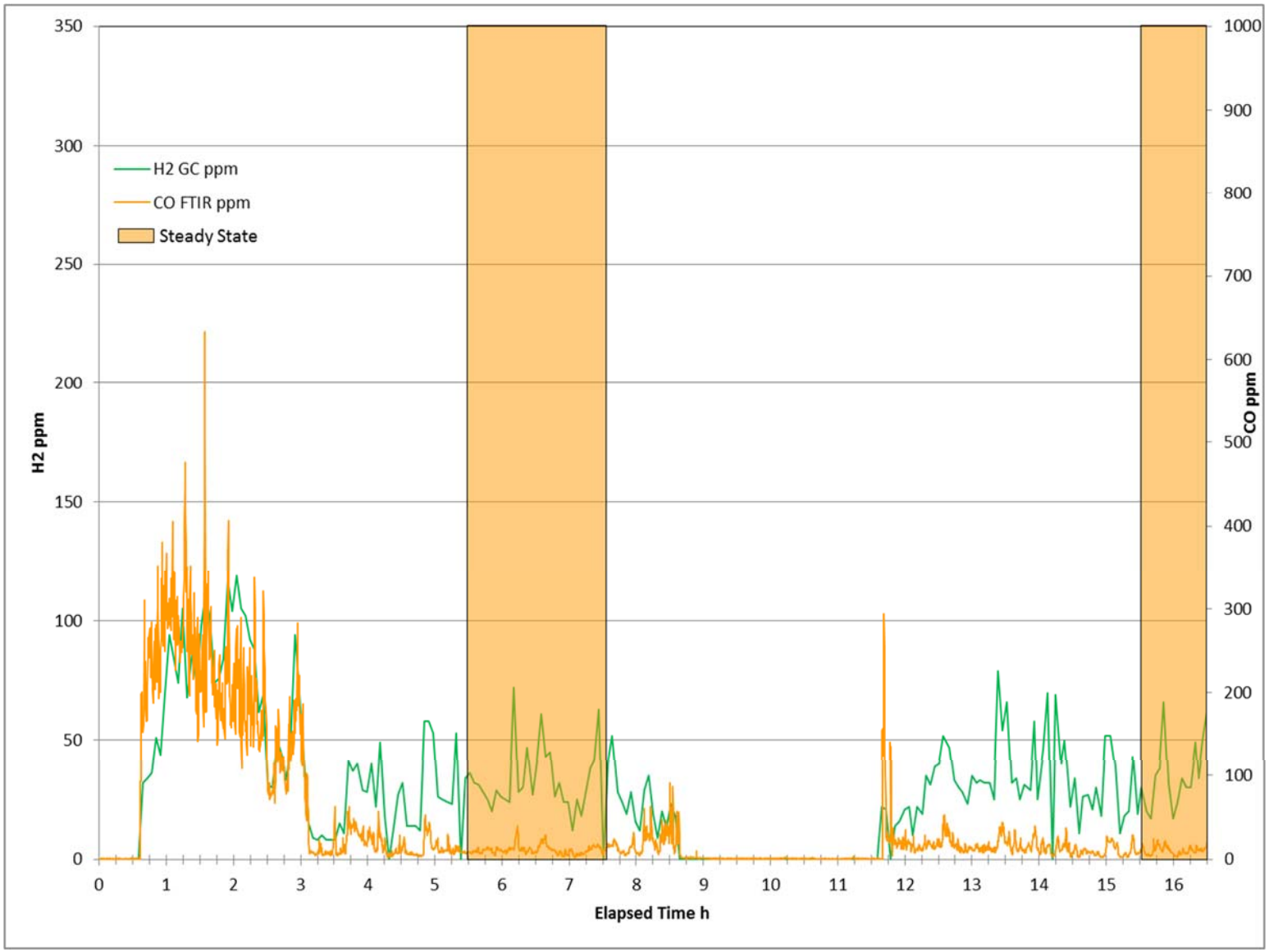

Figure F-4. Nitric-Remediated Feed - H_2 ppm and CO ppm during Low VS Temperature Steady States (381 and 238°C from left to right)

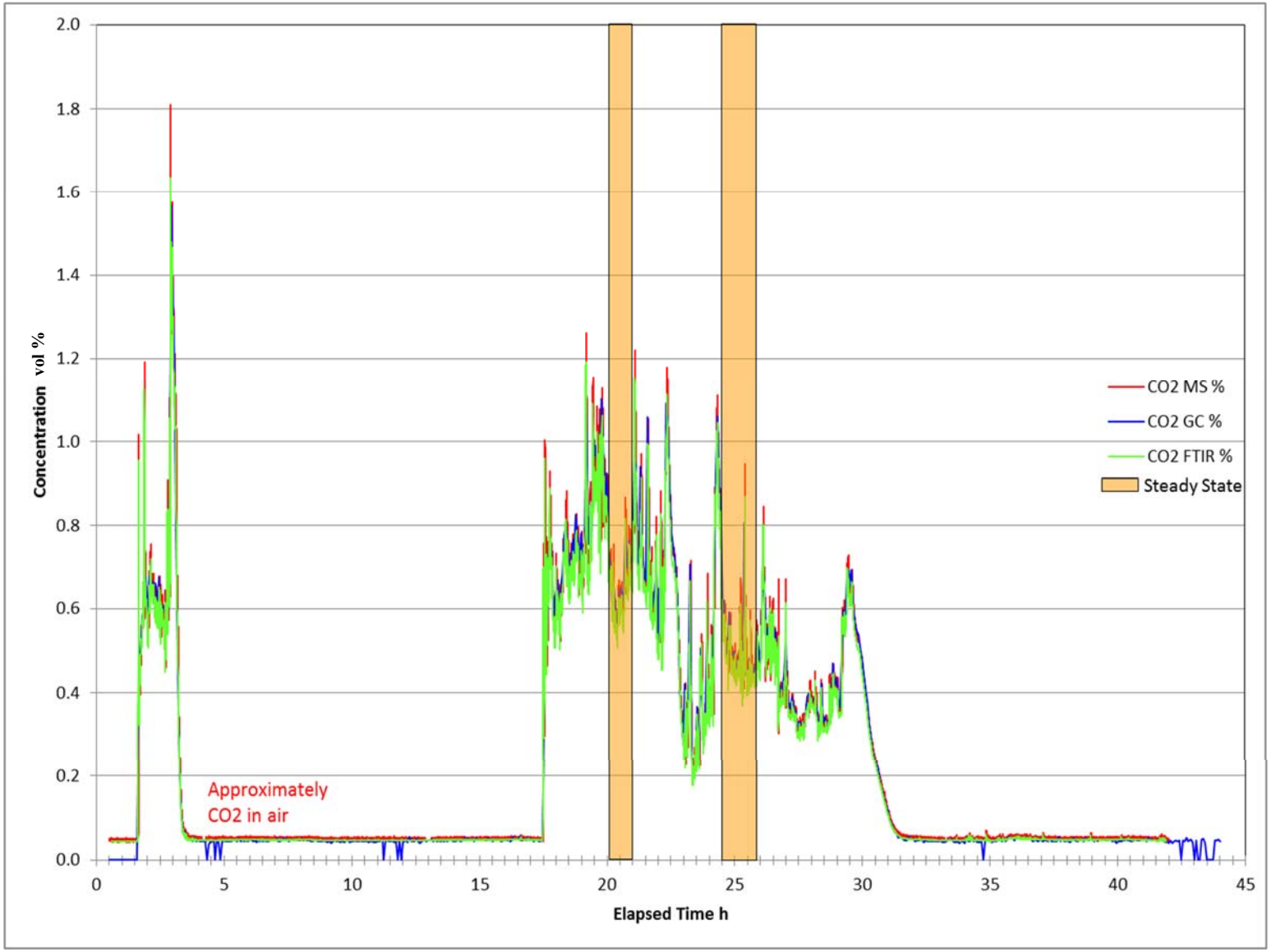

Figure F-5. Nitric-Remediated Feed – CO_2% during High VS Temperature Steady States (628 and 496°C (from left to right)

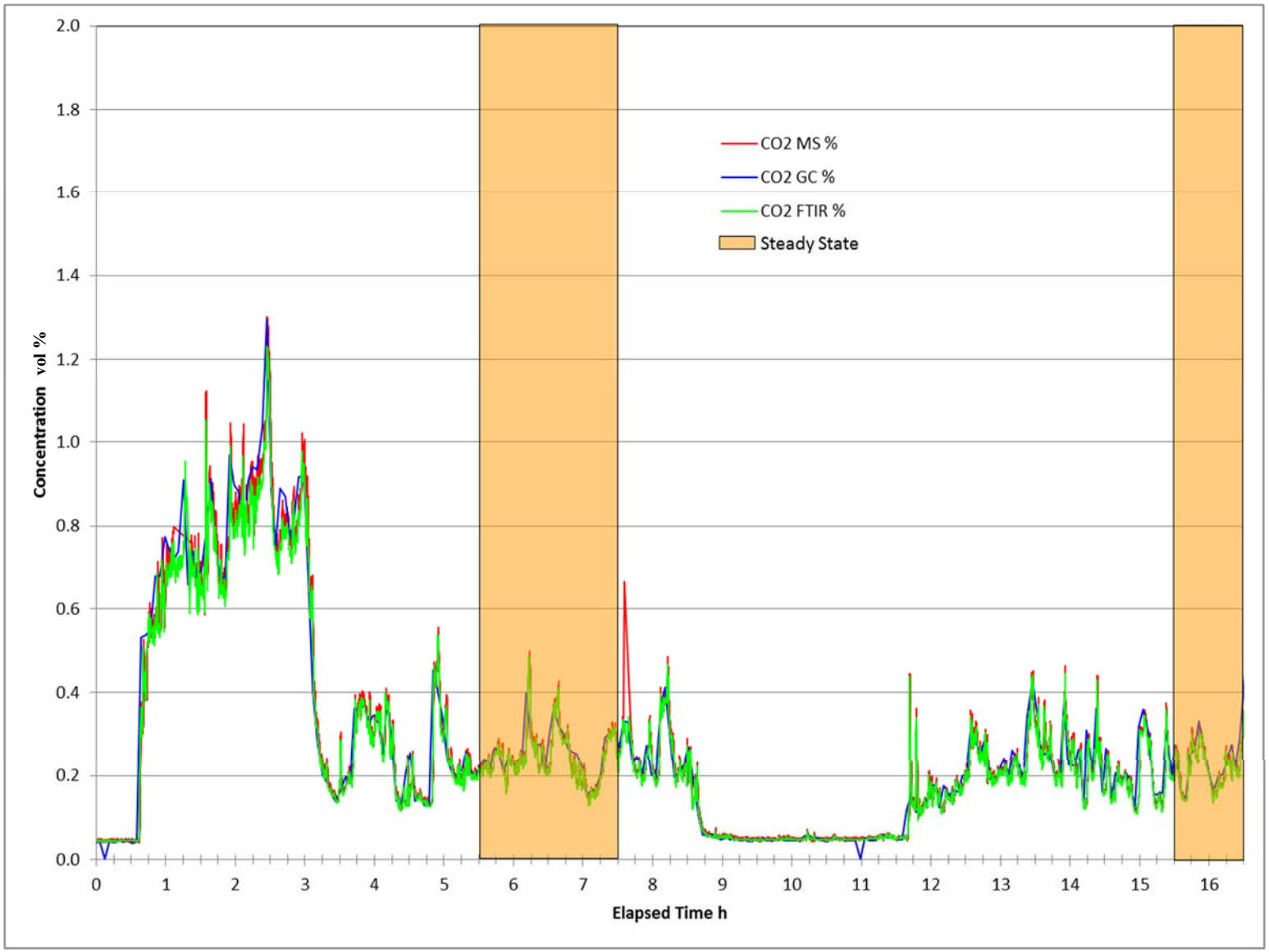

Figure F-6. Nitric-Remediated Feed – CO_2% during Low VS Temperature Steady States (381 and 238°C from left to right)

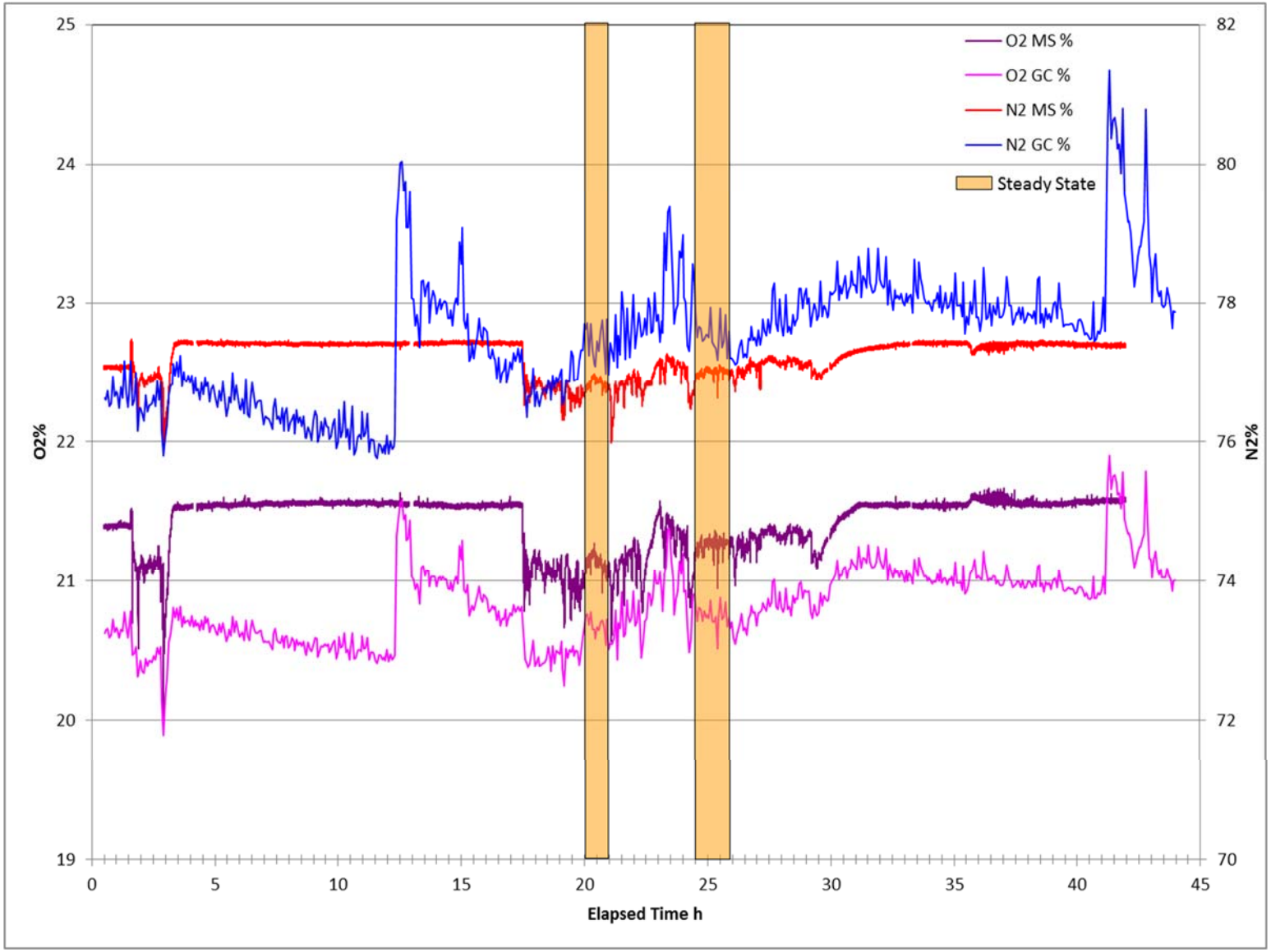

Figure F-7. Nitric-Remediated Feed – N_2% and O_2% during High VS Temperature Steady States (628 and 496°C from left to right)

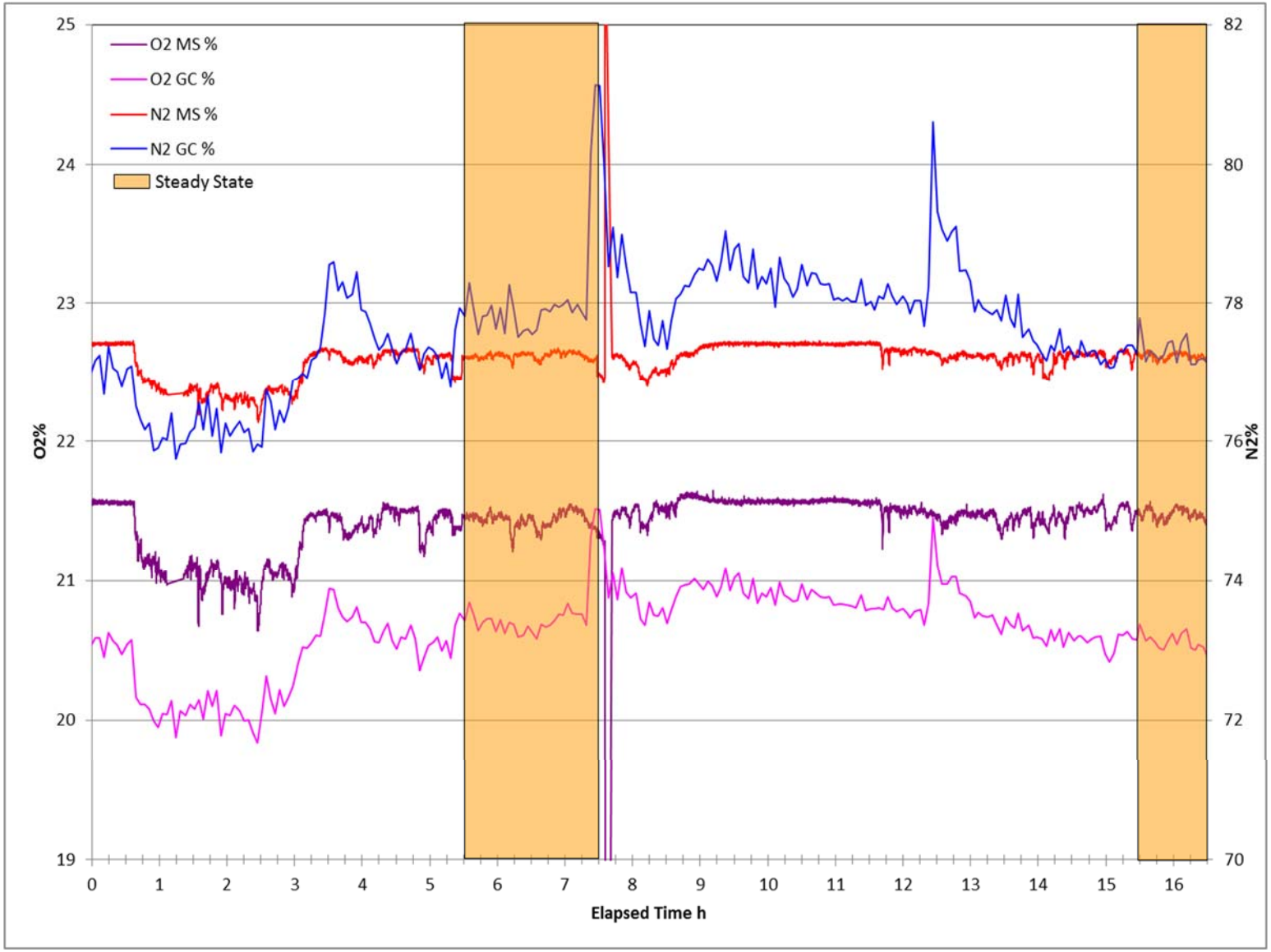

Figure F-8. Nitric-Remediated Feed – N_2% and O_2% during Low VS Temperature Steady States (381 and 238°C from left to right)

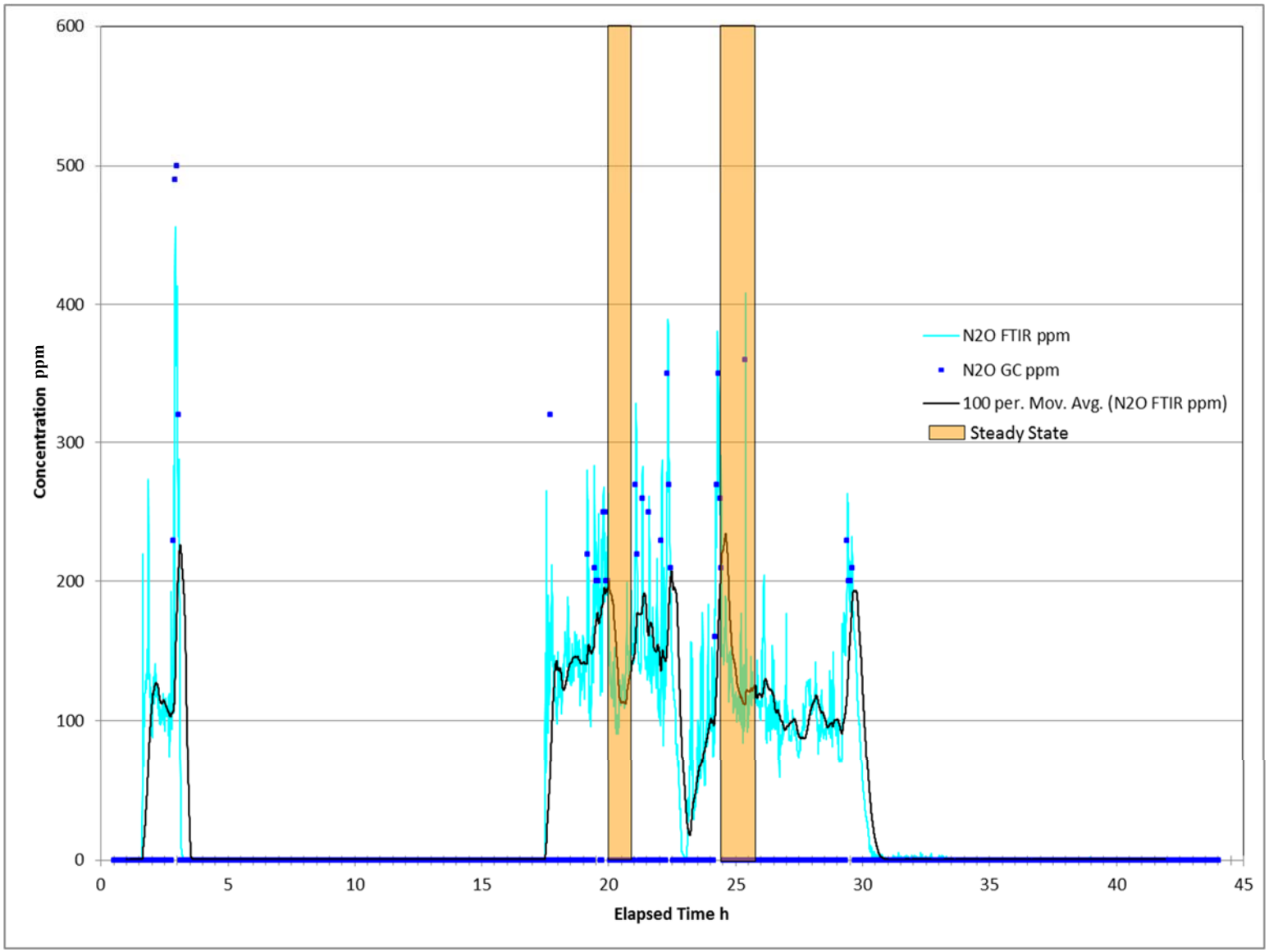

Figure F-9. Nitric-Remediated Feed – N_2O ppm during High VS Temperature Steady States (628 and 496°C from left to right)

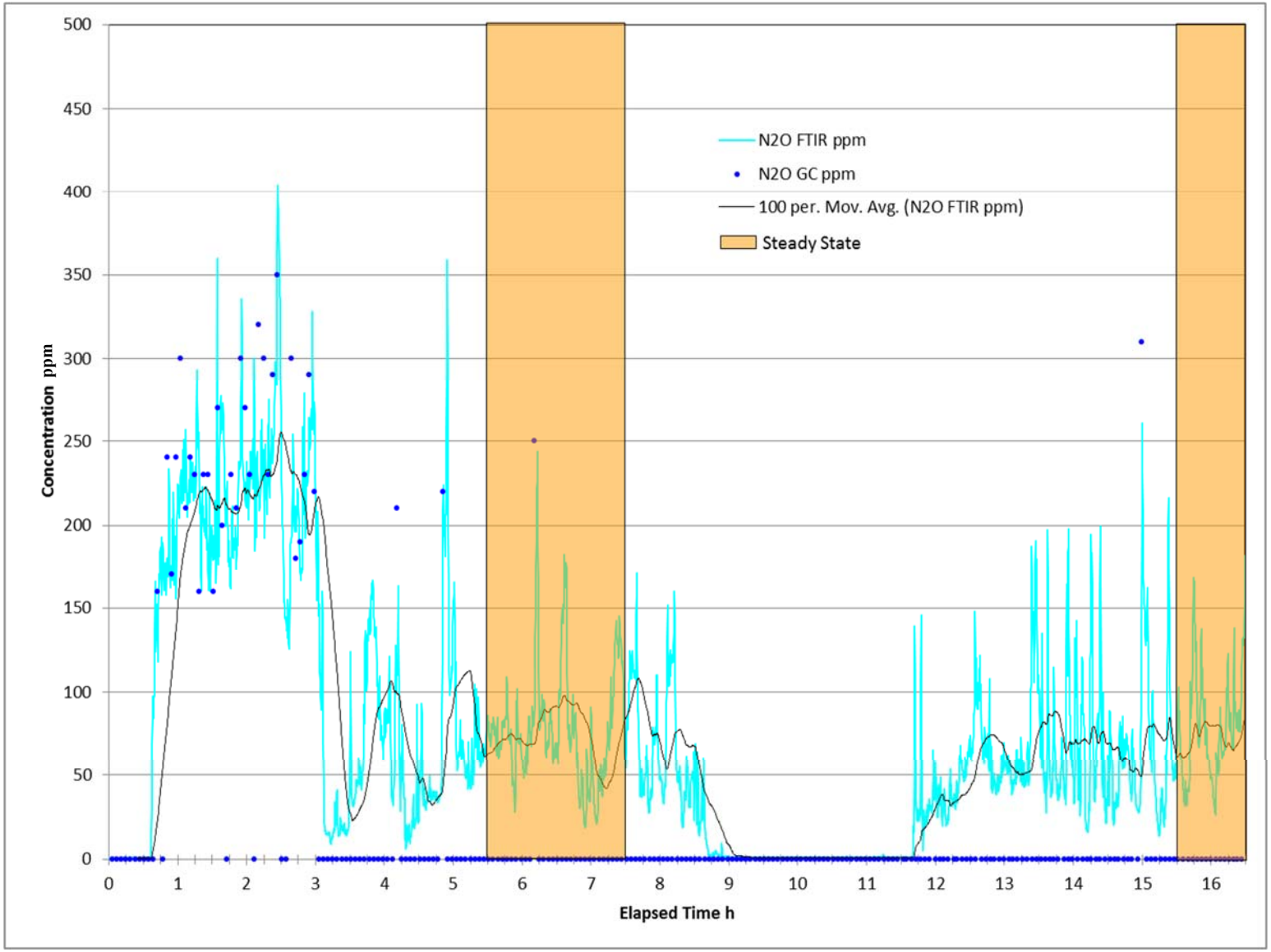

Figure F-10. Nitric-Remediated Feed – N_2O ppm during Low VS Temperature Steady States (381 and 238°C from left to right)

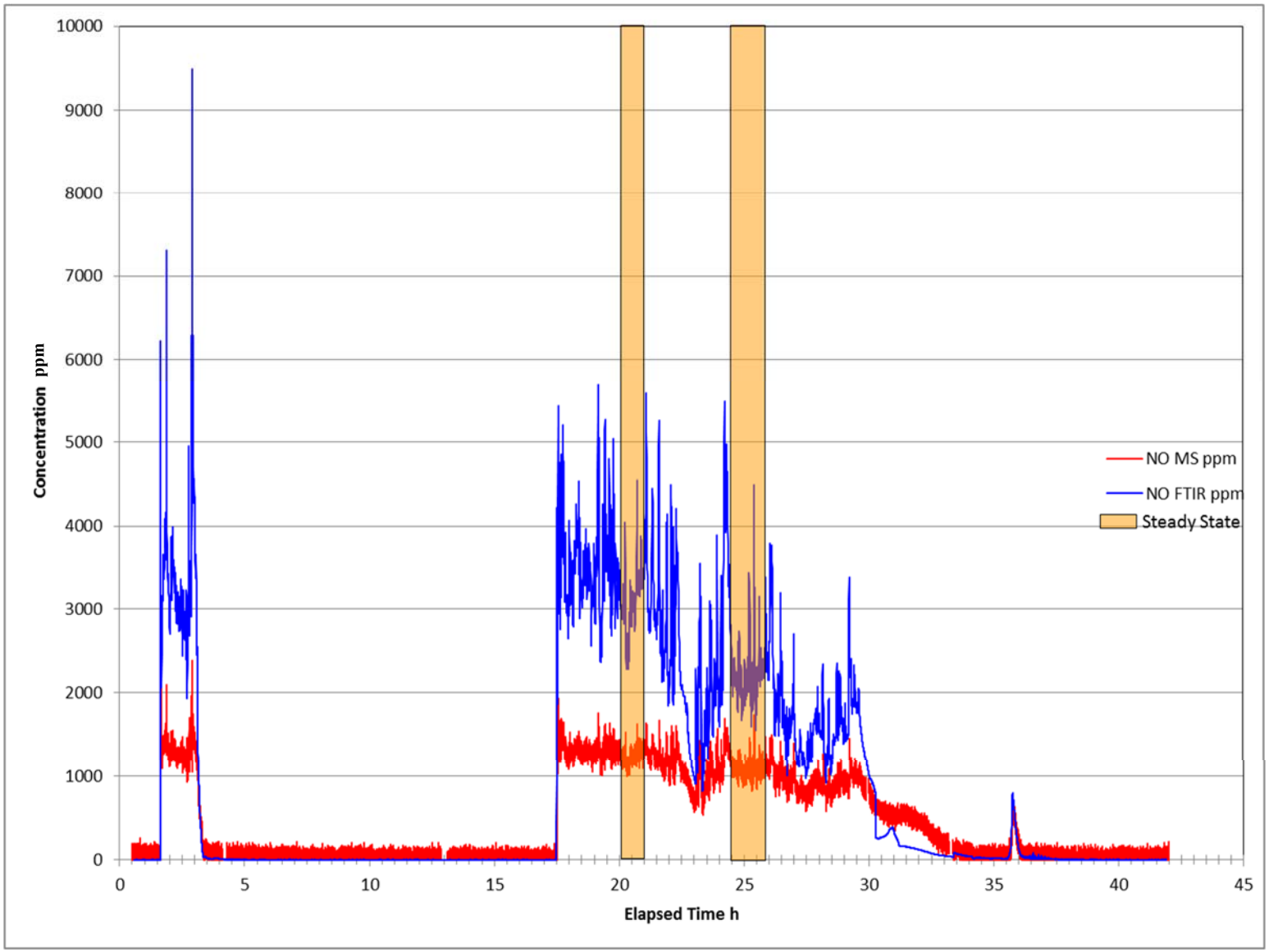

Figure F-11. Nitric-Remediated Feed – NO ppm during High VS Temperature Steady States (628 and 496°C from left to right)

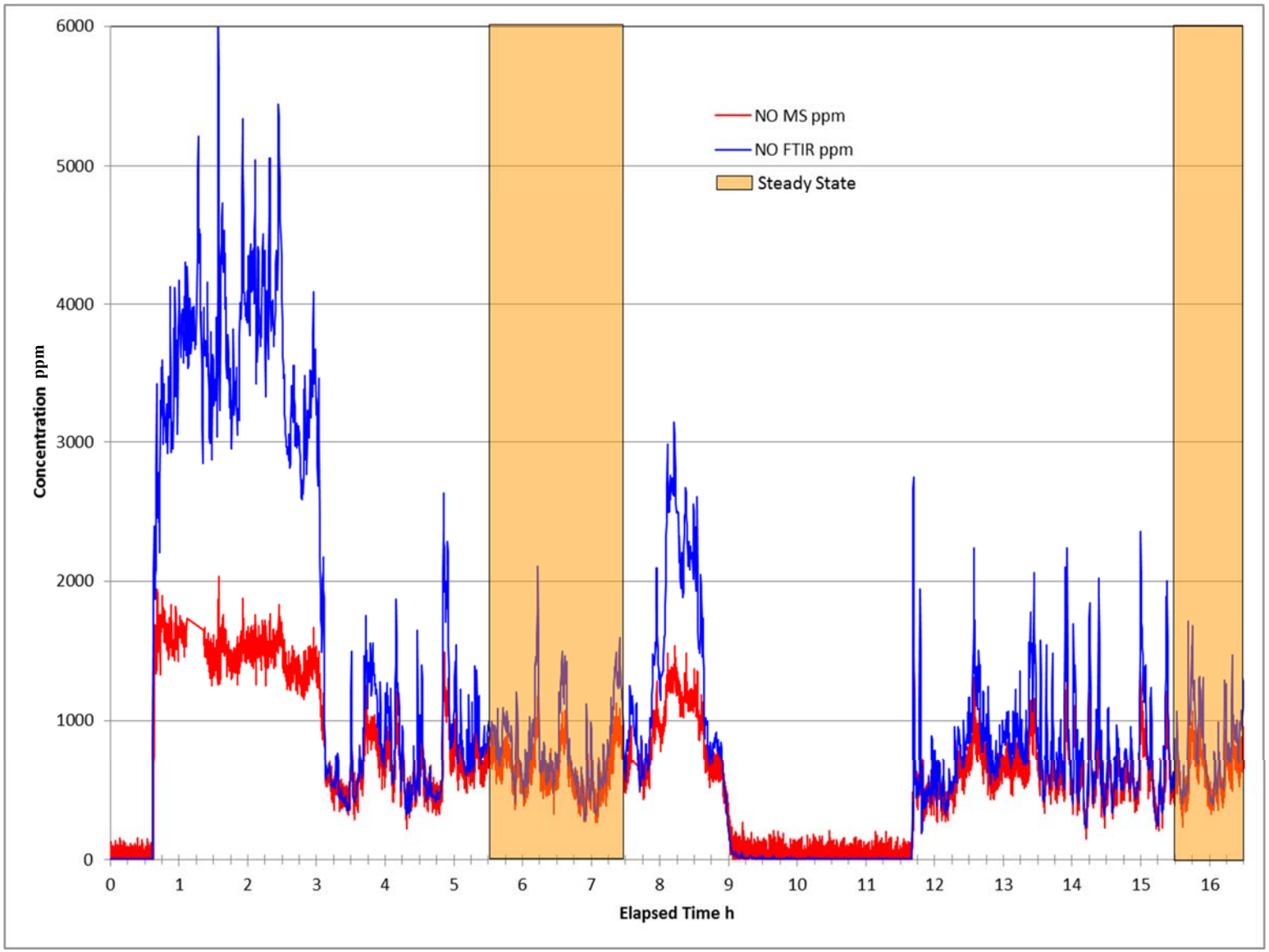

Figure F-12. Nitric-Remediated Feed – NO ppm during Low VS Temperature Steady States (381 and 238°C from left to right)

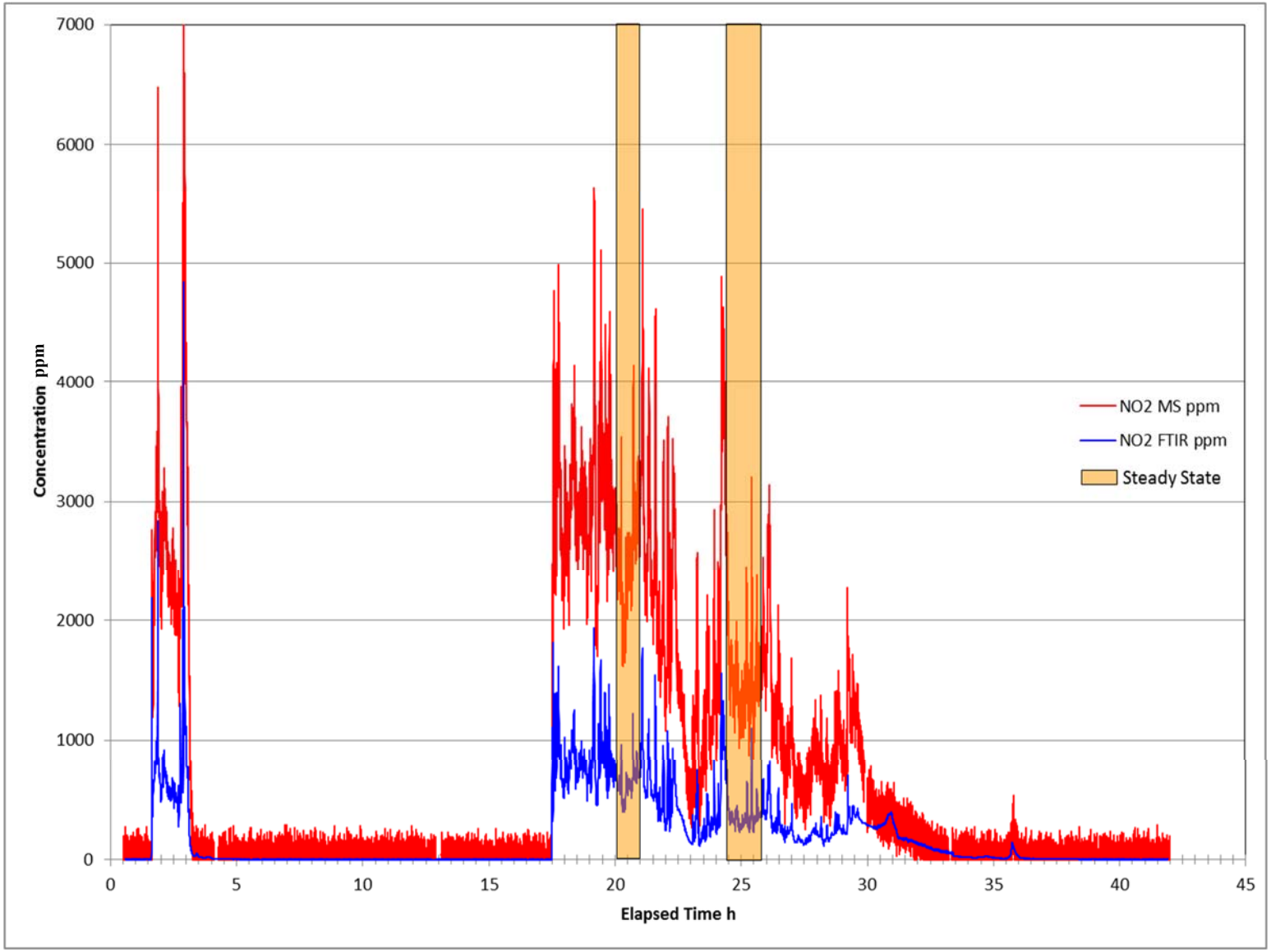

Figure F-13. Nitric-Remediated Feed – NO_2 ppm during High VS Temperature Steady States (628 and 496°C from left to right)

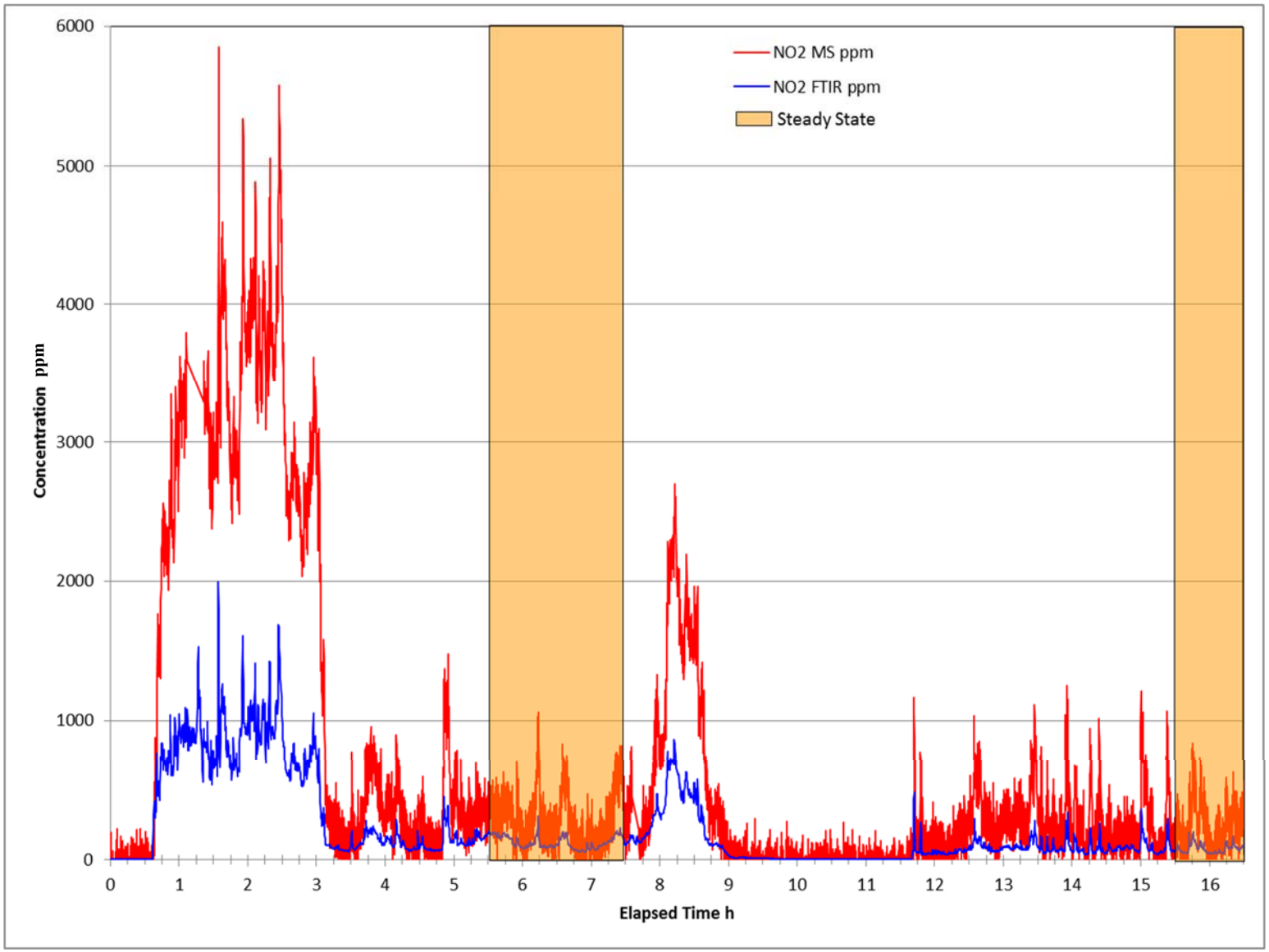

Figure F-14. Nitric-Remediated Feed – NO_2 ppm during Low VS Temperature Steady States (381 and 238°C from left to right)

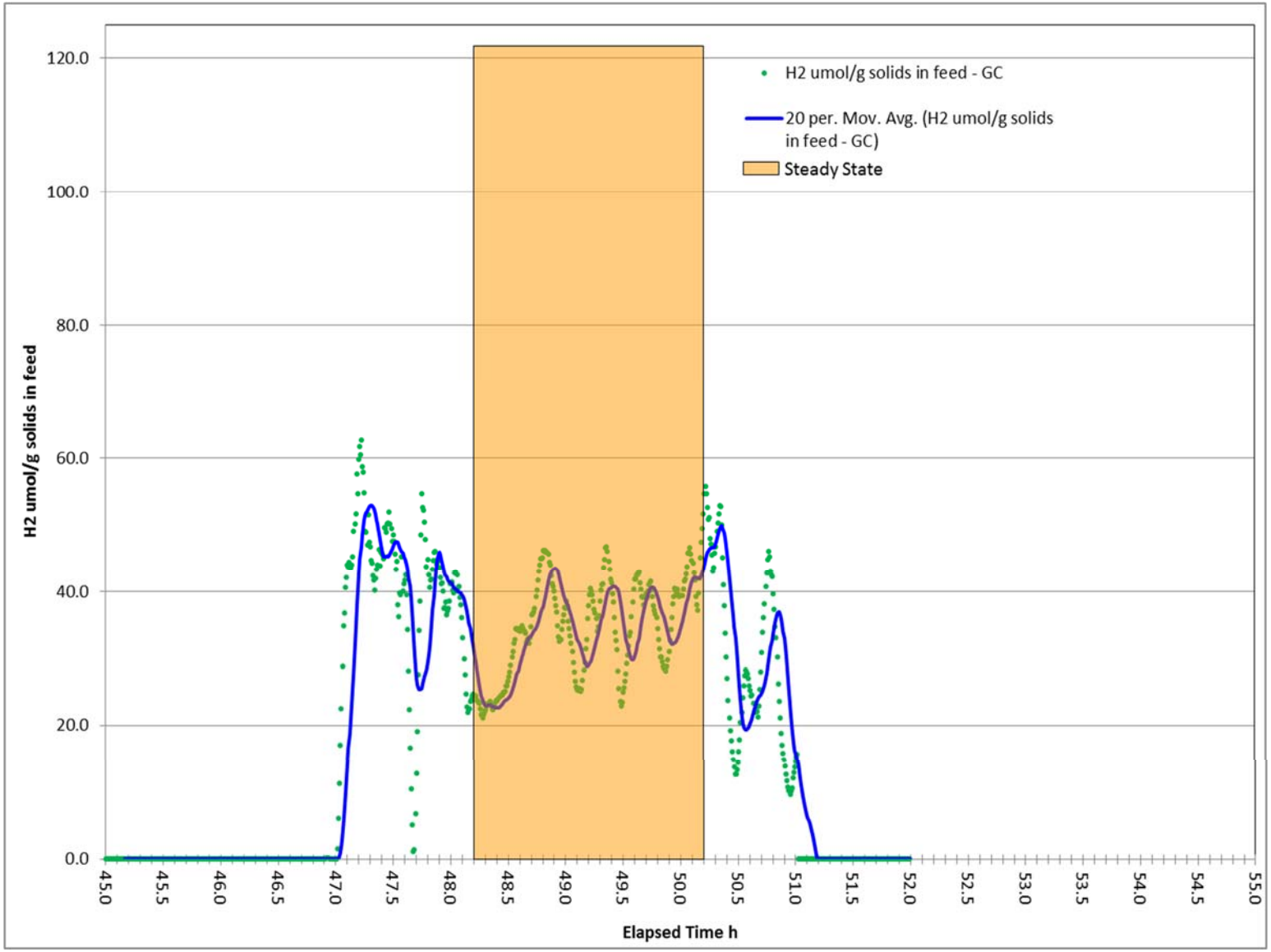

Figure F-15. Unremediated Feed - H_2 µmol per Gram of Solids in Melter Feed as a Function of Time during High VS Temperature Steady State (606°C)

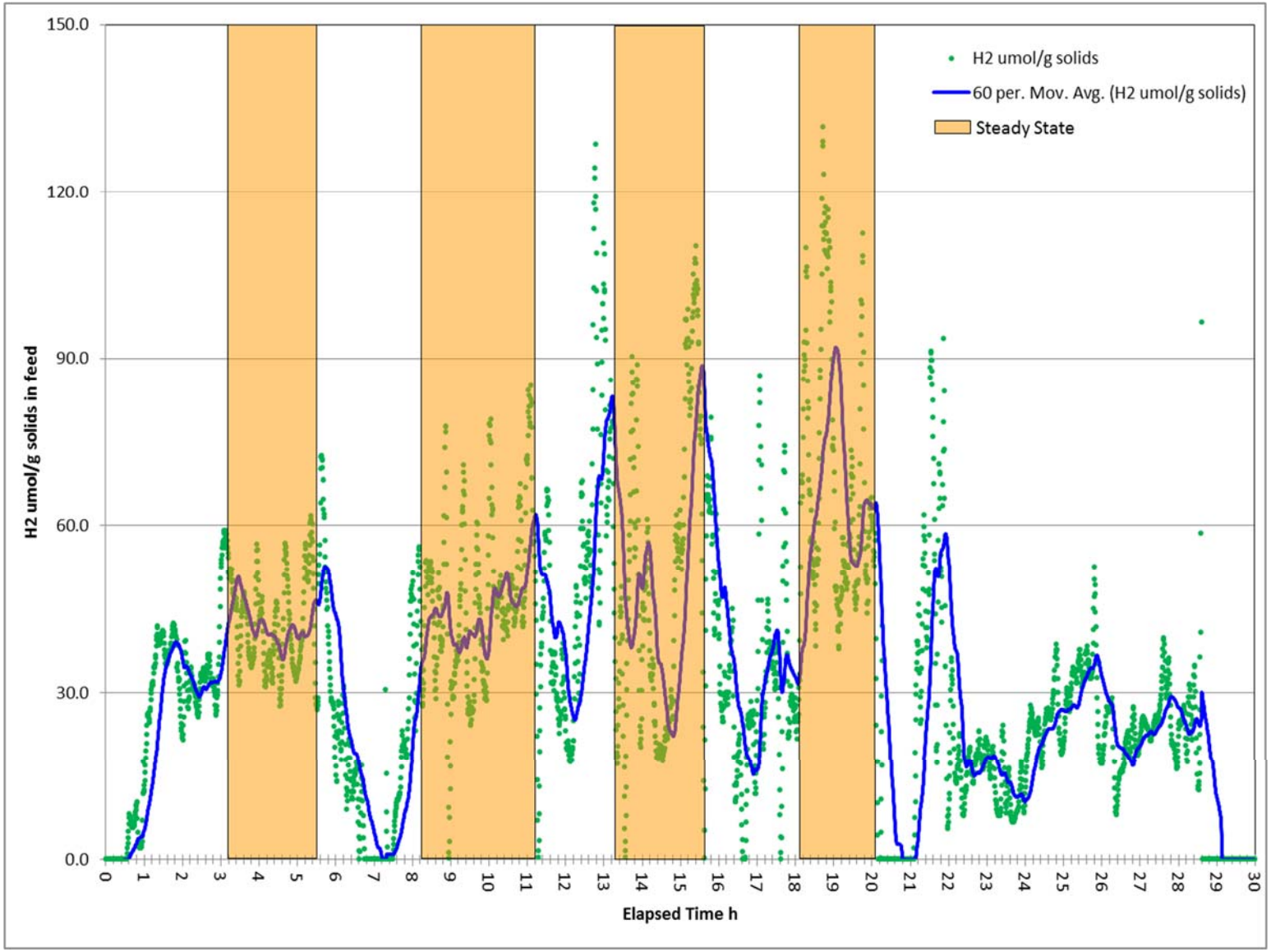

Figure F-16. Unremediated Feed - H_2 µmol per Gram of Solids in Melter Feed as a Function of Time during Low VS Temperature Steady States (501, 432, 321, and 222°C from left to right)

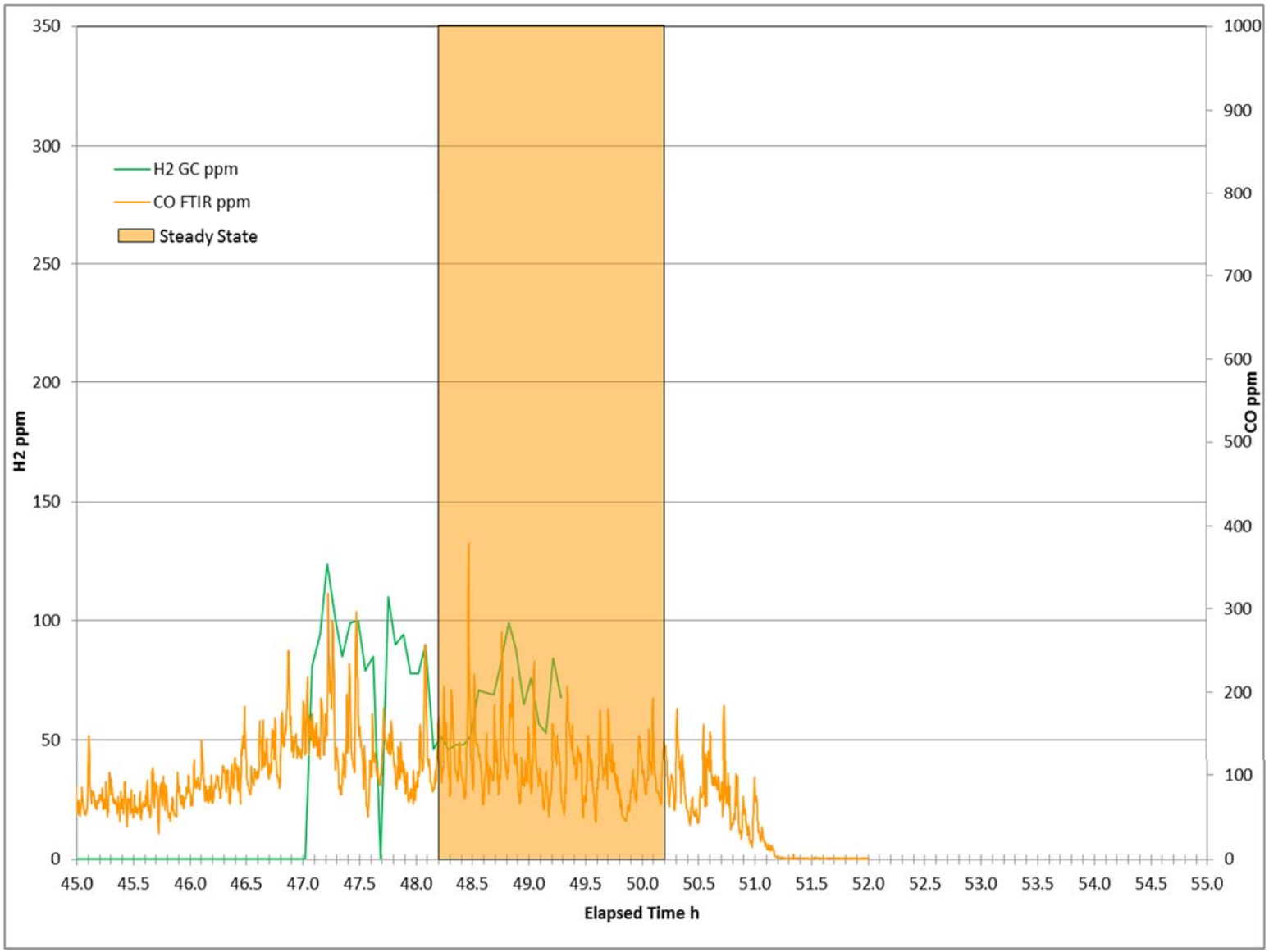

Figure F-17. Unremediated Feed - H_2 ppm and CO ppm during High VS Temperature Steady State (606°C)

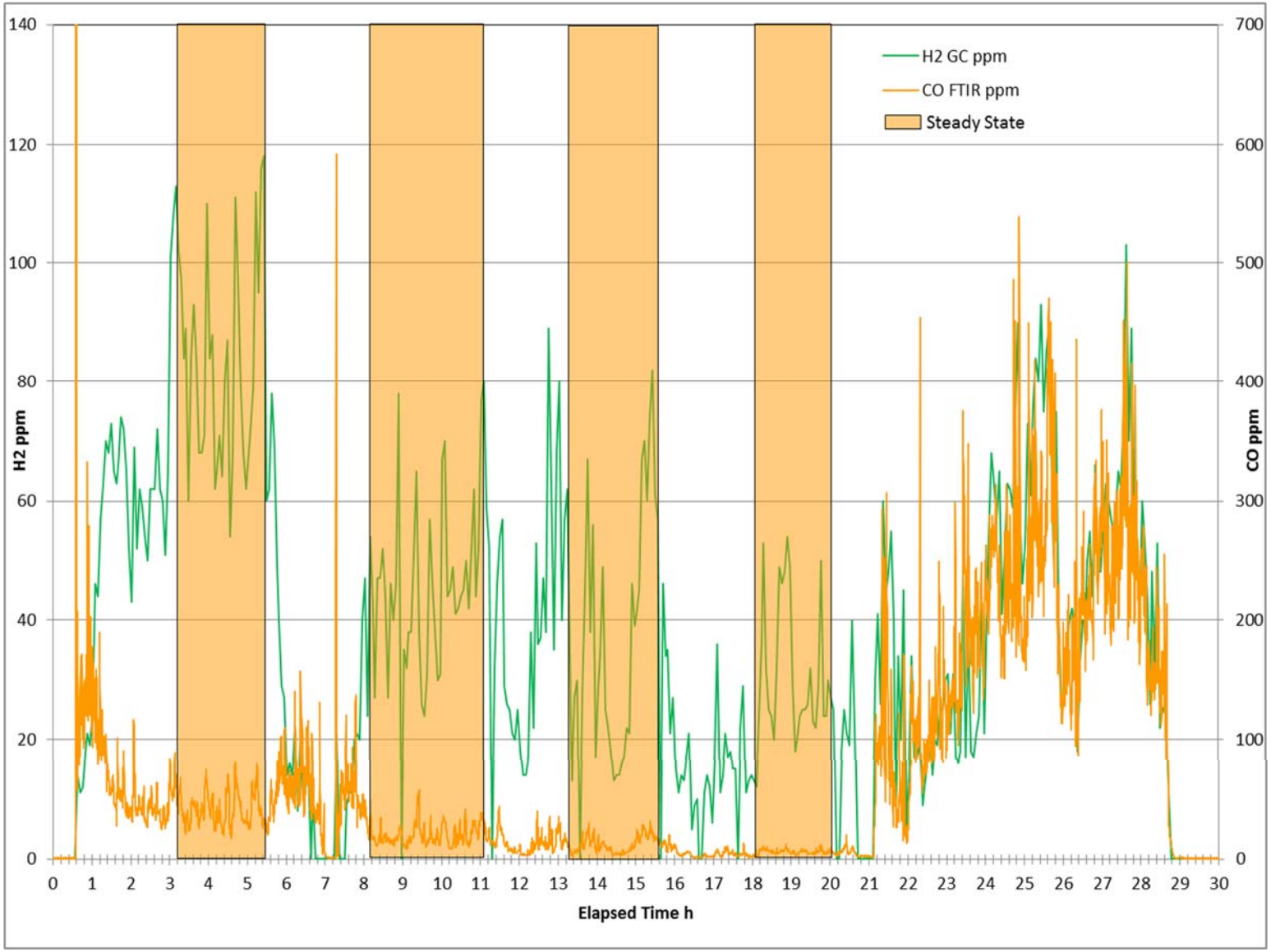

Figure F-18. Unremediated Feed – H_2 ppm and CO ppm during Low VS Temperature Steady States (501, 432, 321, and 222°C from left to right)

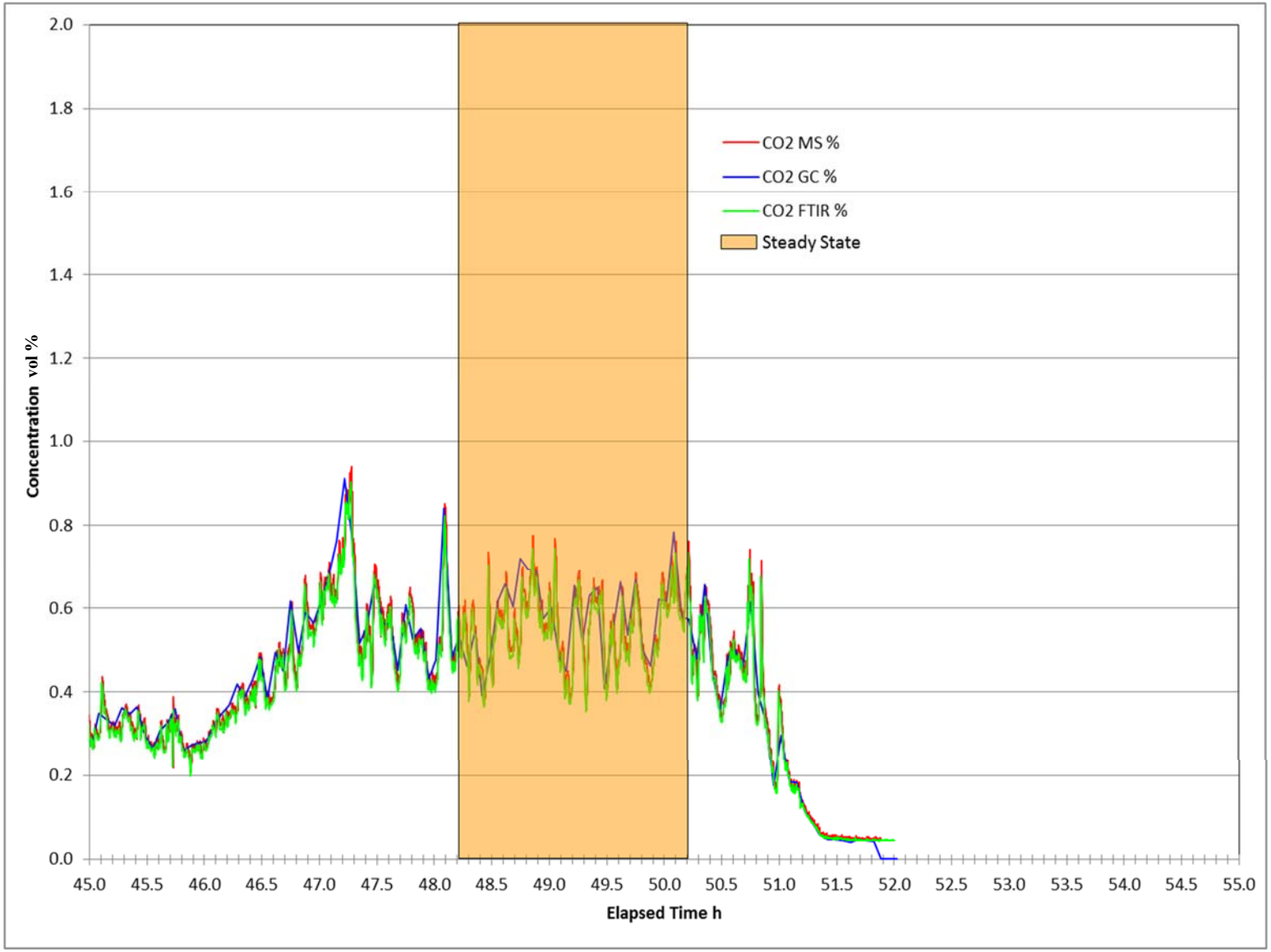

Figure F-19. Unremediated Feed – CO_2% during High VS Temperature Steady State (606°C)

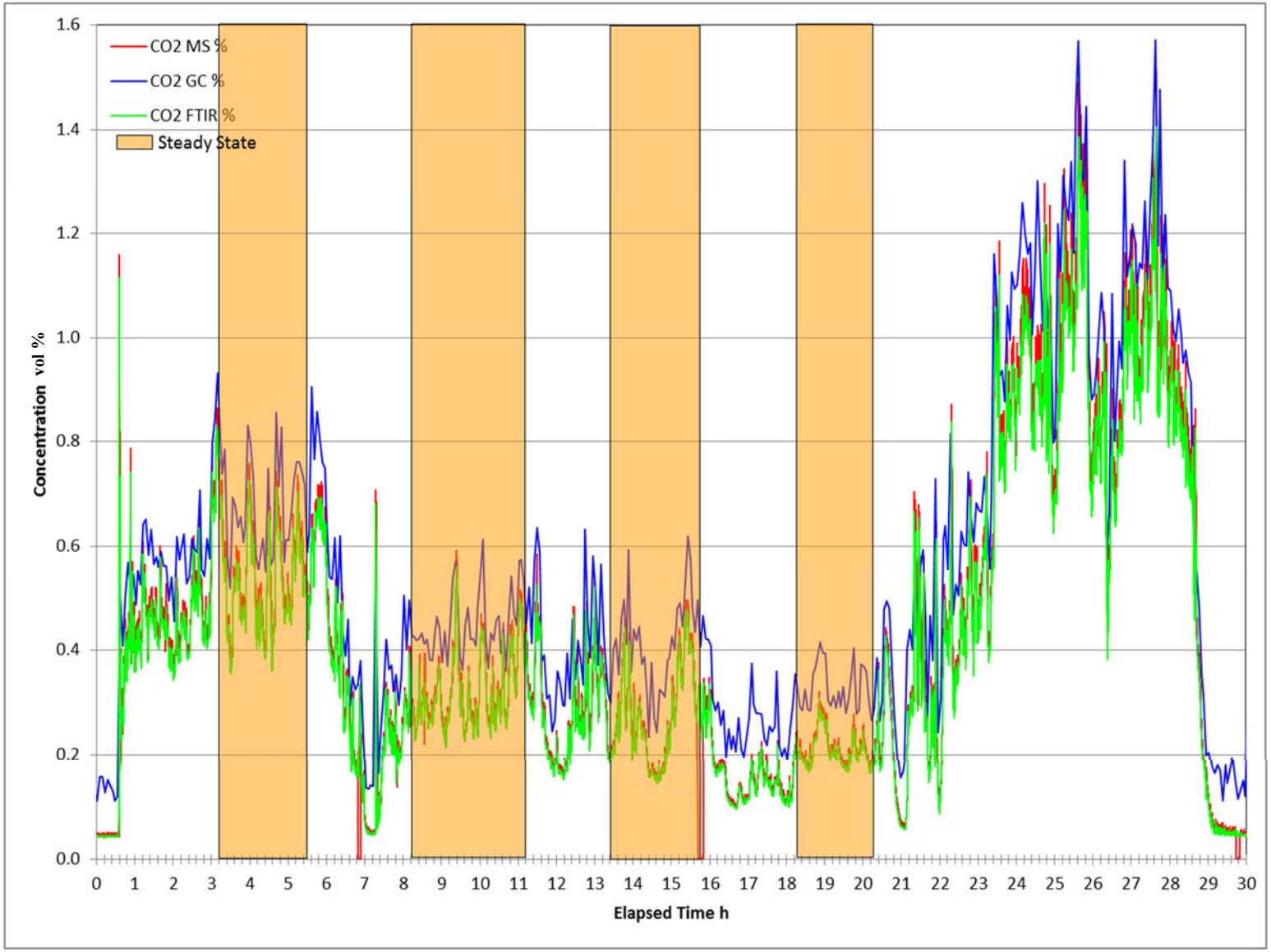

Figure F-20. Unremediated Feed – CO_2% during Low VS Temperature Steady States (501, 432, 321, and 222°C from left to right)

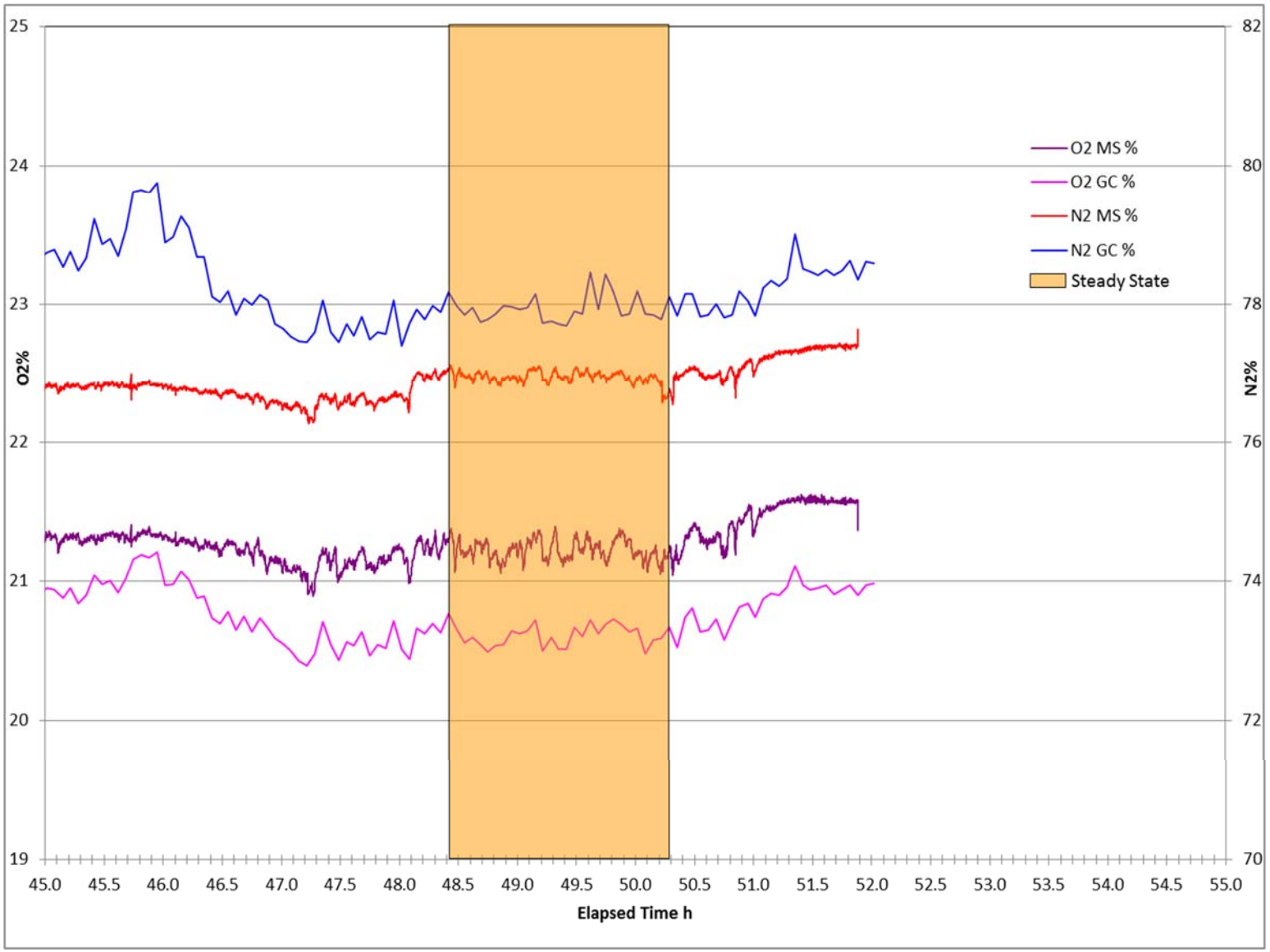

Figure F-21. Unremediated Feed – N_2% and O_2% during High VS Temperature Steady State (606°C)

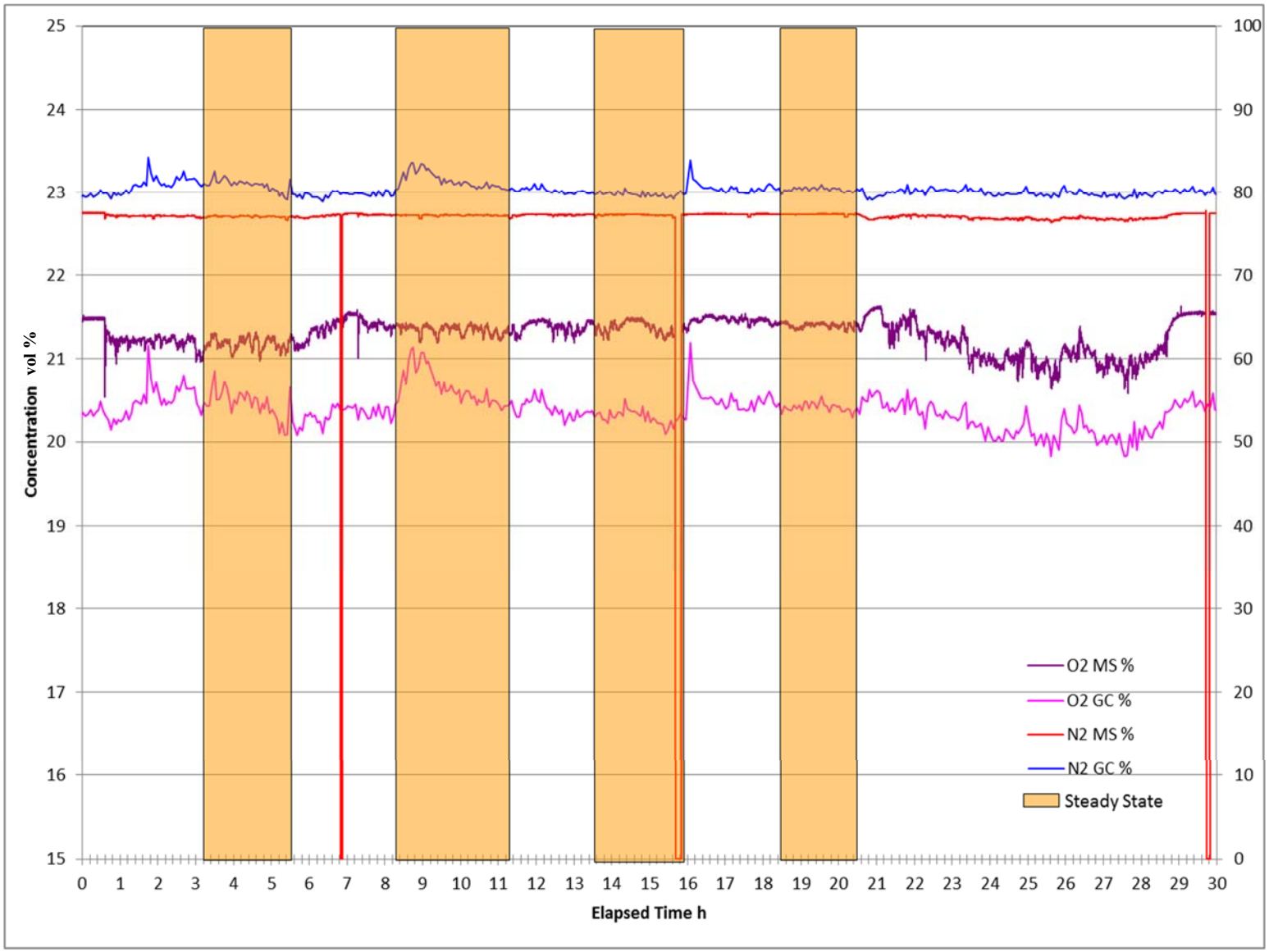

Figure F-22. Unremediated Feed – N_2%and O_2% during Low VS Temperature Steady States (501, 432, 321, and 222°C from left to right)

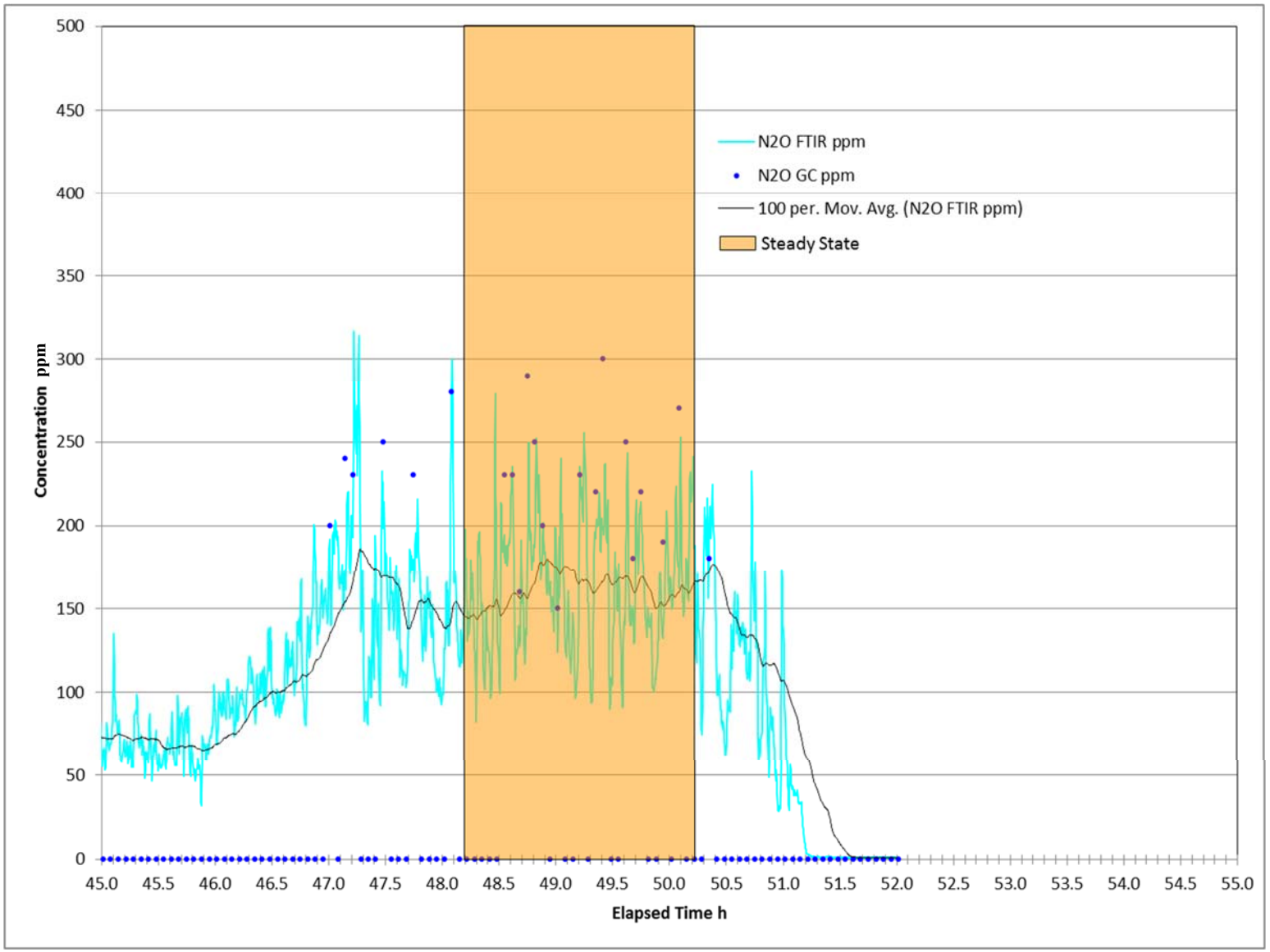

Figure F-23. Unremediated Feed – N_2O ppm during High VS Temperature Steady State (606°C)

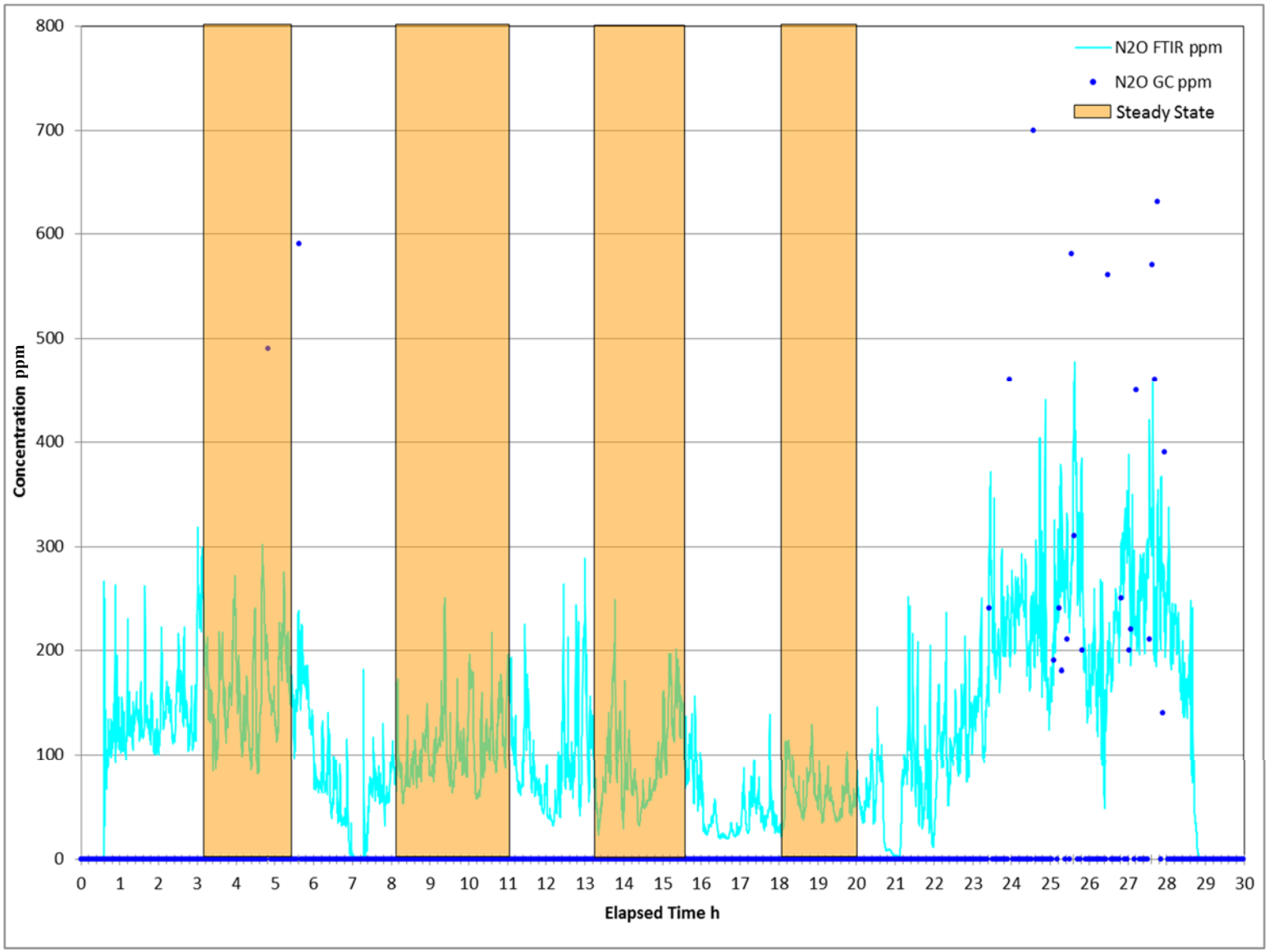

Figure F-24. Unremediated Feed – N_2O ppm during Low VS Temperature Steady States (501, 432, 321, and 222°C from left to right)

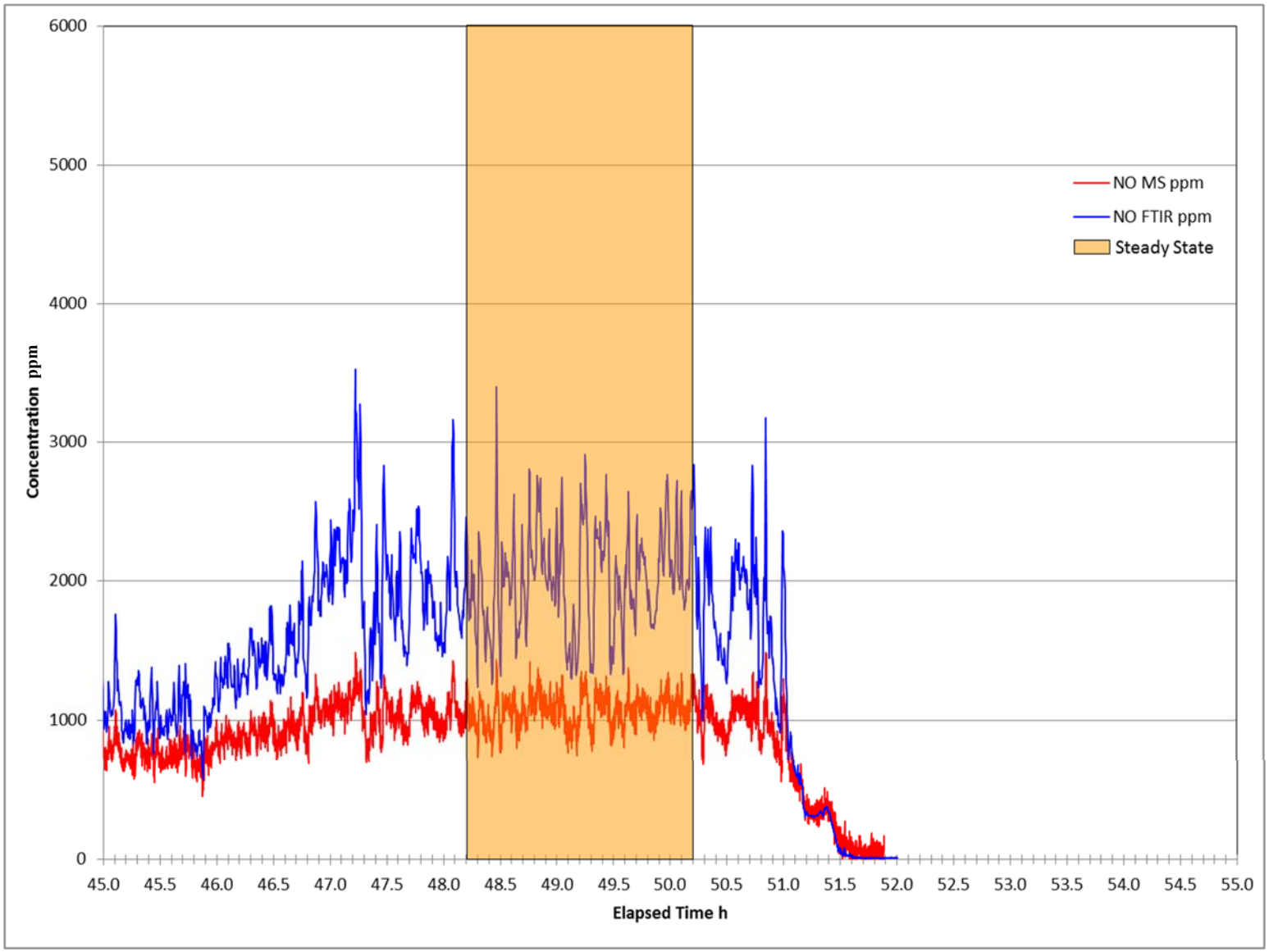

Figure F-25. Unremediated Feed – NO ppm during High VS Temperature Steady State (606°C)

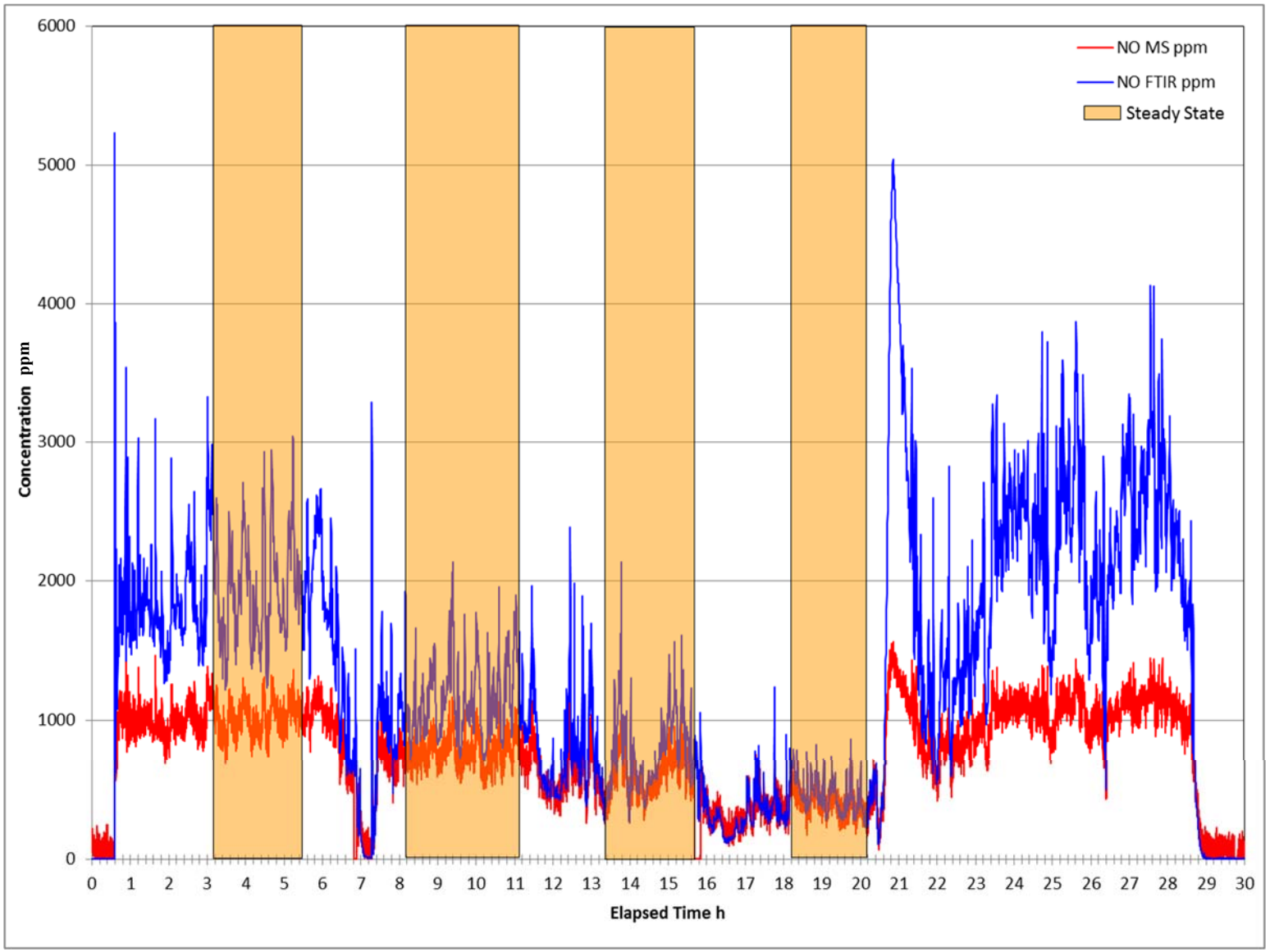

Figure F-26. Unremediated Feed – NO ppm during Low VS Temperature Steady States (501, 432, 321, and 222°C from left to right)

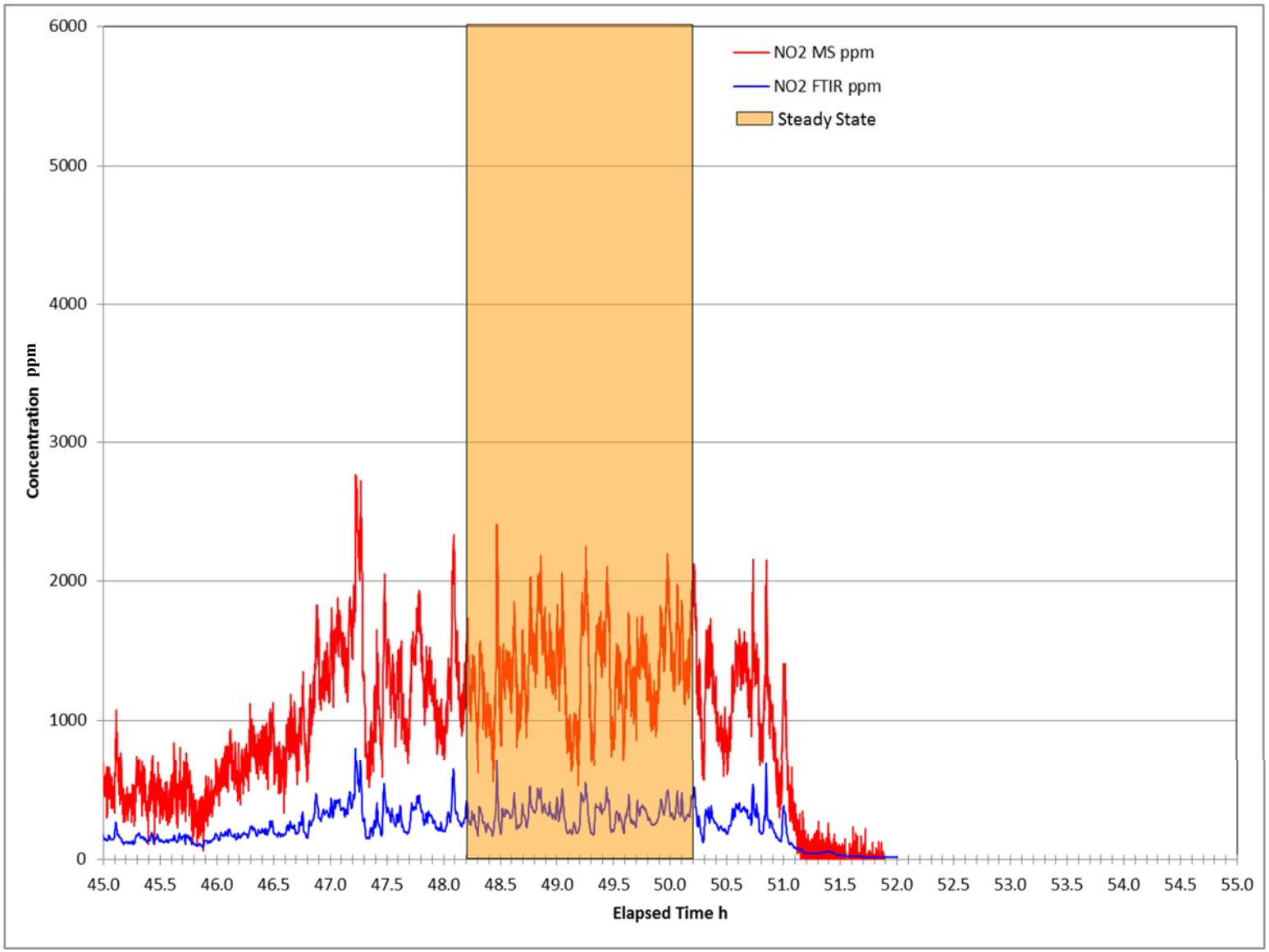

Figure F-27. Unremediated Feed – NO_2 ppm during High VS Temperature Steady State (606°C)

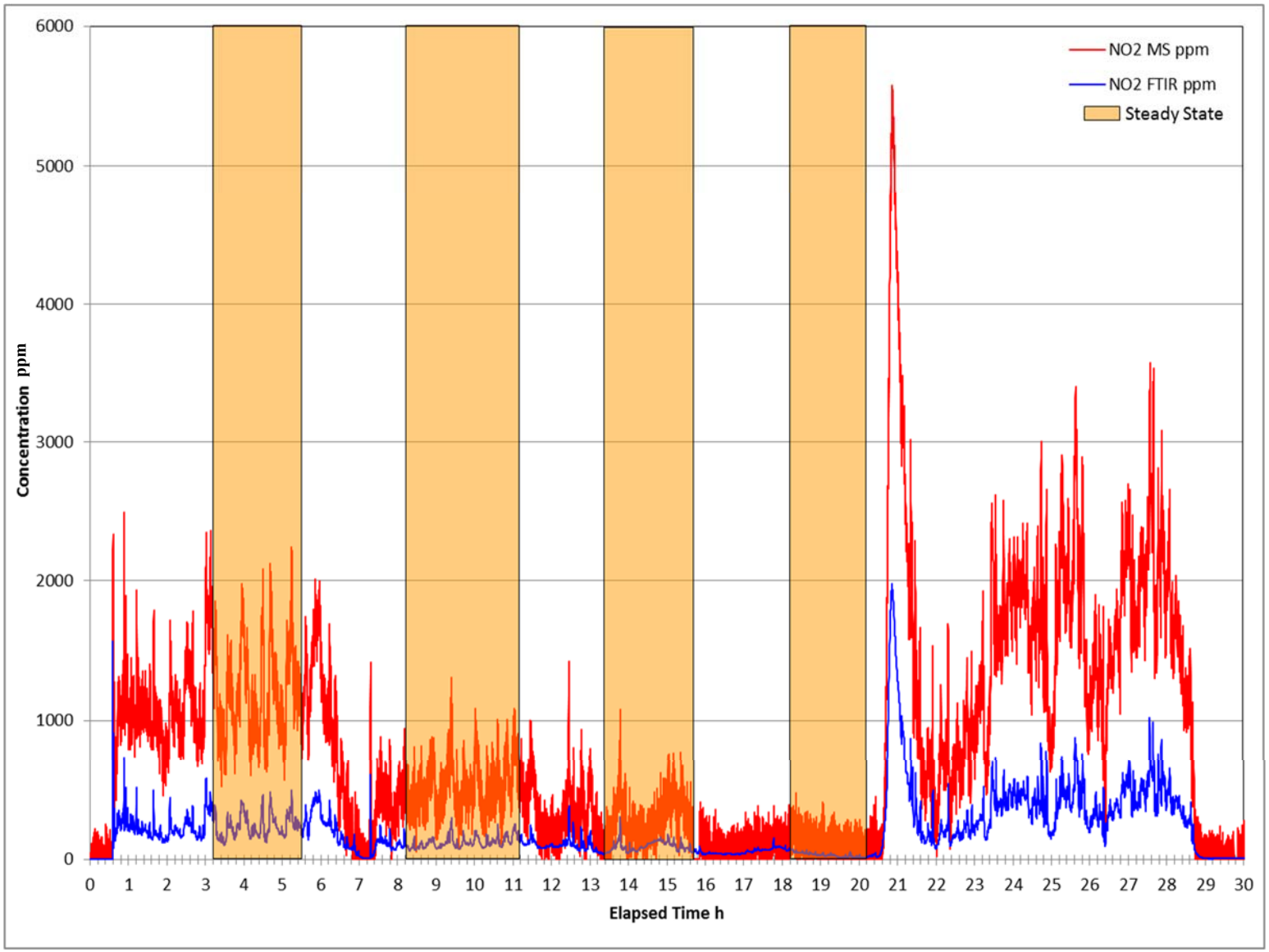

Figure F-28. Unremediated Feed – NO_2 ppm during Low VS Temperature Steady States (501, 432, 321, and 222°C from left to right)

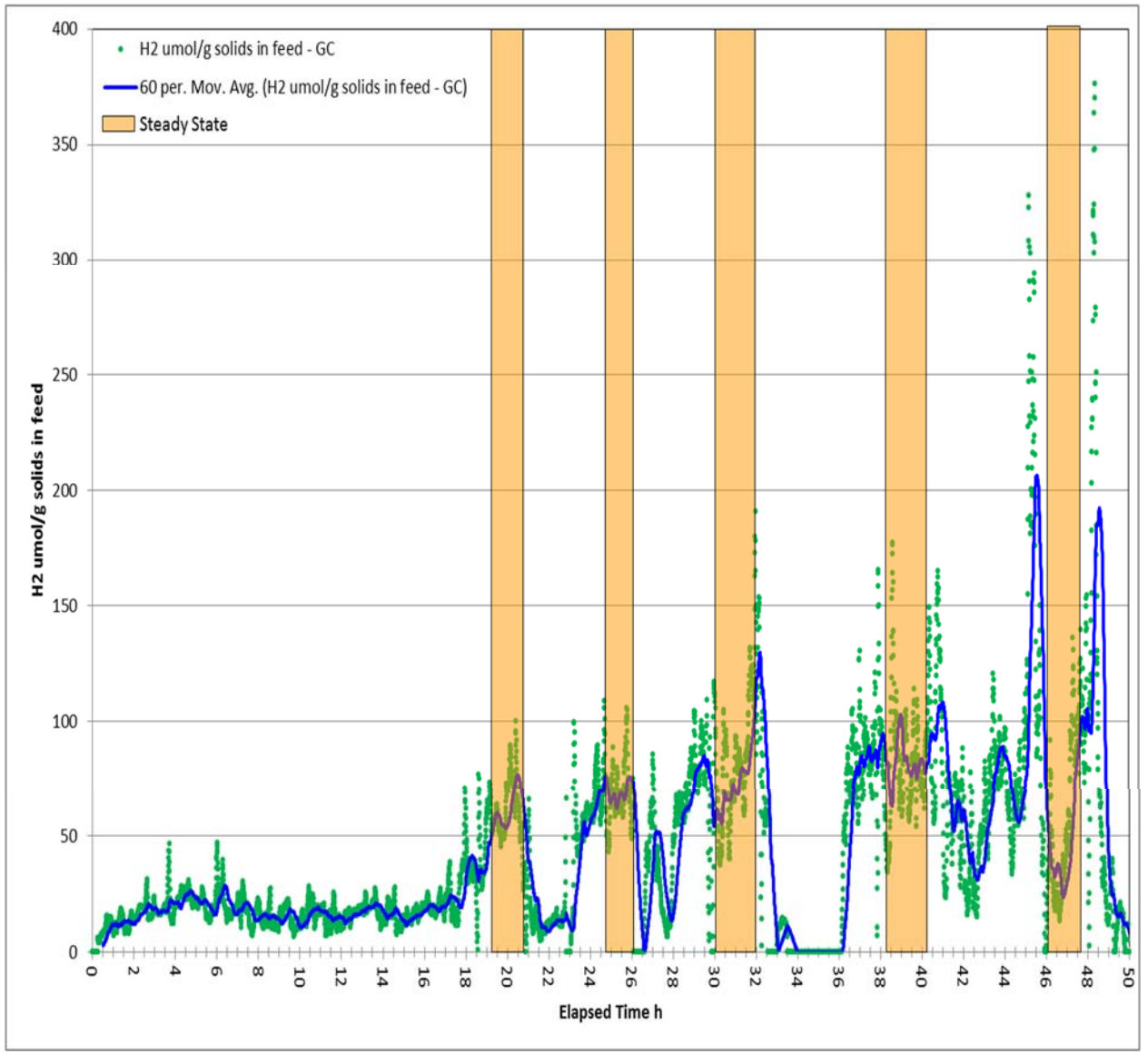

Figure F-29. Glycolic-Remediated Feed – H_2 µmol per Gram of Solids in Melter Feed as a Function of Time during Steady State Testing (616, 529, 422, 324, and 208°C from left to right)

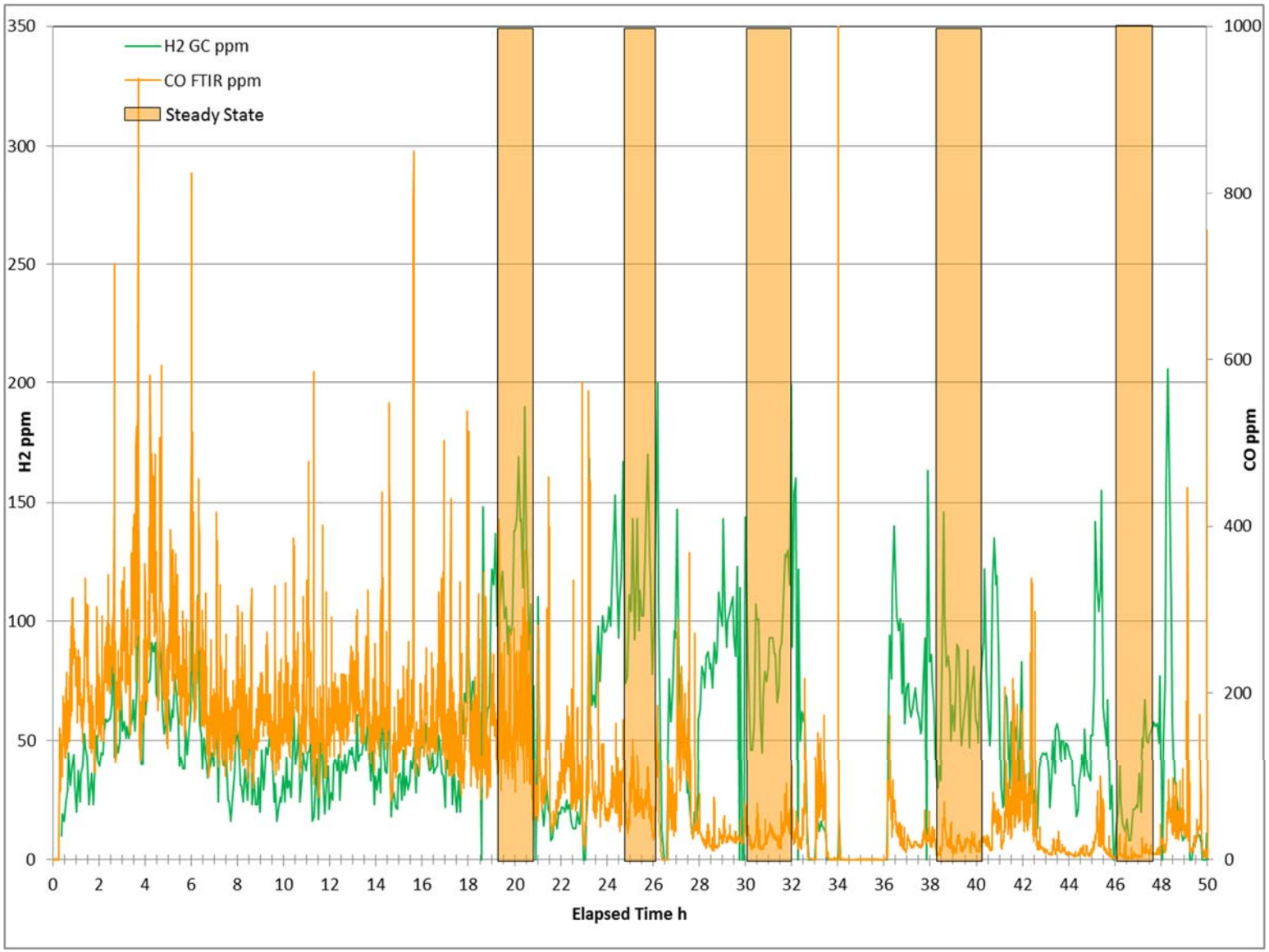

Figure F-30. Glycolic-Remediated Feed – H_2 ppm and CO ppm as a Function of Time during Steady State Testing (616, 529, 422, 324, and 208°C from left to right)

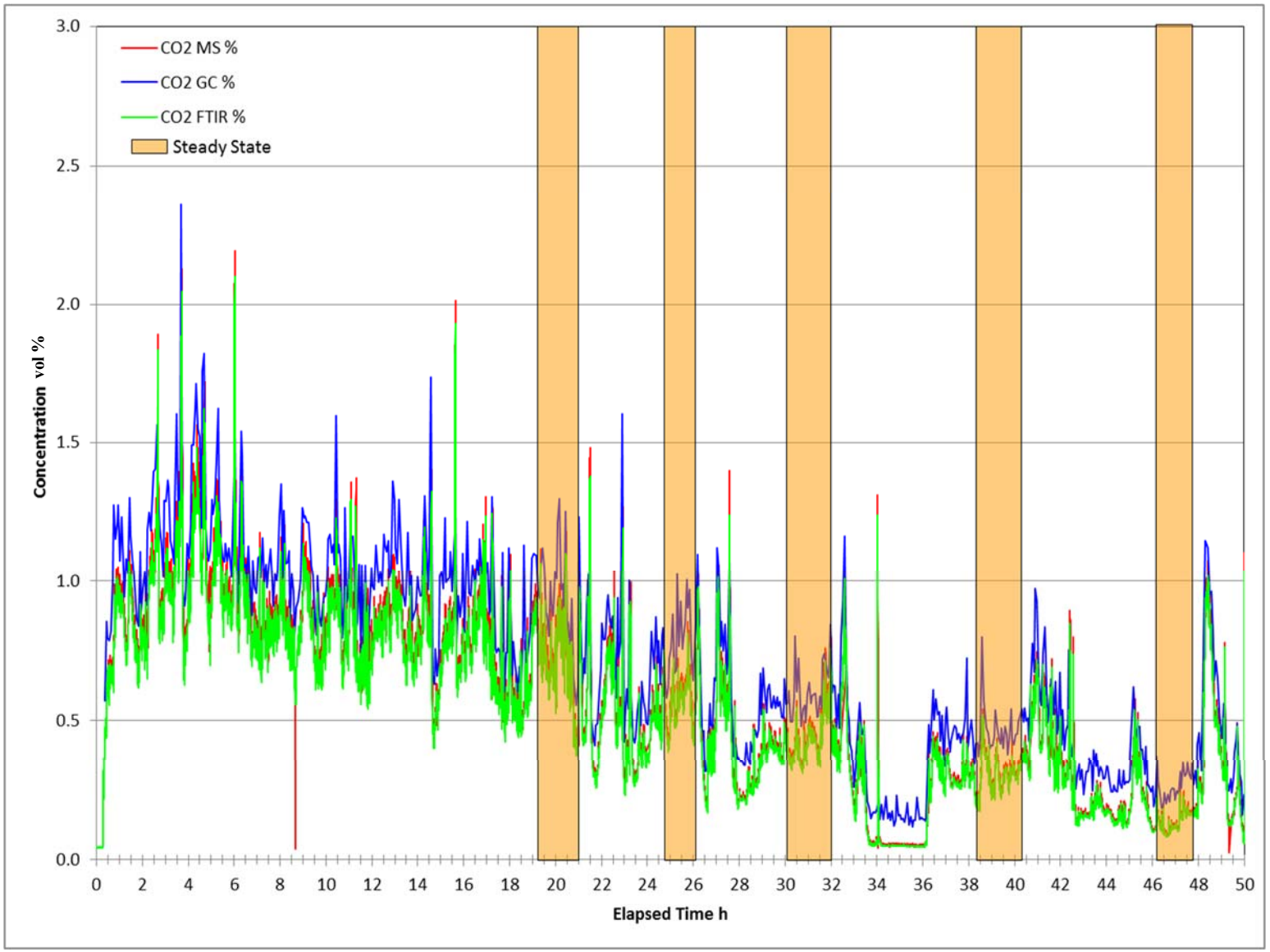

Figure F-31. Glycolic-Remediated Feed – CO_2% as a Function of Time during Steady State Testing (616, 529, 422, 324, and 208°C from left to right)

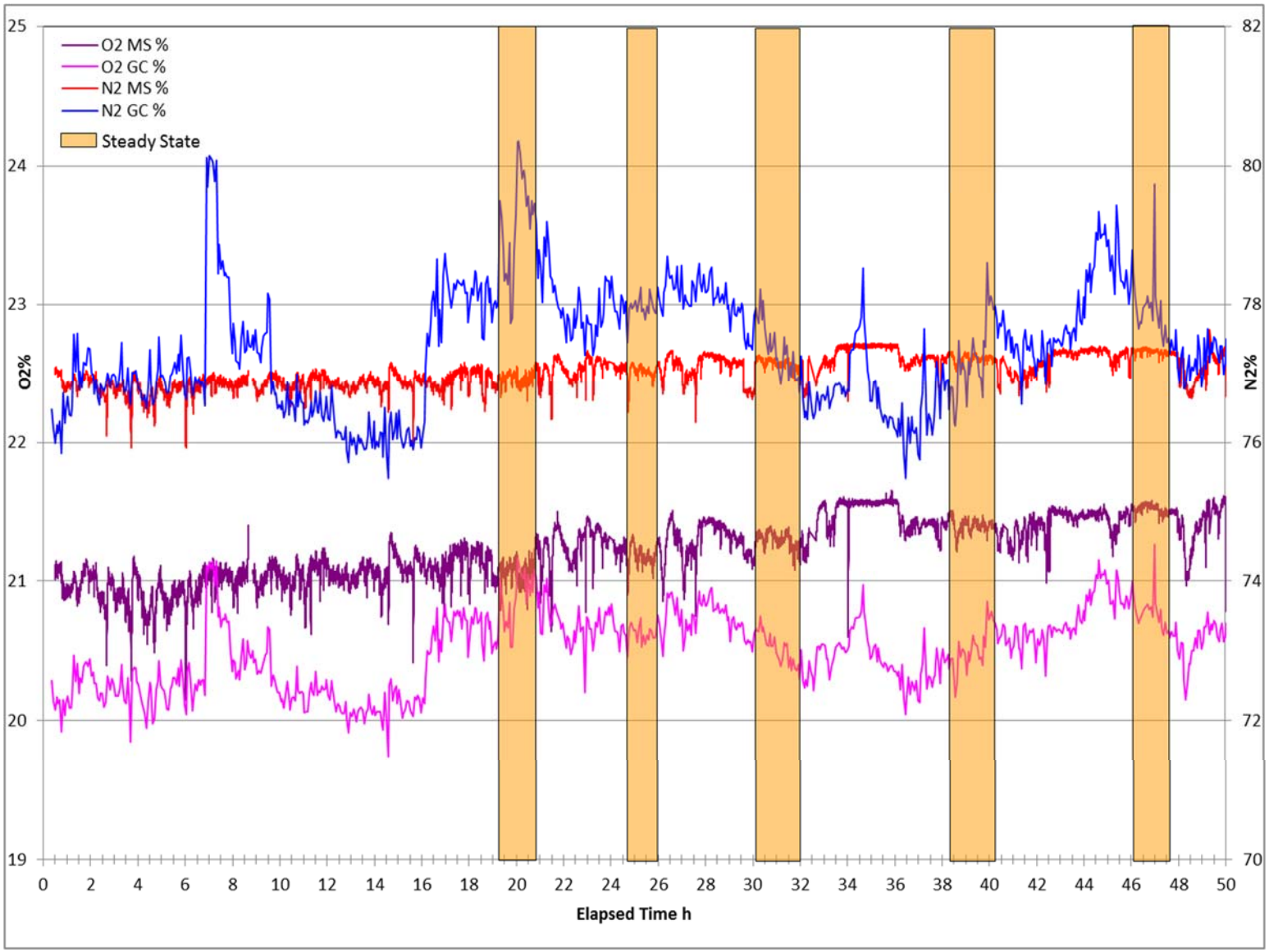

Figure F-32. Glycolic-Remediated Feed – N_2% and O_2% as a Function of Time during Steady State Testing (616, 529, 422, 324, and 208°C from left to right)

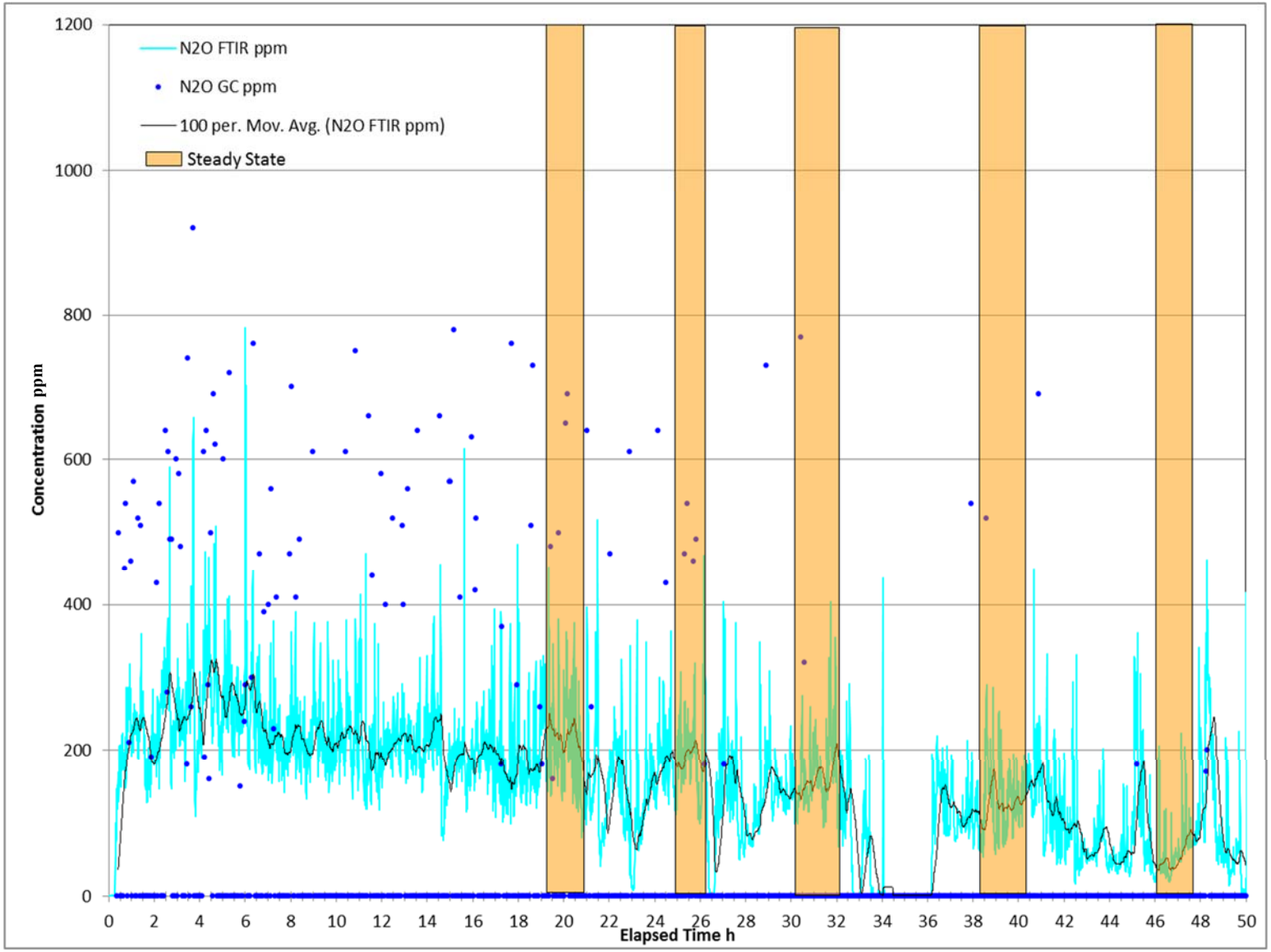

Figure F-33. Glycolic-Remediated Feed – N_2O ppm as a Function of Time during Steady State Testing (616, 529, 422, 324, and 208°C from left to right)

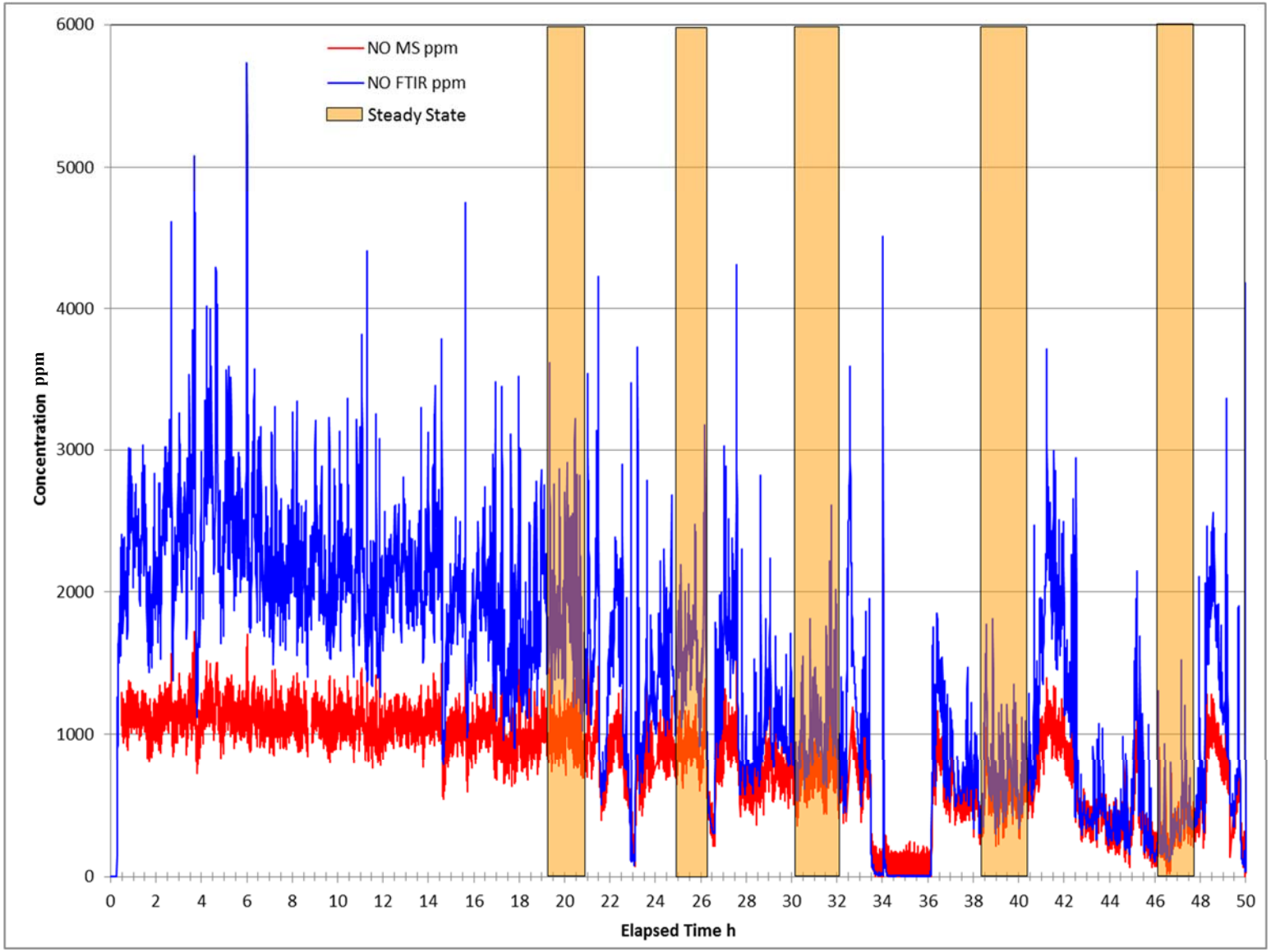

Figure F-34. Glycolic-Remediated Feed – NO ppm as a Function of Time during Steady State Testing (616, 529, 422, 324, and 208°C from left to right)

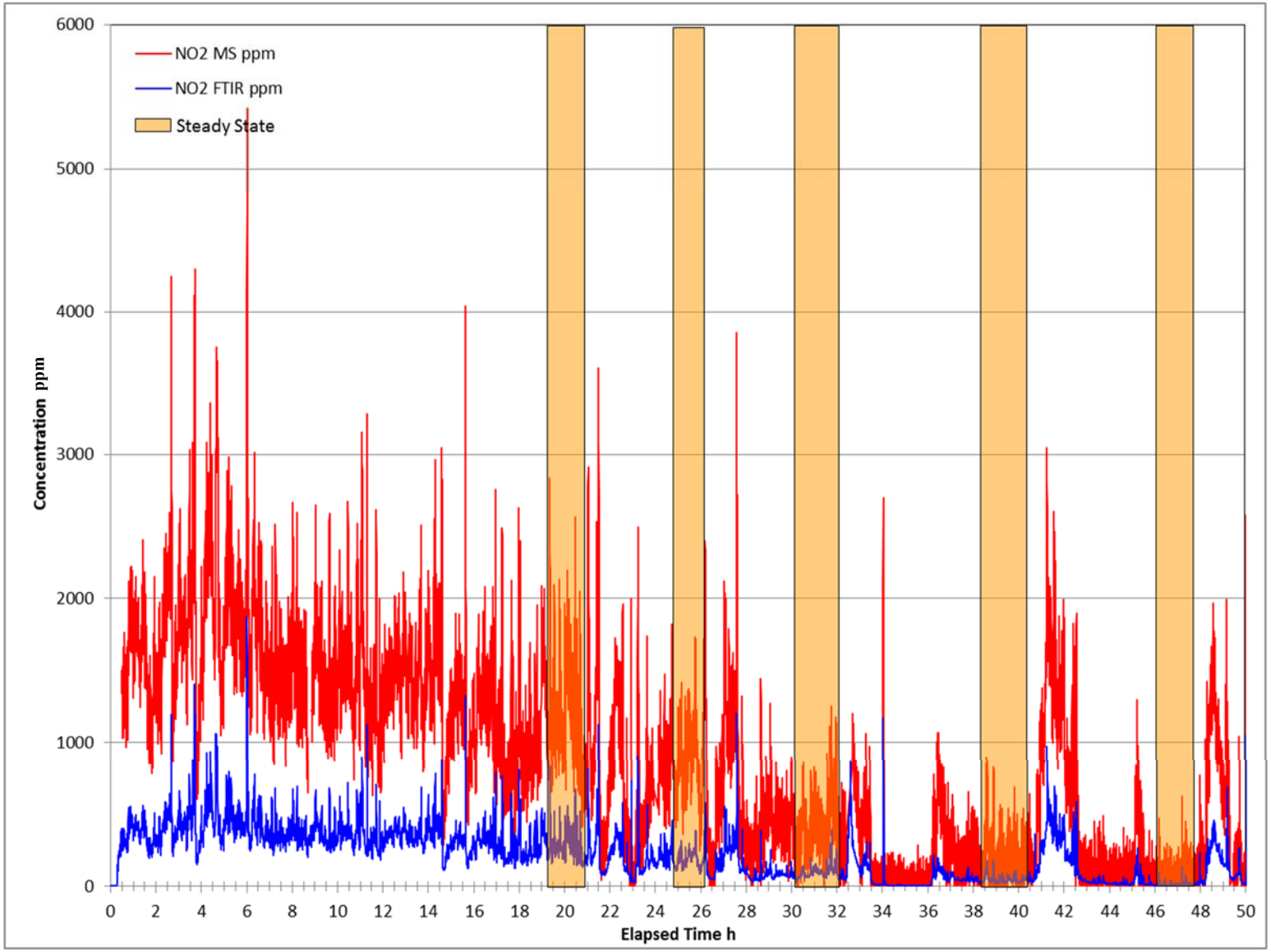

Figure F-35. Glycolic-Remediated Feed – NO_2 ppm as a Function of Time during Steady State Testing (616, 529, 422, 324, and 208°C from left to right)

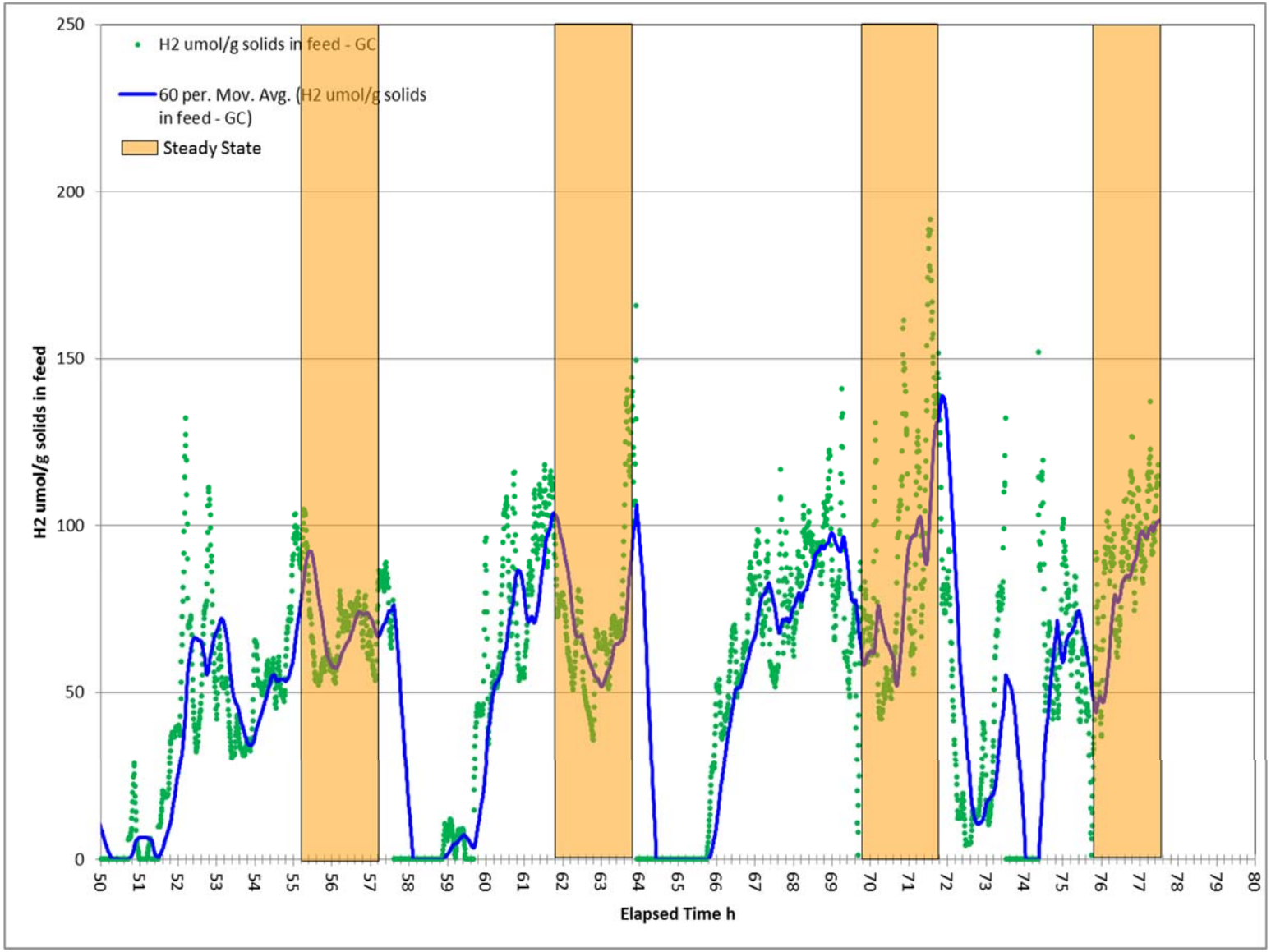

Figure F-36. Bubbled Glycolic-Remediated Feed – H_2 µmol per Gram of Solids in Melter Feed as a Function of Time during Steady State Testing (641, 499, 364, and 239°C from left to right)

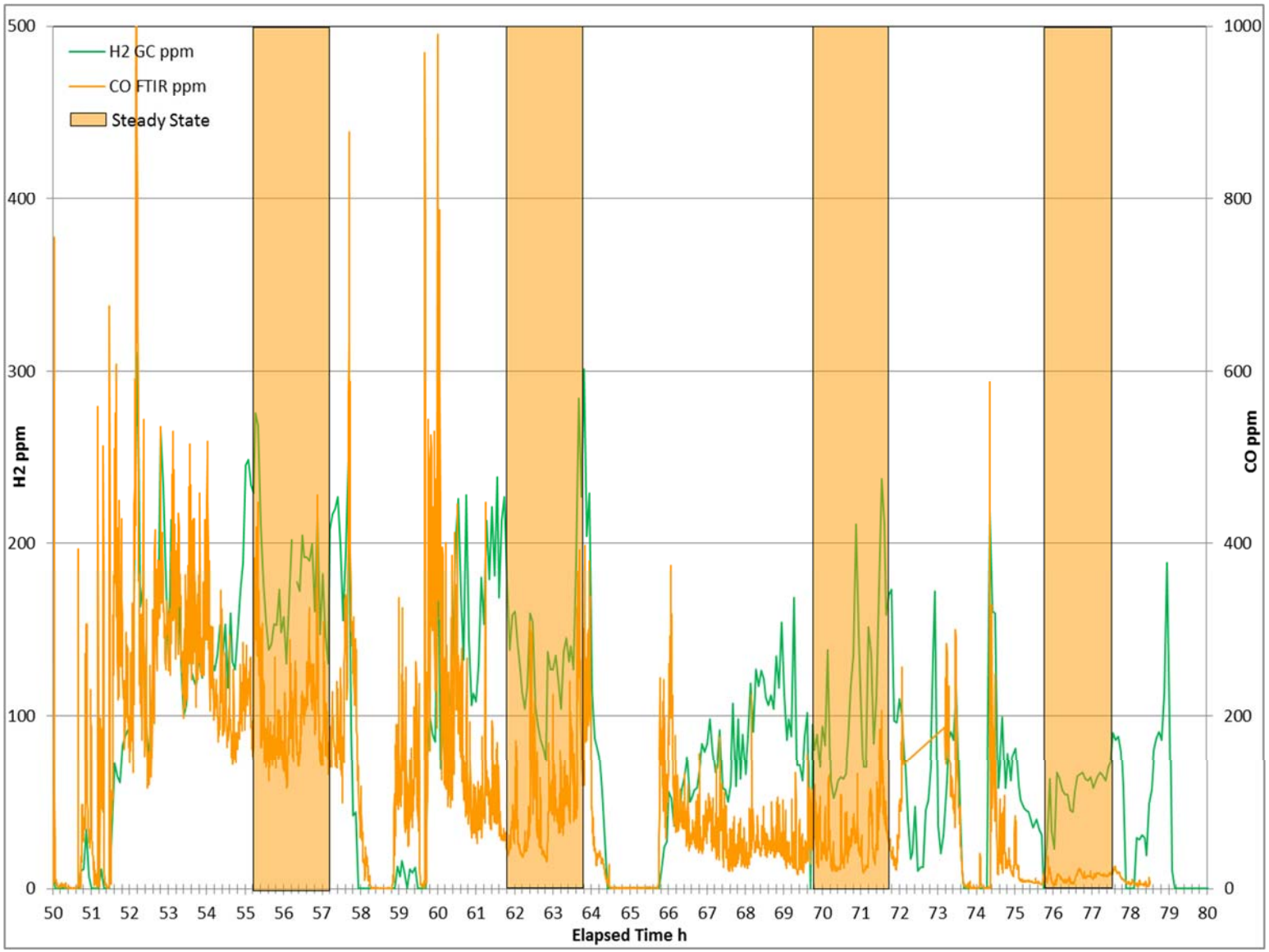

Figure F-37. Bubbled Glycolic-Remediated Feed – H_2 ppm and CO ppm as a Function of Time during Steady State Testing (641, 499, 364, and 239°C from left to right)

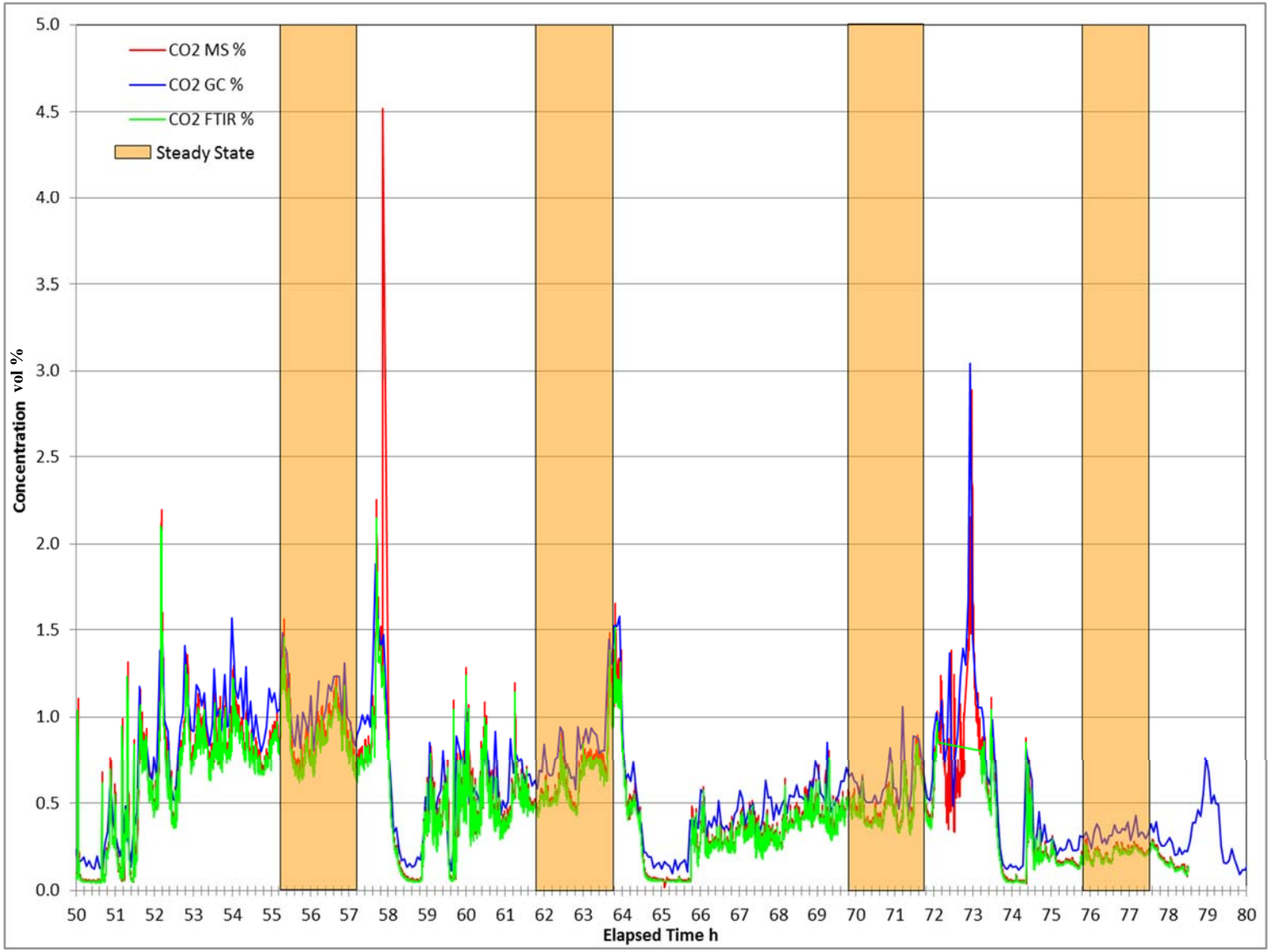

Figure F-38. Bubbled Glycolic-Remediated Feed – CO_2% as a Function of Time during Steady State Testing (641, 499, 364, and 239°C from left to right)

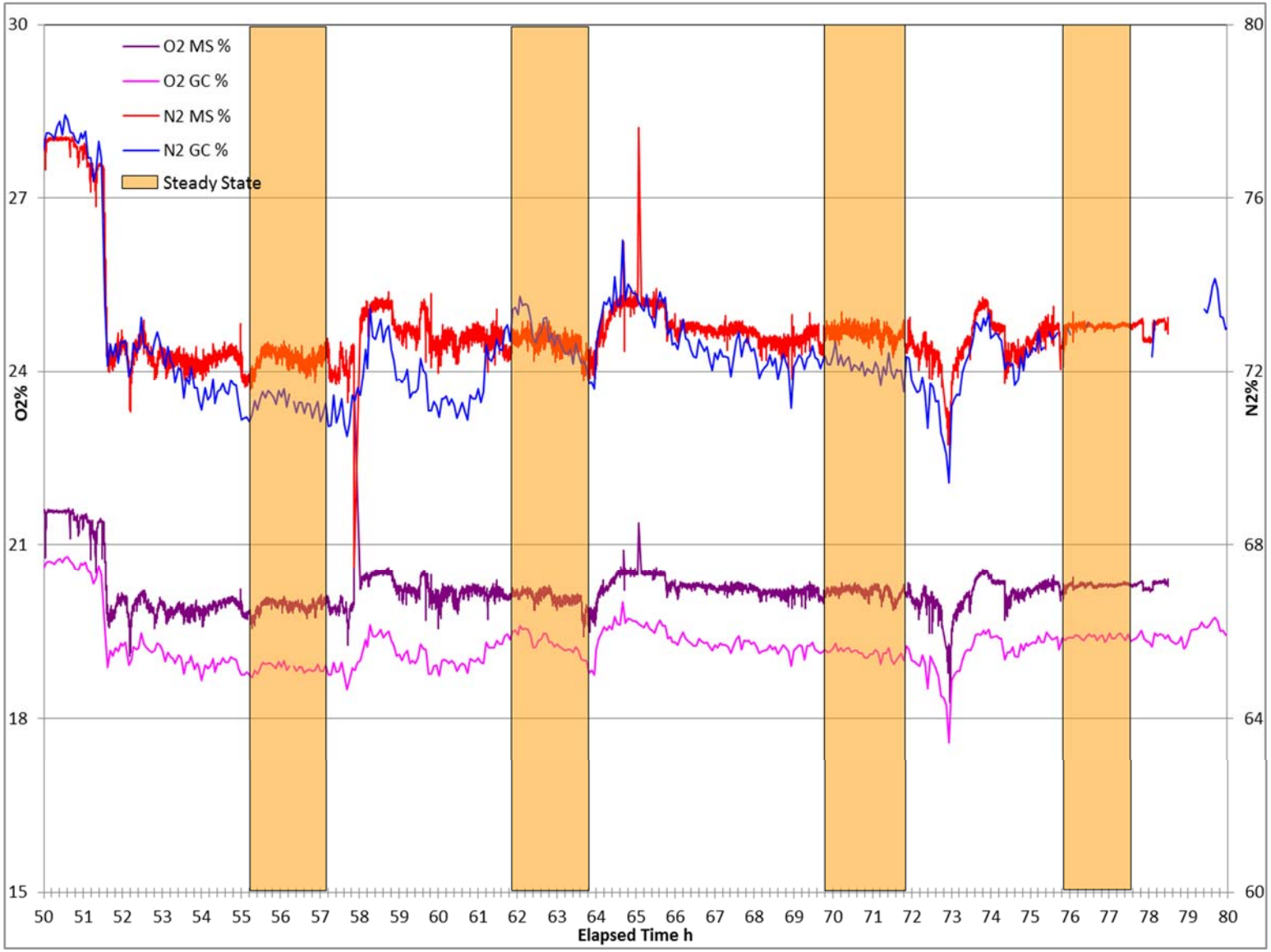

Figure F-39. Bubbled Glycolic-Remediated Feed – N_2% and O_2% as a Function of Time during Steady State Testing (641, 499, 364, and 239°C from left to right)

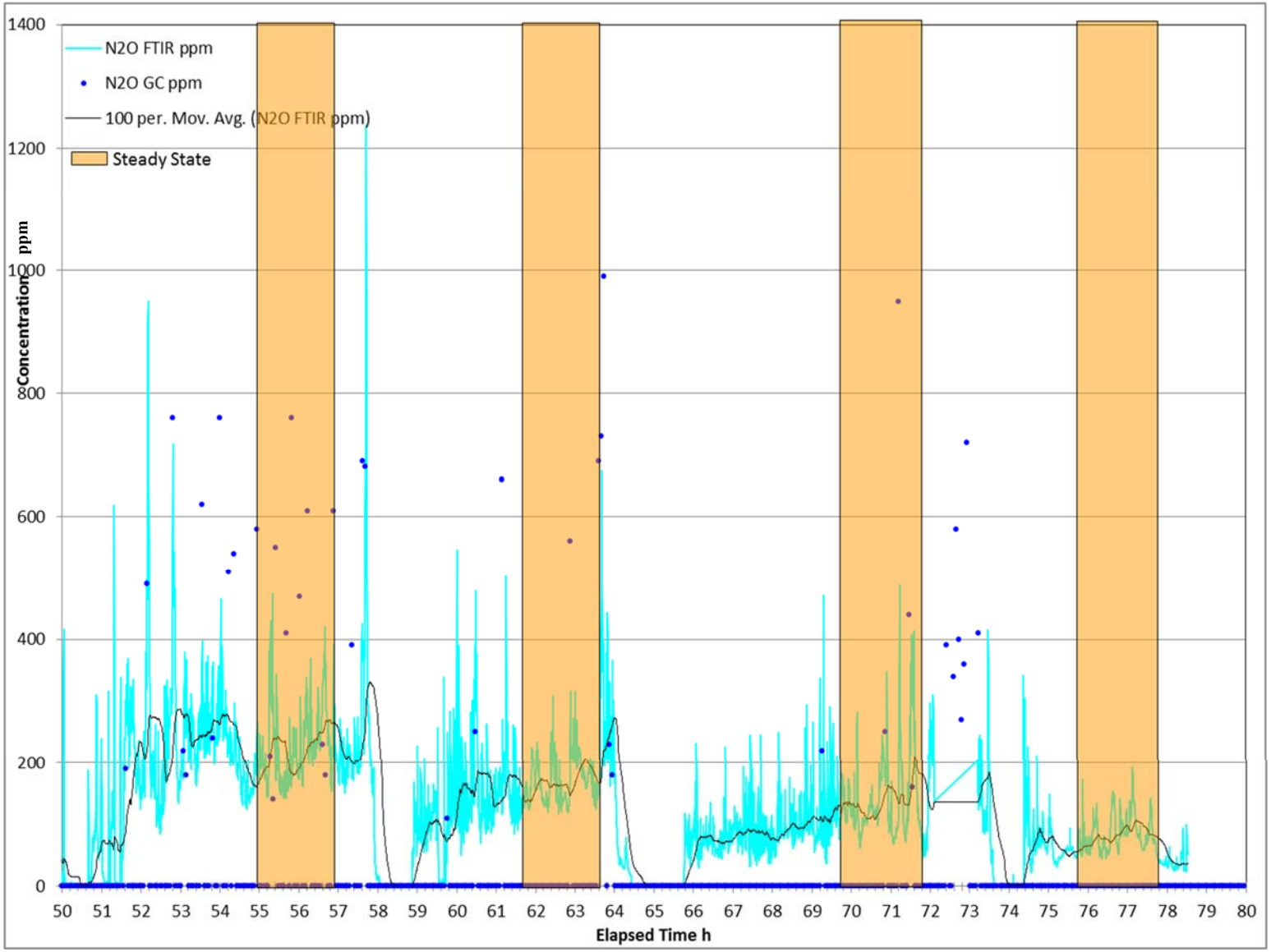

Figure F-40. Bubbled Glycolic-Remediated Feed – N_2O ppm as a Function of Time during Steady State Testing (641, 499, 364, and 239°C from left to right)

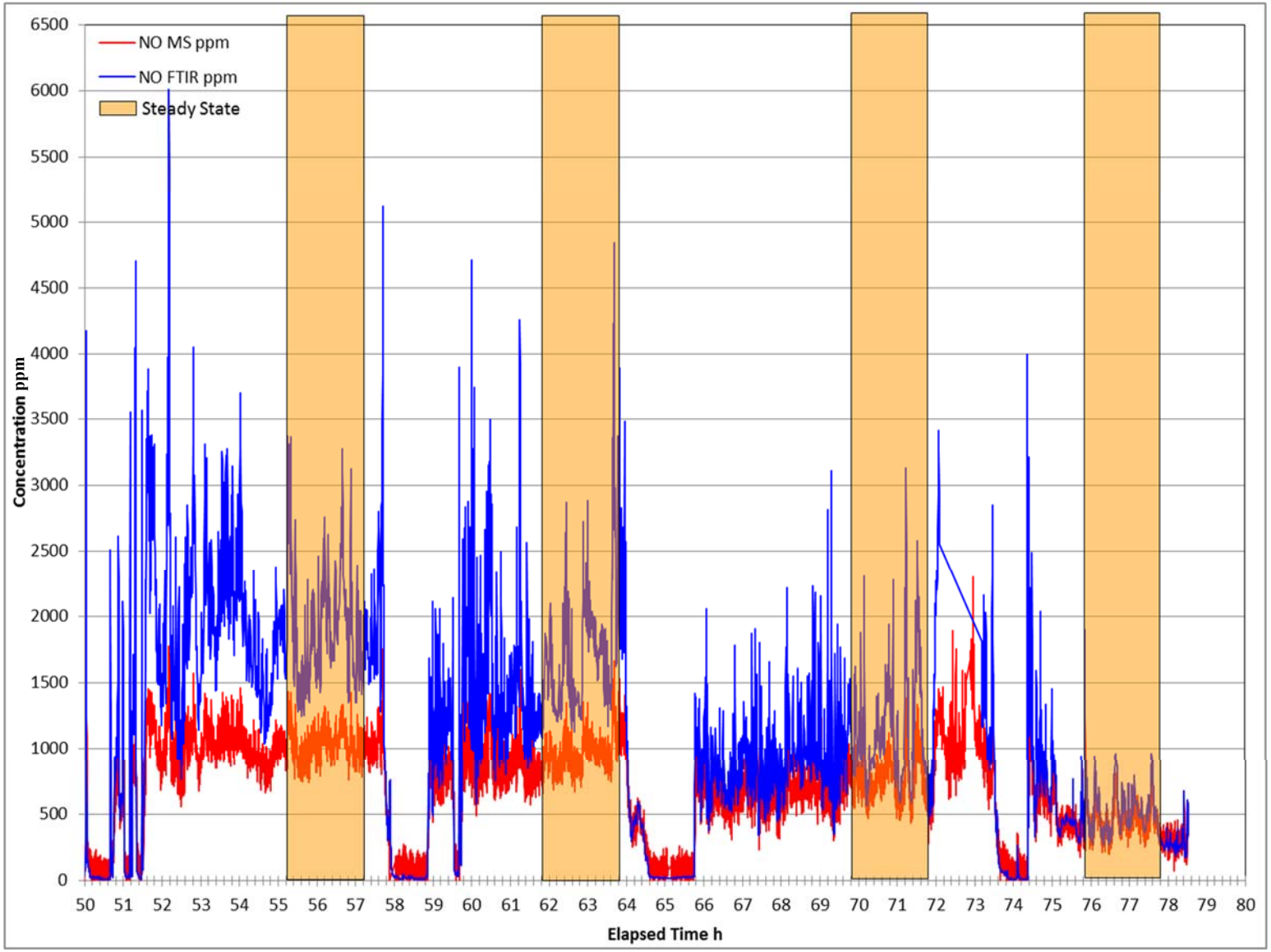

Figure F-41. Bubbled Glycolic-Remediated Feed – NO ppm as a Function of Time during Steady State Testing (641, 499, 364, and 239°C from left to right)

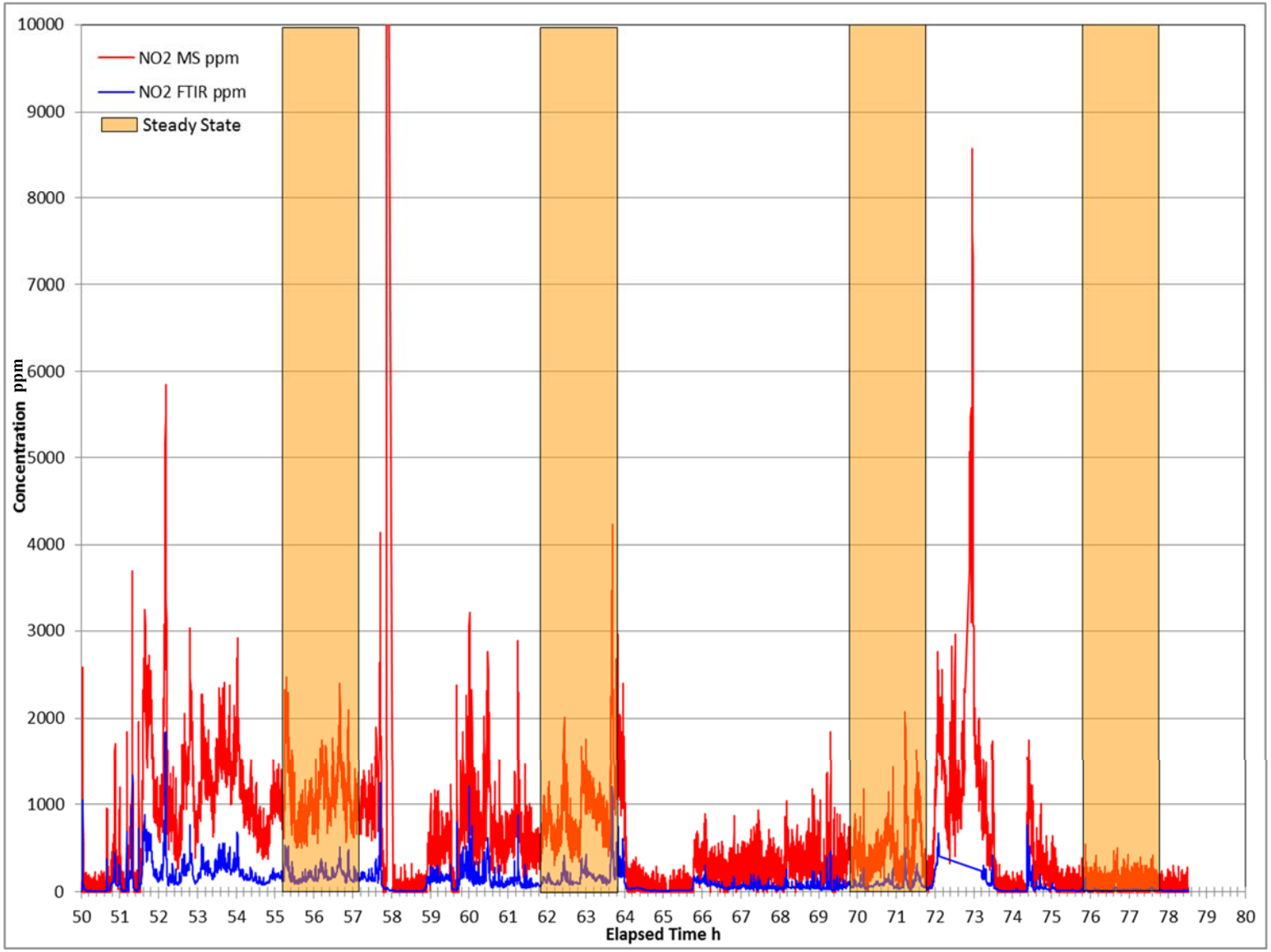

Figure F-42. Bubbled Glycolic-Remediated Feed – NO_2 ppm as a Function of Time during Steady State Testing (641, 499, 364, and 239°C from left to right)

Distribution:

T. B. Brown
M. E. Cercy
D. A. Crowley
D. E. Dooley
A. P. Fellinger
S. D. Fink
C. C. Herman
D. T. Hobbs
E. N. Hoffman
J. E. Hyatt
K. M. Kostelnik
B. B. Looney
T. O. Oliver
F. M. Pennebaker
G. N. Smoland
B. J. Wiedenman
W. R. Wilmarth
Records Administration (EDWS)
P. R. Jackson, DOE-SR
J. A. Crenshaw
H. P. Boyd
J. M. Bricker
J. S. Contardi
T. L. Fellinger
E. J. Freed
J. M. Gillam
B. A. Hamm
E. W. Holtzscheiter
J. F. Iaukea
V. Jain
C. J. Martino
J. W. Ray
P. J. Ryan
M. A. Rios-Armstrong
H. B. Shah
D. C. Sherburne
C. Sudduth
M. S. Williams
M. D. Fowley
J. R. Zamecnik
F. C. Johnson
W. H. Woodham
D. P. Lambert
M. E. Stone
J. D. Newell
W. E. Daniel
J. W. Amoroso
D. J. Adamson
D. L. McClane
A. S. Choi
T. B. Edwards
K. A. Hill
W. P. Kubilius
A. A. Ramsey
S. T. Isom
K. M. Brotherton
V. M. Kmiec
A. V. Staub
L. C. Jamison
A. Samadi-Dezfouli